Self-Assembling Peptide Hydrogels Promote *in vitro* Chondrogenesis of Bone Marrow-Derived Stromal Cells: Effects of Peptide Sequence, Cell Donor Age, and Method of Growth Factor Delivery

by

Paul Wayne Kopesky

S.B. Chemical Engineering
Massachusetts Institute of Technology, 1998

S.M. Chemical Engineering Practice
Massachusetts Institute of Technology, 1999

Submitted to the Department of Biological Engineering
in Partial Fulfillment of the Requirements for the Degree of

Doctor of Philosophy in Biological Engineering

at the

Massachusetts Institute of Technology

June, 2009

Signature of Author_____
Department of Biological Engineering
May 20, 2009

Certified by _____
Alan J. Grodzinsky
Professor of Biological, Electrical, and Mechanical Engineering
Thesis Supervisor

Accepted by _____
Peter C. Dedon
Professor of Toxicology and Biological Engineering
Associate Head, Department of Biological Engineering

Thesis Committee

Dr. Alan J. Grodzinsky
Thesis Advisor
Professor of Biological, Electrical, and Mechanical Engineering
Massachusetts Institute of Technology

Dr. Richard T. Lee
Thesis Committee Chair
Associate Professor of Medicine
Harvard Medical School

Dr. Christopher Evans
Professor of Orthopedic Surgery
Beth-Israel Deaconess Medical Center, Harvard Medical School

Self-Assembling Peptide Hydrogels Promote *in vitro* Chondrogenesis of Bone Marrow-Derived Stromal Cells: Effects of Peptide Sequence, Cell Donor Age, and Method of Growth Factor Delivery

by

Paul Wayne Kopesky

Submitted to the Department of Biological Engineering on May 20, 2009 in Partial Fulfillment of the Requirements for the Degree of Doctor of Philosophy in Biological Engineering at the Massachusetts Institute of Technology

Abstract

The inability of articular cartilage to heal after damage or disease has motivated investigation of novel cartilage tissue engineering technologies. The objective of this thesis was to advance the use of self-assembling peptide hydrogel scaffolds for cartilage repair by encapsulating bone-marrow-stromal cells (BMSCs) and incorporating chondrogenic cues to stimulate differentiation and neotissue production.

To test the hypothesis that self-assembling peptide hydrogels provide cues which enhance the chondrogenic differentiation of BMSCs, a technique for rapid, high-viability BMSC encapsulation was developed. BMSCs were cultured in two peptide hydrogel sequences and compared to agarose hydrogels. BMSCs in all three hydrogels underwent TGF-β1-mediated chondrogenesis as demonstrated by comparable gene expression and ECM biosynthesis. Cell proliferation occurred only in the peptide hydrogels, not in agarose, resulting in higher sulfated-glycosaminoglycan content and more spatially uniform proteoglycan and type II collagen deposition. These data showed that self-assembling peptide hydrogels enhance chondrogenesis compared to agarose.

To evaluate the capacity for BMSCs from young and adult equine donors to produce cartilage-like ECM, neotissue formation was compared to that for animal-matched primary chondrocytes. Young chondrocytes stimulated by TGF-β1 accumulated ECM with higher sulfated-glycosaminoglycan content than adult chondrocytes and BMSCs of either age. BMSCs produced neotissue with higher dynamic stiffness than young chondrocytes. Measurement of aggrecan core-protein and chondroitin-sulfate length by atomic-force microscopy revealed BMSCs produce longer core protein and chondroitin-sulfate, and fewer catabolic-cleavage products than chondrocytes. Therefore, BMSC-produced aggrecan appears to have a younger phenotype than chondrocyte-produced aggrecan. These advantages make BMSCs a potentially superior cell source for peptide-hydrogel-based cartilage repair.

To deliver TGF-β1 to BMSCs via a bioactive scaffold, BMSCs were encapsulated in peptide hydrogels with both tethered and adsorbed TGF-β1 and cultured in TGF-β1-free medium. Chondrogenesis was compared to that of unmodified peptide hydrogels with medium-delivered TGF-β1. Adsorbed-TGF-β1 peptide hydrogels stimulated chondrogenesis of BMSCs as demonstrated by cell proliferation and cartilage-like ECM accumulation, while tethered TGF-β1 was not different from TGF-β1-free controls. TGF-β1 adsorbed to self-assembling peptide hydrogels can stimulate BMSC chondrogenesis.

BMSC-seeded self-assembling peptide hydrogels, modified for controlled delivery of pro-chondrogenic factors, generate cartilage-like neotissue and are compatible with a single-surgery, autologous therapy for cartilage repair.

Thesis Supervisor: Alan J. Grodzinsky, Prof. of Biological, Electrical, Mechanical Engineering

Acknowledgements

This thesis represents not only the culmination of a scientific endeavor for me professionally, but also a journey of personal development and a discovery of identity for which I am profoundly indebted to so many people. When I think back to the goals I set five years ago which provided my motivation to attend graduate school, they were almost exclusively professional: to develop the skills to propose, conduct, and interpret a scientific investigation; to learn to make the day-to-day decisions necessary to successfully complete a long-term investigation, and to contribute to the solution of an unmet societal challenge. While I hope that I have done all of these things, what I did not anticipate was what I learned about myself: the fundamental curiosity to understand the dazzling sophistication of biology; the pride in being a part of a profession and a community of scientists whom I deeply respect; and the fulfillment from both solving the technical challenges of laboratory work as well as from the creative process of generating new hypotheses.

First and foremost I would like to thank Alan Grodzinsky. It is simply not possible to overstate the role he has played in my endeavors both personal and professional. Not only did he assemble a team of brilliant scientists and engineers and provide the resources for us to pursue our education, but he has mentored and guided my education with a leadership style that combines the highest standards for excellence with the freedom for self-discovery. He sets the example everyday and I can not imagine a more ideal environment in which to conduct my graduate work.

I have been privileged to be involved with the Biological Engineering Department throughout my MIT career, starting in the fall of 1995 as an undergraduate in the Biomedical Engineering Minor. My introduction to the field of tissue engineering came at an informational meeting run by Linda Griffith that fall and I still remember being fascinated by her description of seeding hepatocytes into three-dimensional scaffolds and regenerating liver. Through the minor I also met Doug Lauffenburger and am grateful to him for the numerous mentoring discussions we have had over the years. I will always remember his generosity with his time and guidance at many stages of my career. The experiences I had with Doug and Linda were inspirational and formative and I simply would not be where I am without them.

The level of talent in both the Continuum Biomechanics Group and the entire Biological Engineering Department is truly superb. While I could not possibly name everyone who has contributed to my education, there are many whose contributions I would like to acknowledge here. In particular, Eric Vanderploeg has been an exceptional colleague and friend to whom I am deeply indebted for his scientific insight and strategic guidance. Thank you for always tolerating with a smile my repeated barging into your office to discuss whatever half-formed idea happened to be on my mind. Equally instrumental to my education was John Kisiday who literally taught me stem-cell and three-dimensional tissue culture from scratch. I was fortunate to have Rich Lee and Chris Evans on my thesis committee; this thesis has benefited tremendously from your scientific insight. Thank you to Hsu-Yi Lee and Sangwon Byun who have been a pleasure to work with as colleagues and coauthors on numerous studies. The lab simply would come to a grinding halt without the dedication of Han-Hwa Hung, Linda Bragman, and Eliot Frank. I have enjoyed working with you as friends and colleagues. Thank you to all the members of the tissue-

engineering subgroup, Diana Chai, Rachel Miller, Emily Florine, and to all the members of the entire Grodzinsky lab over the last five years. It has been an honor to work with all of you.

Finally, I would like to thank my family. Thank you to my parents and sister who have always supported me and who were so instrumental in inspiring my decision to attend graduate school. You have always motivated me to aim higher and strive to be better. To my wife, Bao-Kim, who listens to my every frustration and expression of self-doubt, there simply are no words to express my gratitude for your unconditional support, companionship, and love.

Table of Contents

List of Tables

List of Figures

Chapter 2
Self-assembling peptide hydrogels modulate *in vitro* chondrogenesis of bovine bone marrow stromal cells

Chapter 3
Adult equine bone-marrow stromal cells undergo chondrogenesis and produce a cartilage-like ECM superior to animal-matched adult chondrocytes

Chapter 4
Controlled delivery of TGF-β1 from self-assembling peptide hydrogels induces chondrogenesis in bone marrow stromal cells via Smad 2/3 signaling

Appendix

Chapter 1. Introduction

1.1 Cartilage Injury and Disease

The high prevalence of joint injury, subsequent osteoarthritis (OA), and the frequent disability that follows[1-4] highlight the urgency for finding treatments that can repair articular cartilage damage, an irreversible step in disease progression. Recent studies have shown that joint injuries, including partial and full-thickness fractures of the articular cartilage surface, joint derangement, and tears of the meniscus and ligaments, can lead to the early onset of OA. Injuries during adolescence and young adulthood increase the risk of OA more than 2-fold from 6% in uninjured individuals to 13.9% in those with injuries[3]. In addition, radiographic evidence of OA was found in 80% of athletes 14 years after ligament tear injury, irrespective of the treatment received[4].

The degenerative changes of OA present a difficult challenge. Often the disease begins attacking joints long before pain and disability become symptomatic, leading to joint tissue damage[2]. Tissue degradation caused by OA includes weakened muscles and tendons, fissured and torn meniscus, osteophyte formation, inflamed synovium, and fissured, torn and destroyed cartilage[2]. Cartilage degradation is particularly critical as it is the major weight-bearing tissue within the joint and lacks the capacity for self-repair, making damage to it irreversible and resulting in approximately one million joint replacements per annum in the US and Europe combined[2]. Thus, while the development of treatments for OA will undoubtedly have to address the range of pathophysiological

processes involved in the disease[2,5], it is likely that strategies which aim to halt OA progression will require a complementary strategy for cartilage repair and regeneration.

1.2 Cartilage Repair

The need to repair damage motivates the significant effort and resources invested in developing cartilage replacement techniques. Surgical procedures in clinical use for repairing cartilage provide symptomatic relief of joint pain, but result in the formation of predominantly fibrous tissue and fibrocartilage with reduced mechanical properties and limited long-term durability[6]. Microfracture is a minimally invasive procedure consisting of drilling holes in the subchondral bone plate at the defect site, inducing therapeutic bleeding and subsequent clot formation. The resulting repair provides good short-term improvements, but deterioration begins 18 months after surgery[7]. Osteochondral autografting or mosaicplasty is an approach to cartilage defect repair involving transplantation of grafts of cartilage cores with similar characteristics to the surrounding tissue. Significant complications to this procedure exist however, including surface discontinuity, unmatched thickness of donor and recipient cartilage, and weak fibrocartilage grouting. Coupled with the inherent donor-site morbidity, these issues raise significant questions about the long-term benefits for this procedure[6].

Autologous chondrocyte implantation (ACI) is an alternative approach to cartilage repair utilizing *ex vivo* expanded chondrocytes. Cartilage slices are obtained from a minor load-bearing area of the injured joint and chondrocytes are isolated and expanded in the laboratory. These chondrocytes are then injected into the joint in a second surgical procedure in which they are retained in the defect by suturing a periosteal

flap to the surrounding cartilage[8]. Advantages over mosaicplasty include a smaller donor site requirement due to the *ex vivo* expansion of chondrocytes and the flexibility to completely fill irregular defects. However, chondrocytes are known to dedifferentiate and lose the ability to produce cartilage ECM components during monolayer expansion[9]. Furthermore, a direct comparison of ACI with microfracture in a randomized trial showed no significant differences between the two treatments at either two or five years[10,11].

1.3 Cartilage Tissue Engineering

Cartilage tissue engineering has the potential to regenerate mature hyaline cartilage for repair in cases of injury or disease. Consisting of a cell source, a three-dimensional scaffold and the appropriate cues for tissue formation, tissue engineering strategies for cartilage repair were initially based on ACI and utilized autologous chondrocytes seeded into absorbable scaffolds[12]. Further improvements included the use of allogeneic cells, chondro-inductive matrix, and *ex vivo* mechanical stimulation with the goals of homogeneous defect fill, a single-surgery treatment, elimination of suturing, and improved material properties[12]. Despite these efforts, no technique has yet succeeded in generating fully-functional cartilage repair[13].

Recently, bone marrow derived stromal cells (BMSCs) have been isolated and shown to have the capacity to differentiate into many lineages, including bone, adipose, muscle, and cartilage[14,15]. Because bone marrow samples can be harvested via minimally invasive techniques, these cells eliminate the need for two surgical procedures, which were necessary with ACI. These cells have the ability to be expanded rapidly in

monolayer culture and then induced to differentiate into a chondrocyte-like phenotype, either by encapsulating them in three-dimensional culture, administering the appropriate growth factors[16], subjecting them to mechanical loading[17], or a combination of these stimuli. It has been shown that type II collagen hydrogels have the potential to induce and maintain BMSC chondrogenesis[18], especially when stimulated by transforming growth factor β1 (TGF-β1). In addition, through the combined use of insulin-like growth factor I and TGF-β1, it is possible to achieve effective proliferation and chondrogenesis of human BMSCs derived from aged individuals (>50 years old)[19]. Due to the expense of long-term growth factor treatment, there may be significant advantages to delivering these factors via functionalized scaffolds, which sustain signaling via growth factor tethering[20].

Self-assembling peptide hydrogels, a new class of biomaterials, have recently been discovered and been shown to have many applications in biotechnology[21,22]. When used as a 3-D environment for cell-culture, these materials allow for study and manipulation of cells that is not possible *in vivo*[23] and may be used as novel scaffolds for tissue engineering[24]. Injection of cell-free peptides into the myocardium can lead to the recruitment of vascular cells to the resulting microenvironment, and promote the survival of endogenous precursor cells[25]. Self-assembling peptide hydrogels have been applied in cartilage repair strategies, and been shown to stimulate ECM production and cell division in primary chondrocyte-laden constructs for cartilage tissue repair[26]. BMSC-laden peptide constructs achieve significant matrix accumulation and mechanical properties over a six-week time course[27]. In addition, bone-marrow derived BMSCs showed 4-fold higher GAG accumulation and nearly 8-fold higher biosynthesis rates when seeded in

peptide hydrogels as compared to agarose hydrogels[28], suggesting the potential for BMSC chondrogenesis and ECM production when encapsulated in peptide hydrogels.

1.4 Thesis Outline

The objective of this thesis was to advance the use of self-assembling peptide hydrogel scaffolds for cartilage tissue repair by encapsulating BMSCs and incorporating chondrogenic cues to stimulate differentiation and neotissue production.

Studies described in chapter 2 investigated self-assembling peptide hydrogel scaffolds to determine if they provide cues that enhance the chondrogenic differentiation of BMSCs. Sequence specific effects of two different peptide hydrogels, KLD12 $(KLDL)_3$ and RAD16 $(RADA)_4$, on BMSC chondrogenesis were evaluated and compared to a reference system of BMSCs encapsulated in agarose hydrogels.

Studies described in chapter 3 explored the effects of cell type and age on chondrogenic potential by determining the capacity for BMSCs and chondrocytes from young and adult equine donors to produce a cartilage-like ECM. Neotissue biochemical and biomechanical properties are used to characterize chondrogenesis as well as molecular properties of neotissue extracted aggrecan.

In studies described in chapter 4, self-assembling peptide hydrogels were modified to deliver TGF-β1, a prochondrogenic growth factor, to encapsulated BMSCs via biotin-streptavidin tethering and growth factor adsorption. Growth factor retention within acellular peptide hydrogels was characterized and chondrogenesis of BMSCs encapsulated within growth-factor modified peptide was evaluated. TGF-β1 signaling in modified-peptide hydrogels via the Smad 2/3 intracellular pathway was also assessed.

Finally, in Chapter 5 the main findings and conclusions are discussed and new questions motivated by this thesis are explored.

Chapter 2. Self-assembling peptide hydrogels modulate *in vitro* chondrogenesis of bovine bone marrow stromal cells

The objective of this study was to test the hypothesis that self-assembling peptide hydrogel scaffolds provide cues which enhance the chondrogenic differentiation of bone marrow stromal cells (BMSCs). BMSCs were encapsulated within two unique peptide hydrogel sequences and chondrogenesis was compared to that in agarose hydrogels. Unique cell morphologies were observed for BMSCs in each peptide hydrogel sequence, with extensive cell-cell contact present for both, whereas BMSCs in agarose remained rounded over 21 days in culture. Differences in cell morphology within the two peptide scaffolds may be related to sequence-specific cell adhesion. BMSCs in all three hydrogels underwent TGF-β1-mediated chondrogenesis as demonstrated by comparable gene expression and biosynthesis of ECM molecules. Expression of an osteogenic marker was unchanged and an adipogenic marker was suppressed by TGF-β1 in all hydrogels. Cell proliferation occurred only in the peptide hydrogels, not in agarose; resulting in higher glycosaminoglycan content and more spatially uniform proteoglycan and collagen type II deposition. The G1-positive aggrecan produced in peptide hydrogels was predominantly the full-length species, whereas that in agarose appeared to be predominantly the aggrecanase product G1-NITEGE. Taken together, this study showed

self-assembling peptide hydrogels enhance chondrogenesis compared to agarose as shown by ECM production, DNA content and aggrecan molecular structure.

2.1 Introduction

Bone marrow stromal cells (BMSCs) have been widely used as a cell source for tissue-engineering strategies aimed at resurfacing articular cartilage[14,16,29]. Significant progress has been made demonstrating the potential for BMSCs to undergo chondrogenesis and produce a cartilage-like extracellular matrix (ECM) when encapsulated in a variety of three-dimensional scaffolds including agarose[30,31], alginate[32], collagen type I[33,34], gelatin/albumin[35], and silk-elastin[36], but challenges in the use of BMSCs in the repair of cartilage defects still remain[13,37]. Improvements in BMSC chondrogenesis and eventual clinical use appear to require optimization of many factors. Among these is the current belief that the scaffold must provide the appropriate cell microenvironment and differentiation cues[38]. An ideal cartilage tissue engineering scaffold should be biocompatible, allow for cell adhesion, migration, and proliferation, and have sufficient porosity and hydration to permit nutrient and waste product flow. It should also stimulate production of an *in vivo*-like cartilage matrix with the appropriate cell-dependent turnover pathways. Finally it should be able to fill irregular defects, integrate effectively with the native recipient tissue, and degrade with the appropriate resorption kinetics[13,38].

Self-assembling peptides are a relatively new class of molecules that have the capacity to form stable hydrogels and encapsulate viable cells for potential therapeutic applications[22,39,40]. One type of these peptides consists of short oligomers of alternating

hydrophilic and hydrophobic residues that trigger self-assembly upon exposure to physiologic pH and ionic strength[22]. These peptides are completely synthetic, which avoids the potential pathogenicity of animal-derived materials[24] and because of their rapid self-assembly, they are useful for cell encapsulation in both *in vitro* and *in vivo* applications. Various sequences have been used as tissue engineering scaffolds including KLD12 ($[KLDL]_3$) for cartilage[26], RAD16-I ($[RADA]_4$) for cartilage[41] and liver[42,43], and RAD16-II ($[RARADADA]_2$) for cardiovascular[20] tissue repair. In addition, a recent study has shown that equine BMSCs encapsulated in KLD12 peptide hydrogels can undergo *in vitro* chondrogenesis[28].

A successful cartilage repair therapy ultimately must generate a tissue with comparable ECM biochemistry and biomechanics to native tissue. Also, it will likely require that cues are provided to guide the BMSCs to closely mimic the temporal sequence of genetic, biochemical, and biophysical events in native chondrogenesis[44,45]. It is thus important that a detailed analysis of chondrogenesis for any cell-based therapy be performed *in vitro* as an assessment of its potential repair capacity *in vivo*. Measurements include chondrogenic gene expression at initial and subsequent timepoints[46], characterization of early time-dependent changes in cell morphology[33], quantification of cell content[32], production and analysis of secreted ECM components[31,47], and assessment of both anabolic and catabolic ECM processing[48]. Previous reports have used these analytical techniques to demonstrate how altering the cell microenvironment impacts BMSC chondrogenesis and neo-tissue formation[32,46,49].

The objective of this study was to evaluate whether two different peptide hydrogels, KLD12 and RAD16-I, provided sequence-specific cues which enhanced

transforming growth factor-β1 (TGF-β1) stimulated chondrogenesis of BMSCs as compared to agarose hydrogel culture. Agarose was chosen as a reference because of its extensive use to study chondrocyte biology in three-dimensional culture[9,50,51] and to evaluate progenitor cell differentiation[28,30,41,48]. Real-time RT-PCR was used to quantitatively assess expression of genes important for differentiation and ECM production. Neo-tissue cell content was measured by construct DNA content. The synthesis rate and accumulation of newly secreted ECM were also assessed biochemically. Changes in cytoskeleton morphology were characterized via F-actin imaging, and immunohistochemistry and immunoblotting were used to determine the type of ECM molecules and catabolic products. Time-points for this study were chosen from 1-21 days of culture with the goal of understanding how peptide sequence impacts the initial stages of chondrogenesis.

2.2 Materials and Methods

Materials

Low-melting-point agarose was from Invitrogen, (Carlsbad, CA). KLD12 peptide with the sequence AcN-$(KLDL)_3$-CNH_2 was synthesized by the MIT Biopolymers Laboratory (Cambridge, MA) using an ABI Model 433A peptide synthesizer with FMOC protection. RAD16-I peptide with the sequence $(RADA)_4$ was a gift of Puramatrix from 3DM, Inc. (Cambridge, MA). All other materials were purchased from the suppliers noted below.

Cell isolation and expansion

BMSCs were isolated as described previously[31]. Briefly, bone marrow was harvested aseptically from three newborn bovine calves (Research 87, Marlborough, MA). Following centrifugation at 1000g for 15 min, the cell pellet was washed in PBS and plated at $1x10^6$ mononuclear cells/cm^2 in expansion medium (EM) consisting of low glucose DMEM plus 10% ES-FBS (Invitrogen), HEPES, and PSA (100 U/mL penicillin, 100 μg/mL streptomycin, and 250 ng/mL amphotericin) plus 1 ng/mL bFGF (R&D Systems, Minneapolis, MN). Non-adherent cells were removed by a medium change after 48 hours, and colonies were harvested with 0.05% trypsin/1mM EDTA (Invitrogen) after approximately 7 days (passage 0) and cryopreserved. Six days prior to peptide hydrogel encapsulation, cells were thawed and plated at $6x10^3$/cm^2 in EM plus 5 ng/mL bFGF. After 3 days, cells were detached at ~$3x10^4$ cells/cm^2 (passage 1) and reseeded at $6x10^3$/cm^2. This expansion was repeated during the subsequent 3 days after which cells were detached for encapsulation in 3D peptide hydrogels.

Hydrogel Encapsulation and Culture

BMSCs were encapsulated in either 2% (w/v) low-melting point agarose, 0.35% (w/v) KLD12 peptide, or 0.5% (w/v) RAD16-I peptide at a concentration of 10^7 cells/mL. The different concentrations for the self-assembling peptides were chosen so that initially the hydrogels would have similar mechanical characteristics[52,53], and 2% agarose was selected for comparison with previously published studies[30,31,41,48]. Hydrogel disks with 50μL initial volume were cast in neutral-buffered, acellular agarose molds to initiate self assembly (Fig. 2.1) and cultured in high glucose DMEM (Invitrogen) supplemented with 1% ITS+1 (Sigma-Aldrich, St. Louis, MO), 0.1 μM dexamethasone (Sigma-Aldrich),

37.5 μg/mL ascorbate-2-phosphate (Wako Chemicals, Richmond, VA), PSA, HEPES, Proline, and NEAA, with (+TGF-β1) or without (Cntl) 10 ng/mL recombinant human TGF-β1 (R&D Systems), with medium changes every 2-3 days.

Histology and Immunohistochemistry

Hydrogels were fixed in 10% neutral-buffered formalin overnight at 4°C. For F-actin staining, 3D hydrogel samples were sliced to ~700 μm thick, and permeabilized in PBS with 0.1% Triton-X at room temperature for 1 hour. Samples were washed 2-3 times with PBS and stained for 1 hour at room temperature with Texas Red conjugated phalloidin to show F-actin fibers and Hoechst dye to visualize cell nuclei. Samples were washed 2-3 times with PBS and imaged with a Nikon Eclipse fluorescent microscope or with a Zeiss LSM510 confocal microscope. For ECM staining, formalin fixed hydrogels were embedded in paraffin and sliced to 7 μm using a sledge-microtome (Leitz, Wetzlar, Germany). Sections were deparaffinized, treated with 0.1% pepsin for 30 minutes, rinsed with TBS, treated with 0.6% H_2O_2 in methanol, and rinsed again with TBS. Samples were then treated with either mouse anti-collagen type II IgG (Clone CII C1, DSHB, 1:1000 in TBS) or mouse anti-collagen type I IgG (Sigma, diluted 1:1000 in TBS) for 1 hour[54]. After incubation with rabbit anti-mouse IgG (horseradish peroxidase [HRP] conjugated, diluted 1:200 in TBS containing 1% bovine serum; Dako-P0260) for 30 min, the sections were rinsed and incubated for 30 min with goat anti-rabbit IgG (HRP conjugated, diluted 1:100 in TBS containing 1% bovine serum; Dako-P0448). Samples were stained with diaminobenzidine (DAB kit; Vector Laboratories, Burlingame, CA), and cell nuclei were counterstained with Mayer's hemalum. Finally, stained samples

were embedded on microscope slides, using Aquatex (Merck KGaA, Darmstadt, Germany). Additional sections were stained for proteoglycans using toluidine-blue dye solution (0.0714% toluidine blue, Merck; 0.0714% pyronin Y, Fluka; and borax [0.143% di-sodium-tetra-borate], Merck) for 6 minutes as previously described[26]. For cell adhesion and spread area analyses, soluble KLD12 or RAD16-I (500 μg/mL in tissue culture water) were incubated overnight at 37°C in non-treated polystyrene culture plates. Plates were washed thoroughly with water and then incubated for at least 1 hour with the ITS+ media described above. BMSCs at $1.2x10^4$ cells/cm^2 were cultured for 2 hours in TGF-β1-containing medium before being fixed and processed for cytoskeletal imaging as described above. Five random fields were imaged using a Nikon Eclipse fluorescent microscope, and the cell area and number of cells per field were measured with the Matlab Image Processing Toolbox (The MathWorks, Natick, MA).

Real-time Reverse-transcription Polymerase Chain Reaction

RNA was extracted as described previously[55]. BMSC-seeded hydrogel disks were flash frozen in liquid nitrogen, pulverized, and homogenized in TRIzol reagent (Invitrogen). RNA was extracted using an RNeasy Mini Kit (Qiagen, Valencia, CA) and quantified using a Nanodrop 1000 Spectrophotometer (Agilent Technologies, Santa Clara, CA). Absorbance measurements at 260 nm were used to determine the RNA concentration, and 1 μg of each sample was reverse transcribed using the AmpliTaq-Gold Reverse Transcription Kit (Applied Biosystems, Foster City CA). Real-time RT-PCR was performed using the Applied Biosystems 7900HT and SYBR Green Master Mix (Applied Biosystems). Expression of type I collagen, type II collagen, aggrecan, SOX9,

osteocalcin, PPAR-γ, and 18S were quantified using previously published primer sequences[32,55,56]. For each timepoint and hydrogel sample, gene expression levels were first normalized by the corresponding 18S level for that sample, and then normalized by levels expressed by BMSC samples taken immediately prior to hydrogel encapsulation (Day 0)[57].

Biochemistry

During the final 24 hours of culture at each timepoint, medium was additionally supplemented with 5 μCi/mL of ^{35}S-sulfate and 10 μCi/mL of ^{3}H-proline to measure cellular biosynthesis of proteoglycans and proteins, respectively. Upon completion of culture, four 30-minute rinses in excess non-labeled sulfate and proline were performed for all samples to wash out free radiolabel. Hydrogels were then weighed wet, lyophilized, and weighed dry. Samples were digested in 0.25 mg/mL proteinase-K (Roche Applied Science, Indianapolis, IN) overnight at 60°C. Digested samples were assayed for total retained sulfated glycosaminoglycan (sGAG) content by DMMB dye binding assay[58], DNA content by Hoechst dye binding[59], and radiolabel incorporation with a liquid scintillation counter. Conditioned culture medium collected throughout the study was also analyzed for sGAG content by DMMB dye binding.

Aggrecan Extraction and Western Analysis

Aggrecan was extracted from hydrogel disks and analyzed as described previously[60]. Hydrogel disks were saturated with PBS and Complete Protease Inhibitors (Roche) and frozen at -20°C until extraction. Gels were extracted for 48 hours in 4M

guanidinium hydrochloride, deglycosylated, and the resulting digest was lyophilized. Samples were reconstituted and 20 μg sGAG/lane was run on a 4-15% Tris-HCl gel at 100V for 1 hour. Proteins were transferred to a nitrocellulose membrane and probed with affinity-purified antibodies for aggrecan G1 domain (JSCATEG)[60].

Statistical analysis

DNA and sGAG content, and proteoglycan and protein biosynthesis, were reported as mean ± SEM with four samples from each of three animals (n=12). RT-PCR results are reported as mean ± SEM using pooled samples from n=3 animals. All data were log-transformed to ensure normality and analyzed by multi-factor ANOVA (with animal as a random factor) and *post hoc* Tukey tests with significance set at $p<0.05$.

2.3 Results

Cell and Actin Morphology

Spherical, isolated, uniformly seeded cells were observed in all three scaffolds immediately after casting on day 0 (Fig. 2.2A) in both medium conditions (+TGF-β1 and Cntl). By day 4 in TGF-β1-supplemented medium, distinct morphologies were apparent in each of the hydrogels (Fig. 2.2B). Cell-cell contact appeared to be a feature for both peptide hydrogels with a spread, networked morphology in RAD16-I peptide and a clustered morphology in KLD12 peptide. In control medium, cell spreading and apparent cell-cell contact were observed in both peptide hydrogels, similar to but less extensive than the respective +TGF-β1 conditions (not shown). At day 4, cells in agarose in both medium conditions maintained the same spherical, isolated morphology as at day 0,

suggesting that these cells did not reorganize their actin cytoskeleton (Fig. 2.2B). Despite these early differences, cells in all three hydrogels cultured with TGF-β1 had a more chondrocyte-like rounded morphology by day 21 (Fig. 2.2C), showing that the apparent cell-cell contact seen at day 4 in peptide hydrogels was a temporary feature. Using confocal microscopy, this predominantly-rounded cell morphology was confirmed for all three scaffolds at day 21 (Fig. 2.2D). To investigate the differences in BMSC morphology in RAD16-I and KLD12 hydrogel culture further, BMSCs were seeded on polystyrene surfaces with adsorbed RAD16-I or KLD12 peptide monomers. After two hours, cells attached and spread to a significantly greater degree on RAD16-I surfaces than KLD12 (Fig. 2.3A). Quantitative image analysis showed greater numbers of attaching cells per field, and more than double the area per cell, on RAD16-I peptide than on KLD12 surfaces (Fig. 2.3B).

Chondrogenic, Osteogenic, and Adipogenic Gene Expression

Evidence that chondrogenesis occurred in all three hydrogels was provided by the upregulation of three cartilage-associated genes, type II collagen, aggrecan, and SOX-9 (Fig. 2.4B-D). As expected, TGF-β1-supplementation stimulated >100-fold upregulation of type II collagen and >1000-fold upregulation of aggrecan by day 4, with maximum upregulation at day 9 of >1000-fold and nearly 10,000-fold for type II collagen and aggrecan, respectively. In contrast, type I collagen, which is expressed by undifferentiated BMSCs and early in chondrogenesis[45], was upregulated just 10-fold by day 4 with no further significant upregulation detected (Fig. 2.4A). Upregulation of type II collagen and aggrecan also occurred in control medium, but the magnitude was 10 to

100-fold lower than with TGF-β1 (Figs. 2.4B & 2.4C). No upregulation of type I collagen or SOX-9 was seen in control medium. In all cases, these data showed no differences among the scaffolds, resulting in a similar overall gene expression pattern.

Neither osteogenic nor adipogenic gene expression was observed in any of the scaffolds. No significant differences were seen among scaffolds or medium conditions for osteocalcin, a marker for osteogenesis. At day 1, osteocalcin was downregulated by nearly 4-fold (Fig. 2.4E), but returned to baseline on days 4 through 9, and finally dropped again on day 14 to an average of 3-fold below day 0 levels. PPAR-γ expression, a marker for adipogenesis, was upregulated in control medium at days 4, 7, 9, and 14 by ~5-fold in all three scaffolds (Fig. 2.4F); however, the addition of TGF-β1 reduced its expression to nearly baseline levels at all timepoints.

Hydrogel DNA Content, sGAG Content, and ECM Biosynthesis

Increases in DNA content were stimulated by TGF-β1-supplemented medium for both peptide hydrogels, but not in agarose, throughout the entire culture period (Fig. 2.5A, $p<0.05$). This resulted in significantly higher DNA content for RAD16-I peptide than for agarose at all timepoints ($p<0.001$) and higher DNA content for KLD12 than for agarose cultures at days 14 and 21 ($p<0.001$). In addition, DNA content increased with time for both RAD16-I and KLD12 disks cultured in TGF-β1 supplemented medium resulting in significantly higher DNA content at day 21 vs. day 7 ($p<0.001$).

TGF-β1 also stimulated a ~5-fold increase in sGAG content of all scaffolds at day 7 (Fig. 2.5B, $p<0.001$) and a >10-fold increase at days 14 and 21 ($p<0.001$) relative to controls. sGAG content increased with time for all three hydrogels through day 14

($p<0.001$). However, sGAG content only increased from day 14 to day 21 for the RAD16-I and KLD12 peptide hydrogels ($p<0.001$) resulting in nearly 2-fold higher sGAG content for both peptides compared to agarose ($p<0.005$). The percentage of sGAG retained in agarose hydrogels decreased with time in culture and was lower compared to RAD16-I or KLD12 peptides at day 21 (Table 1, $p<0.001$). In contrast, both RAD16-I and KLD12 peptides maintained constant sGAG retention throughout the culture period (Table 1) with modestly higher retention levels for RAD16-I peptide compared to KLD12 ($p<0.05$).

Protein biosynthesis rates normalized to DNA content were 4-9 fold higher with TGF-β1 supplementation throughout the entire culture period (Fig. 2.5C, $p<0.001$), and decreased with time by a factor of 2-3 for day 21 vs. day 7 in all three hydrogels ($p<0.005$). No differences in protein biosynthesis were seen among the three hydrogels. TGF-β1 stimulated 2-10 fold higher ^{35}S-proteoglycan biosynthesis rates at all timepoints in all three hydrogels (Fig. 2.5D, $p<0.01$). Surprisingly (given the higher final sGAG content of the peptide hydrogels), ^{35}S-proteoglycan biosynthesis, on a per-DNA basis, was 3-fold higher for agarose than for RAD16-I peptide ($p<0.001$). However, proteoglycan biosynthesis increased in RAD16-I peptide by day 14 ($p<0.05$) (when proliferation had essentially stopped) and no significant differences were seen among the three hydrogels in TGF-β1-supplemented medium at days 14 or 21.

Hydrogel Wet Weights and Contraction

Both peptide hydrogels contracted 50%-60% within the first week of culture in the presence of TGF-β1 as assessed by changes in wet mass (Fig. 2.5E). No further

contraction was observed after one week. In control medium, contraction of both peptide hydrogels was 30%-45% in the first week with no further contraction at later timepoints. No contraction was observed in agarose hydrogels in either medium condition.

Hydrogel Histology - Accumulation of Proteoglycans and Collagen Types I and II

Spatially uniform, metachromatic staining for the presence of sGAG was observed throughout both RAD16-I and KLD12 peptide hydrogels by day 21; in agarose, however, staining was largely confined to the immediate pericellular matrix (Fig. 2.6A). Positive type II collagen staining was also more intense and uniformly distributed throughout the RAD16-I and KLD12 peptide hydrogels than in the agarose, where again it was mainly in the pericellular matrix (Fig. 2.6B). Less intense non-uniform type I collagen staining was also visible in both peptide hydrogels, primarily in cell-associated regions whereas little or no staining was seen in agarose hydrogels (Fig. 2.6C).

Aggrecan Western Blot

GuHCl extracts from all three hydrogels revealed the presence of a large macromolecular species as detected by anti-G1 aggrecan Western blotting, running at the molecular weight of full length aggrecan (Fig. 2.7). In both RAD16-I and KLD12 hydrogels, this full length aggrecan was the predominant species detected, while in agarose hydrogels a doublet-band near 65 kDa was the major immunoreactive product detected. This is consistent with the virtual absence of aggrecanase activity in the peptide gels in contrast to a high level in the agarose. Since the agarose nonetheless accumulated quite high levels of GAG, it appears that it accumulates the CS-rich catabolic product of

aggrecanase activity cleaving the interglobular domain and resulting in the formation of abundant G1-NITEGE. This product is normally lost from cartilage explants[61].

2.4 Discussion

The capacity for self-assembling peptide hydrogels to support and enhance chondrogenesis of 3D-encapsulated BMSCs was compared to that in agarose hydrogel culture. Both the DNA content and the accumulation of a cartilage-like ECM were higher for TGF-β1-stimulated BMSCs in RAD16-I and KLD12 hydrogels than in agarose. Due to contraction of both peptide hydrogels, but not agarose, normalization of data to wet mass (Fig. 2.5) would exaggerate the higher DNA content and ECM accumulation for peptide hydrogels. Thus, the motivation for presenting the data on a per-hydrogel sample basis was to allow for a direct comparison of the neo-tissue construct in each hydrogel given an equal initial cell content and hydrogel size. The results are consequently consistent with a recent report where wet mass-normalized KLD12 peptide hydrogels had higher sGAG content than agarose hydrogels[28], but are in contrast with the findings of Erickson[41] which report higher sGAG content in agarose than in RAD16-I hydrogels.

No significant differences in DNA-normalized protein and proteoglycan biosynthesis rates were observed for any of the three hydrogels in the presence of TGF-β1 (with the exception of ^{35}S-sulfate incorporation at day 7), however both DNA and sGAG content were higher for RAD16-I and KLD12 than for agarose. Thus, by presenting proteoglycan synthesis rates on a per-DNA basis, we have shown similar biosynthesis rates in both peptides and agarose. The finding that the biosynthetic rates were similar but the sGAG content was lower in agarose can probably be explained by

the lower cell content in agarose, the lower sGAG retention in agarose, or the presence of an intrinsic endocytotic removal mechanism for aggrecan sGAG in the agarose system especially.

The three distinct cytoskeletal morphologies observed during the first week of culture suggest that unique biophysical signals are generated in each hydrogel. The mechanisms responsible for these differing cell morphologies are not known but may include the state of differentiation of the cells, the scaffold mechanical stiffness and cell-scaffold adhesion[44]. For example, the equilibrium modulus of 2% agarose is ~10 kPa[50,51] which is approximately 10-fold higher than RAD16-I (~1 kPa storage modulus)[53], while RAD16-I and KLD12 have stiffness values within 25% of each other[52]. The stiffer agarose thus likely confines cells to a spherical morphology and prevents cell mediated hydrogel contraction, consistent with recent reports where BMSC-seeded agarose maintained nearly constant volume and did not contract during long term culture[30,41]. Since the stiffness of RAD16-I and KLD12 are similar, differences in cell-scaffold adhesion/cell differentiation are likely more important for explaining the differences between the network of cell-cell contacts observed in RAD16-I and the multi-cell clusters in KLD12. To investigate this possibility, BMSCs were seeded onto 2D peptide-coated surfaces. More cells-per-field and greater spread-area per cell were observed for BMSCs on RAD16-I than on KLD12 during 2-hour adhesion experiments (Fig. 2.3). A recent report on HUVEC adhesion and spreading on RAD16-I and KLD12 hydrogels[53] also showed more cells attaching and greater spreading per cell when seeded on RAD16-I compared to KLD12 hydrogels. These differences in adhesion are consistent with the 3D scaffold effects observed here, where more intimate cell-scaffold contact created by the

network morphology in RAD16-I may be due to greater cell-scaffold adhesion, while cell clusters in KLD12 may result from weaker cell-scaffold interactions.

Two features seen in common to both peptides, but not agarose, were hydrogel contraction and extensive cell-cell contact. In a recent review of biophysical signals in pre-natal chondrogenic condensations, Knothe Tate *et al*.[44] reported that increasing cell density and cell-cell contact stimulates mitotic activity. Furthermore, the formation of cell condensations amplifies the number of cells which subsequently undergo overt chondrogenesis[62,63]. Thus, greater cell proliferation in both RAD16-I and KLD12 peptide hydrogels compared to agarose, as evidenced by higher DNA content, may be stimulated by cell-cell contact and the increased cell density generated by contraction of the peptide scaffolds. Interestingly, a similar effect of contraction-stimulated mitotic activity was observed for chondrocytes seeded in a collagen-GAG scaffold[64], although in this system, blocking contraction resulted in higher proteoglycan biosynthesis[64,65]. This contrasts with our current study, and may be a result of lower chondrogenic capacity of monolayer-expanded chondrocytes compared to BMSCs. Given the importance of biophysical signals in chondrogenesis[44], differences between the spread-network (RAD16-I) and clustered (KLD12) morphologies observed here (Fig. 2.2) may have important consequences for the final cell phenotype and neo-tissue composition produced in each peptide hydrogel, motivating more detailed studies of these differences.

Two major chondrogenic ECM genes, type II collagen and aggrecan, were upregulated by over three orders of magnitude in all three hydrogels in the presence of TGF-β1 (Fig. 2.4). Consistent with recent reports on chondrogenesis of BMSCs in pellet[66,67], agarose[31,68], PEG[46], and alginate[18,32] culture, the sharpest increases in mRNA

transcript levels for type II collagen and aggrecan occurred during the first 3-7 days in culture, and transcript levels were nearly flat during the second week of culture (Fig. 2.4). Type I collagen, an important ECM molecule during early chondrogenesis in the developing limb bud[44,45], was upregulated at day 4 with TGF-β1, but by substantially less than either type II collagen or aggrecan. SOX9 transcript levels were an order of magnitude higher with TGF-β1 by day 7, also consistent with recent reports in alginate[32,46]. Markers for osteogenesis (osteocalcin) and adipogenesis (PPAR-γ) were unchanged from their day 0 undifferentiated values in the presence of TGF-β1, demonstrating specific chondrogenic differentiation. Given that changes in cell morphology, hydrogel contraction, and the resulting cell-cell contacts occurred in peptide hydrogels during the first week of culture, and that concomitant upregulation of chondrogenic genes occurred in both agarose and peptide hydrogels during the first week, it is likely that critical cell differentiation decisions occur within the first few days after BMSC encapsulation in 3-D culture and exposure to TGF-β1. While no gene expression differences were measured between peptide and agarose hydrogels during this time, it is possible that the chondrogenic program can be easily modulated early in culture, suggesting further, detailed study of this phase of chondrogenesis.

sGAG retention in agarose hydrogels dropped dramatically in the final week of culture but was maintained in both peptides. This is in contrast to sGAG release from chondrocyte-seeded agarose cultures, which is constant over time[50], but consistent with our results showing no additional accumulation of sGAG in agarose in the final week. sGAG accumulation in both peptide hydrogels, however, significantly increased during this time. Thus, while BMSCs in agarose and peptide hydrogels had similar DNA-

normalized proteoglycan synthesis rates, the sGAG produced in agarose cultures was preferentially lost to the medium while that in peptide cultures was retained. This was confirmed by toluidine blue staining which indicated much higher negative charge content in the peptide gels compared to agarose cultures. The potential mechanisms for these differences in sGAG retention may be catabolic (i.e., the action of proteases cleaving aggrecan and thereby increasing release of sGAG) or anti-anabolic (i.e., the relative lack of production of ECM components necessary for aggrecan-sGAG retention such as link protein and/or hyaluronan, or the lower ECM density in agarose due to contraction differences). To further understand the relative importance of these contrasting mechanisms, Western analysis with anti-G1 aggrecan antiserum was performed on hydrogel protein extracts (Fig. 2.6). Results showed a doublet at ~65 kDa in the agarose hydrogels samples only, consistent with aggrecanase-generated NITEGE-neoepitope containing fragments[61]. Thus, an apparent high level of catabolic enzyme activity may have led to decreased sGAG retention in agarose, suggesting an important difference between the chondrogenic programs executed in agarose and peptide hydrogels.

2.5 Summary

The importance of scaffold design in promoting chondrogenesis of BMSCs for cartilage tissue engineering has been demonstrated through differences in ECM protein production, retention, and cell morphology. Peptide hydrogels enhanced early chondrogenesis compared to agarose, and unique signals generated by each peptide sequence subtly altered the chondrogenic differentiation program. In addition to the

importance of scaffold-generated, biophysical signals, TGF-β1 was a critical biochemical signal necessary to promote chondrogenesis. By further optimizing self-assembling peptide hydrogels, it may be possible to incorporate biochemical signals into the scaffold[20]. Self-assembling peptide hydrogels thus have the potential to incorporate both the appropriate biophysical and biochemical chondrogenic stimuli, making them a promising candidate for use in a clinically-feasible, cartilage repair therapy.

2.6 Acknowledgements

Thank you to Eric Vanderploeg for assistance with study design and protocol development. Thank you to Hsu-Yi Lee for performing the quantitative image analysis of 2D BMSC morphology, Bodo Kurz for performing the proteoglycan histology and collagen immunohistochemistry, and John Sandy for providing the α-G1 aggrecan antibody. Finally, thank you to Alan Grodzinsky for his scientific insight and leadership.

This work was funded by the National Institutes of Health (NIH EB003805), a National Institutes of Health Molecular, Cell, and Tissue Biomechanics Training Grant Fellowship (P.W.K.), and an Arthritis Foundation Postdoctoral Fellowship (E.J.V.).

2.7 Tables

Table 2.1 Percent sGAG Retained in Hydrogels Cultured with TGF-β1
(mean±sem; ^{D7}, ^{D14}, ^{A}, ^{R}, vs. Day 7, Day 14, Agarose, and RAD, respectively, $p<0.05$)

	Day 7	**Day 14**	**Day 21**
Agarose	62±3	59±2	$44\pm3^{D7,D14}$
RAD16-I	80 ± 4^{A}	74 ± 1^{A}	73 ± 1^{A}
KLD12	57 ± 4^{R}	60 ± 4^{R}	$59\pm5^{A,R}$

2.8 Figures

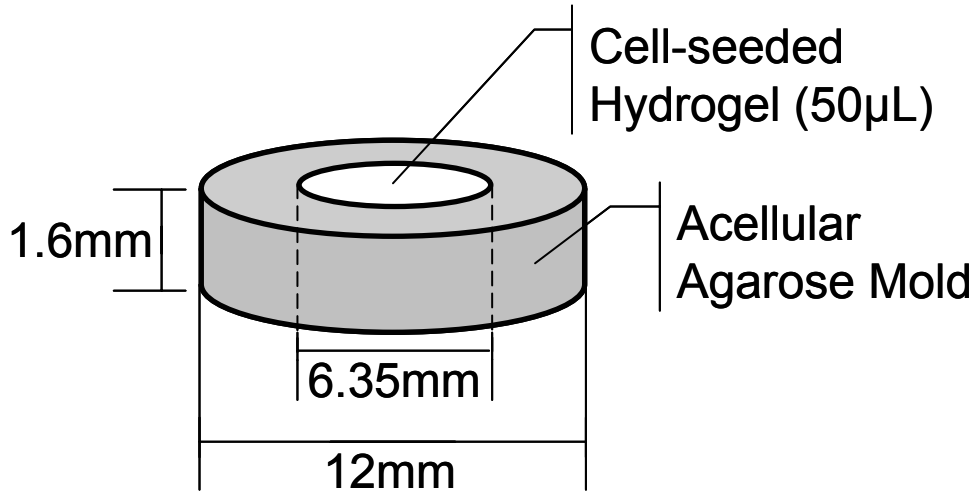

Figure 2.1 Cell-encapsulation and self-assembly mold.
The acelluar-agarose annulus mold is made by injecting 2% agarose into a custom, autoclavable frame. 50µL of cell-hydrogel suspension (BMSCs in RAD16-I, KLD12, or agarose) is then injected into the center to initiate self assembly.

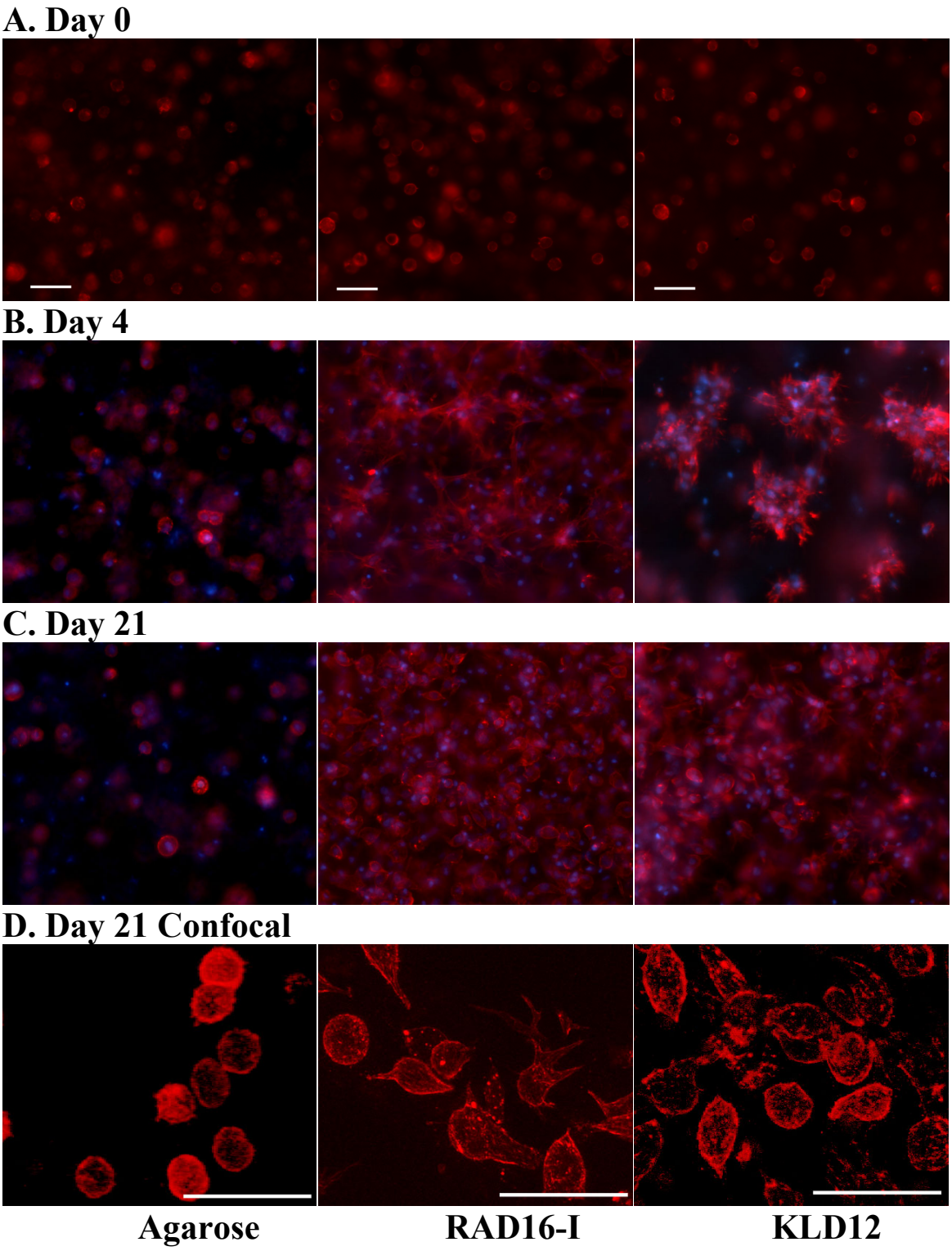

Figure 2.2 BMSC F-actin Morphology in 3D Agarose, RAD16-I, and KLD12
Representative 3D F-actin morphology images for BMSCs cultured with TGF-β1 supplementation and encapsulated in agarose (left column), RAD16-I (center column) and KLD12 (right column). Culture duration was **(A)** 0 days, **(B)** 4 days, or **(C)** 21 days. **(D)** High

magnification, confocal images at day 21. Red indicates F-actin, blue indicates cell nuclei. Scale bar in (A) is applicable to (B) & (C), in all cases scale bar=50µm.

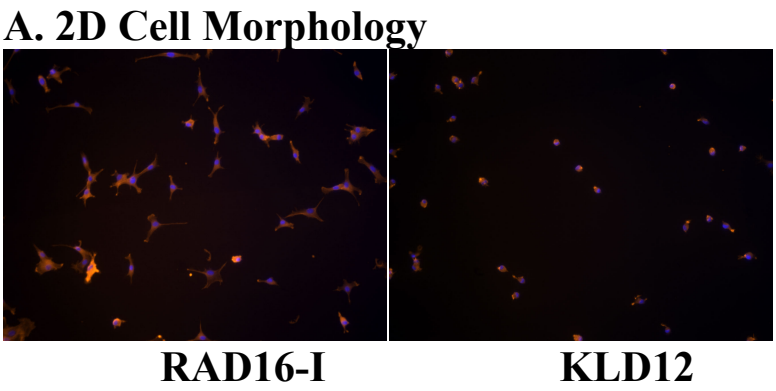

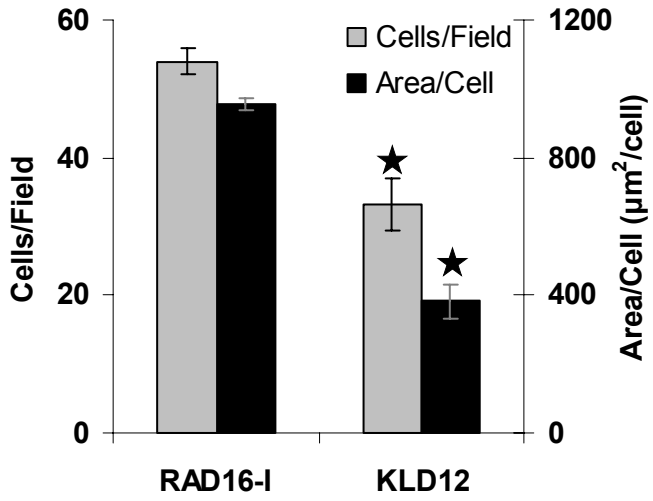

Figure 2.3 BMSC F-actin morphology on 2D RAD16-I & KLD12 Surfaces
(A) Representative 2D F-actin morphology for BMSCs seeded onto RAD16-I (left) and KLD12 (right) surfaces for 2 hours. Red indicates F-actin, blue indicates cell nuclei. **(B)** Quantification of 2D images, n=5 fields, field area = 5.61 x 10^{-3} cm^2, ★ vs. RAD16-I, $p<0.01$.

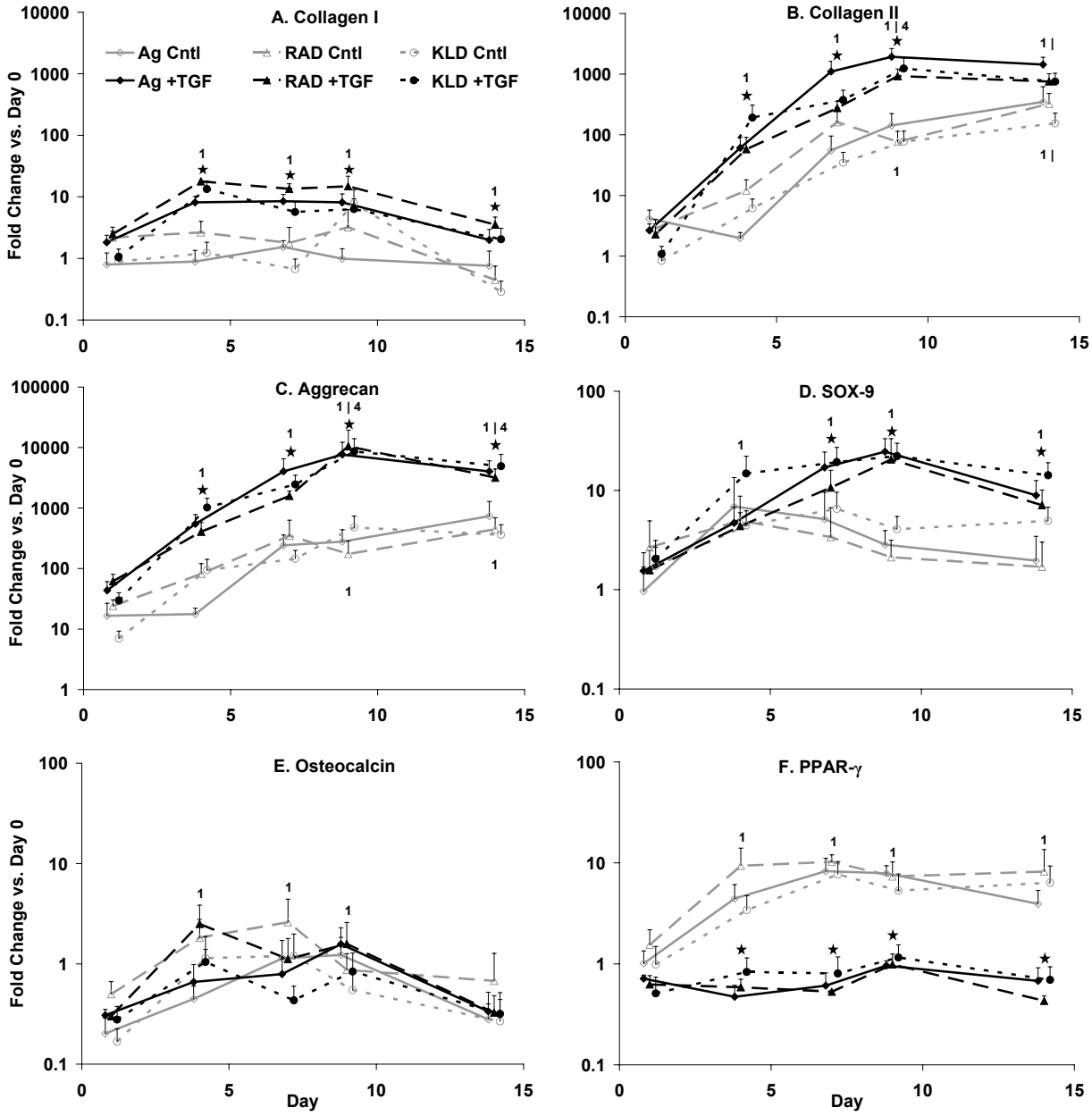

Figure 2.4 Gene expression of 3D-encapsulated relative to monolayer BMSCs
Cultured in control **(Cntl**) or TGF-β1 supplemented **(+TGF)** medium and encapsulated in agarose **(Ag)**, RAD16-I **(RAD)**, or KLD12 **(KLD)**. All scaffolds measured at the same timepoints, but offset for readability. **Stats:** mean±sem; n=3 animals; ★ vs. Cntl medium; **1** or **4** vs. day 1 or day 4, respectively; $p<0.05$.

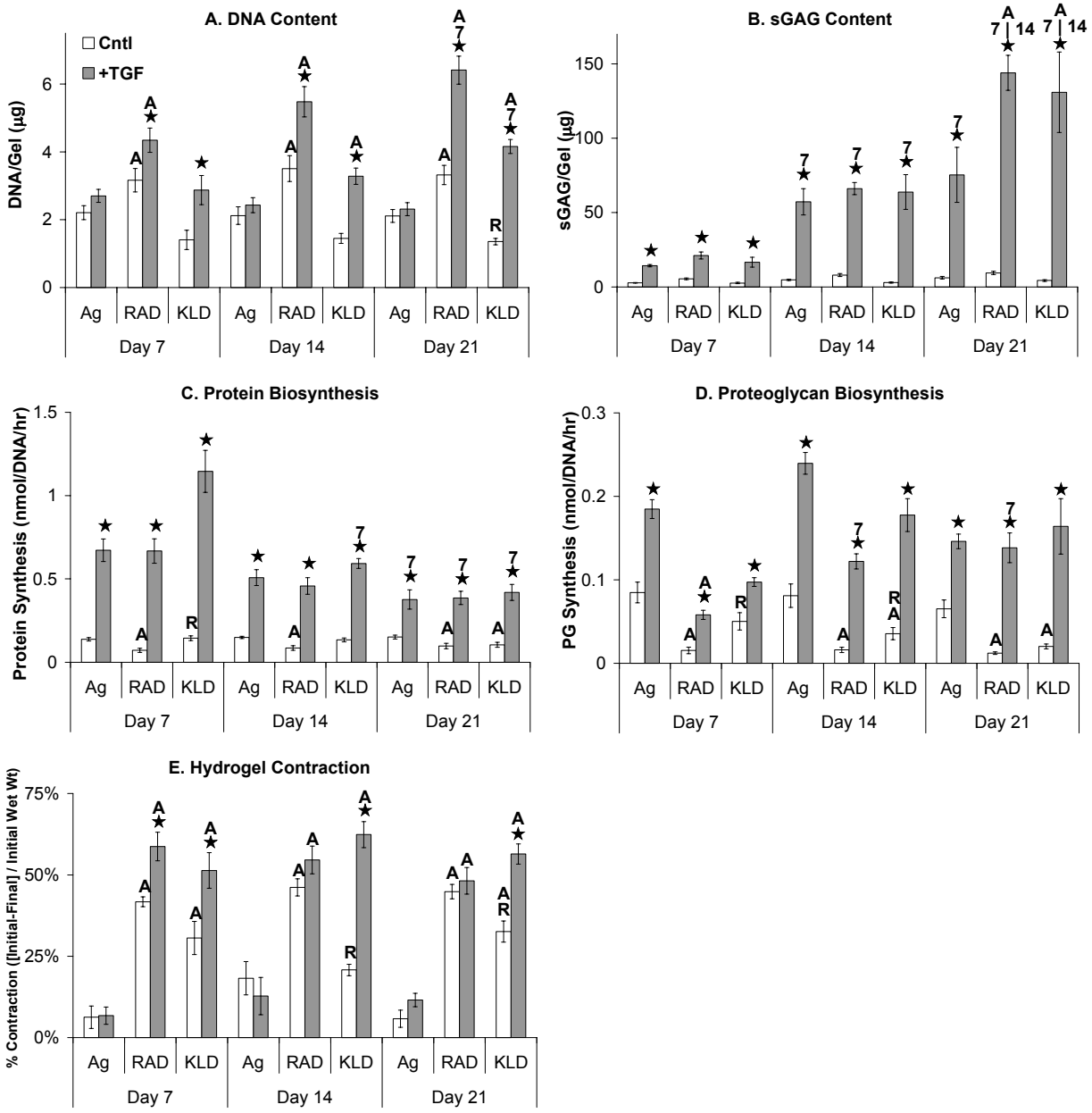

Figure 2.5 Hydrogel Biochemistry and ECM Biosynthesis Rates
Cultured in control **(Cntl**) or TGF-β1 supplemented **(+TGF)** medium and encapsulated in agarose **(Ag)**, RAD16-I **(RAD)**, or KLD12 **(KLD)**. **(A)** DNA Content, **(B)** sGAG Content, **(C)** Protein Biosythesis, **(D)** Proteoglycan Synthesis. **Stats:** mean±sem; n=12 (4 gels x 3 animals); ★ vs. Cntl medium; **7** or **14** vs. day 7 or day 14, respectively; **A** or **R** vs. Agarose or RAD16-I, respectively; $p<0.05$.

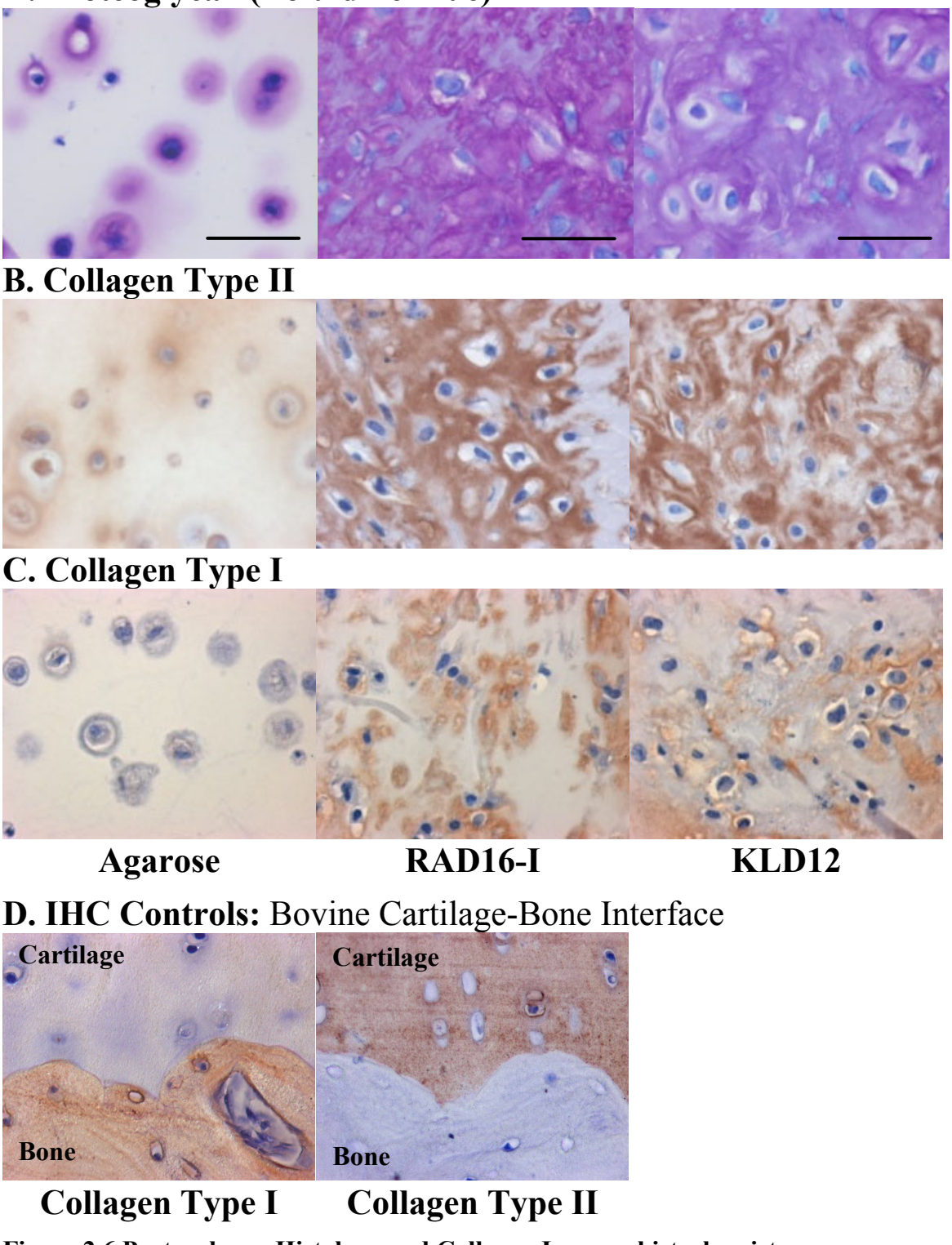

Figure 2.6 Proteoglycan Histology and Collagen Immunohistochemistry
(A) Representative toluidine blue staining for sGAG, and **(B)** collagen type II and **(C)** Type I immunohistochemistry images for BMSCs cultured with TGF-β1 supplementation in agarose (left column), RAD16-I (center column) and KLD12 (right column). (See Methods for details.)

Culture duration was 21 days. **(D)** Collagen I & II immunohistochemistry in bovine cartilage-bone plugs as controls. Scale bar in (A) is applicable to (B), (C), & (D), in all cases scale bar=50μm.

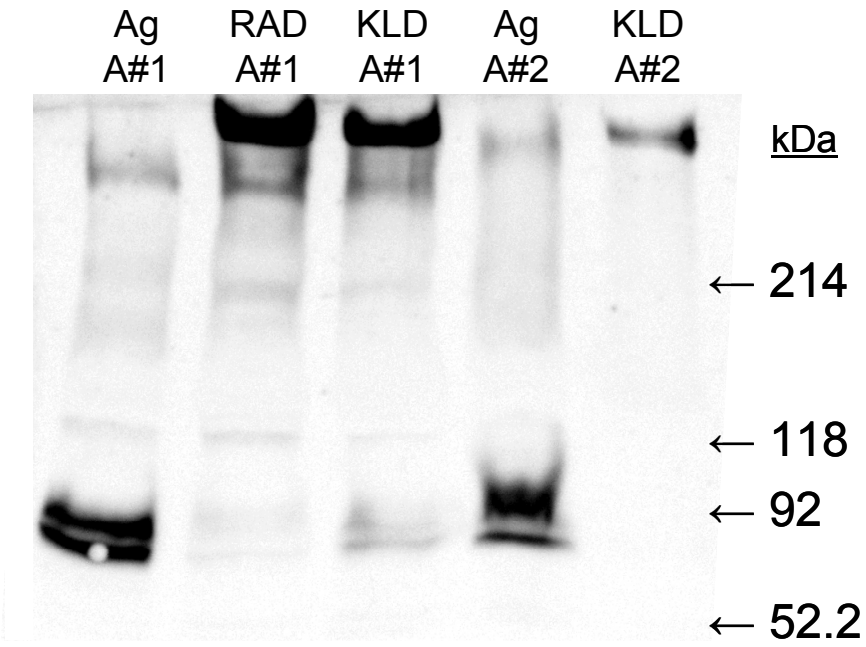

Figure 2.7 Aggrecan Western Analysis
Aggrecan extracted from BMSC-seeded agarose **(Ag)**, RAD16-I **(RAD)**, or KLD12 **(KLD)** hydrogels after 21 days in culture with TGF-β1 supplementation. Lanes 1-3 extracted from animal #1; lanes 4-5 extracted from animal #2.

Chapter 3. Adult equine bone-marrow stromal cells undergo chondrogenesis and produce a cartilage-like ECM superior to animal-matched adult chondrocytes

The capacity for bone-marrow-stromal cells (BMSCs) and chondrocytes from young and adult equine donors to produce a cartilage-like ECM was investigated. Cells were isolated from animal-matched bone marrow and cartilage tissue, encapsulated in a self-assembling-peptide hydrogel, and cultured in a chemically-defined medium with and without TGF-β1 supplementation. BMSCs and chondrocytes from both donor ages were encapsulated with high viability. Young, but not adult chondrocytes proliferated in response to TGF-β1 while BMSCs from both ages proliferated with TGF-β1. Young chondrocytes stimulated by TGF-β1 accumulated ECM with 10-fold higher sulfated-glycosaminoglycan content than adult chondrocytes and 2-3-fold higher than BMSCs of either age. The opposite trend was observed for hydroxyproline content, with BMSCs accumulating 2-3-fold more than chondrocytes, independent of age. BMSCs of either age produced neotissue with higher dynamic stiffness than young chondrocytes. Size-exclusion chromatography of extracted proteoglycans showed that an aggrecan-like peak was the predominant sulfated proteoglycan for all cell types. Measurement of aggrecan core-protein length and chondroitin-sulfate-chain length by atomic-force microscopy revealed that independent of age, BMSCs produce longer core protein and chondroitin-

sulfate chains, and fewer catabolic-cleavage products than chondrocytes, indicating that the BMSC-produced aggrecan has a younger phenotype than chondrocyte-produced aggrecan. Taken together these data suggest advantages for BMSCs over chondrocytes as a source for cell-based cartilage repair, especially for autologous applications with adult patients.

3.1 Introduction

Because of their capacity to undergo chondrogenesis[14,16,66], bone-marrow derived stromal cells (BMSCs) have been the focus of numerous studies with the ultimate goal of repairing cartilage tissue damaged through disease or injury[28,30,48]. Recent reports have suggested a robust chondrogenic and tissue forming capacity for BMSCs that is sustained with aging[19,69,70], in contrast with primary chondrocytes which have decreased matrix synthesis and tissue repair potential with age[71-74]. Decreased matrix production with age for primary chondrocytes may be due in part to their reduced sensitivity to pro-anabolic growth factors such as insulin-like growth factor-I or transforming growth factor-β1 (TGF-β1)[75-77].

Several recent studies have encapsulated BMSCs in 3D hydrogel culture with TGF-β1/3 stimulation to induce chondrogenesis and compared the differentiated cell phenotype with that of primary chondrocytes[30,41,48]. While these studies have shown that chondrocytes produce a more cartilage-like and mechanically-functional ECM than BMSCs, these studies have all used a young bovine tissue source. Given the known phenotypic changes that occur with age for both chondrocytes and BMSCs, evaluation of

these cell types at multiple times during development and aging is important, especially in light of the potential advantages of using autologous tissue for cartilage repair[29,78].

To achieve cartilage repair, a successful cell-based strategy will be required to recapitulate the fine structure of the native cartilage ECM in order to produce a mechanically functional tissue. Aggrecan, a large aggregating proteoglycan, is the primary cartilage ECM molecule that provides the compressive stiffness and load distribution functions of the tissue[79]. Given the extensive changes in aggrecan biosynthesis[80,81], processing[82,83], aggregation[72] and degradation[79] with age, it will likely be important to evaluate the quality of aggrecan produced by any cell type used in a cartilage repair therapy. An intensively studied molecule, numerous techniques exist for the study of aggrecan including chromatography[84] and Western analysis[61], which assess size distribution and cleavage products in an entire population of molecules, and imaging techniques such as electron microscopy[85] and atomic force microscopy (AFM)[60], which allow for detailed measurements of individual molecules.

For this study, animal-matched equine bone marrow and cartilage tissue was harvested from both immature foal and skeletally-mature adult horses. BMSCs and chondrocytes were isolated and encapsulated in a self-assembling peptide hydrogel that has been shown to enhance chondrogenesis of BMSCs[28] (Chapter 2). These peptides are being developed for use in cardiovascular[20,86], liver[42], and cartilage[26], and have been successfully used in animal studies without inducing inflammation or immune response[20,86], making them a candidate *in vivo* tissue engineering scaffold. Using TGF-β1 to stimulate chondrogenesis and matrix production, we characterized the tissue forming capacity of BMSCs and chondrocytes from both young and adult animal sources over the

initial 21 days of tissue growth and quantitatively measured ECM synthesis and accumulation. The mechanical function of the developing ECM was assessed by dynamic compression testing. To further characterize the quality of the ECM, proteoglycans were extracted and characterized by size exclusion chromatography to examine the distribution of proteoglycan monomers. Proteoglycan extracts were also purified and imaged by atomic force microscopy to enable detailed morphological measurements of individual aggrecan molecules.

3.2 Materials and Methods

Materials

KLD12 peptide with the sequence AcN-$(KLDL)_3$-CNH_2 was synthesized by the MIT Biopolymers Laboratory (Cambridge, MA) using an ABI Model 433A peptide synthesizer with FMOC protection. All other materials were purchased from the suppliers noted below.

Tissue Harvest

Cartilage tissue was harvested aseptically from the femoropatellar groove and bone marrow was harvested from the sternum and iliac crest of two immature (2-4-month-old foals) and three skeletally-mature (2-5-year-old adults) mixed-breed horses as described previously.[28] Horses were euthanized at Colorado State University for reasons unrelated to conditions that would affect either tissue. Bone marrow and cartilage tissue samples were animal-matched, as they were always harvested from the each animal.

Cell Isolation

Chondrocytes were isolated by sequential pronase (Sigma-Aldrich, St. Louis, MO), collagenase (Roche Applied Science, Indianapolis, IN) digestion as described previously.[87] Marrow samples were washed in PBS and fractionated by centrifugation to remove red blood cells. BMSCs were isolated from the remaining nucleated cell pellet by differential adhesion as described previously.[28] After BMSC colonies reached local confluence, cells were cryopreserved and stored in liquid nitrogen. Prior to peptide hydrogel encapsulation, BMSCs were thawed and plated at $6x10^3$ cells/cm^2 in low glucose DMEM plus 10% ES-FBS (Invitrogen Carlsbad, CA), HEPES, and PSA (100 U/mL penicillin, 100 μg/mL streptomycin, and 250 ng/mL amphotericin) plus 5 ng/mL bFGF (R&D Systems, Minneapolis, MN). After 3 days, cells were detached with 0.05% trypsin/1mM EDTA (Invitrogen) at ~$3x10^4$ cells/cm^2 (passage 1) and reseeded at $6x10^3$ cells/cm^2. Over the subsequent 3 days, this expansion was repeated for passage 2 after which cells were detached for encapsulation in peptide hydrogels.

Hydrogel Encapsulation and Culture

BMSCs and chondrocytes were encapsulated in 0.35% (w/v) KLD12 peptide at a concentration of $10x10^6$ cells/mL using acellular agarose casting molds to initiate peptide assembly as described previously (Chapter 2). Hydrogel disks with 50 μL initial volume and 6.35 mm diameter were cultured in high glucose DMEM (Invitrogen) supplemented with 1% ITS+1 (Sigma-Aldrich, St. Louis, MO), 0.1 μM dexamethasone (Sigma-Aldrich), 37.5 μg/mL ascorbate-2-phosphate (Wako Chemicals, Richmond, VA), PSA, HEPES, Proline, sodium pyruvate, and NEAA, with (+TGF) or without (Cntl) 10 ng/mL

recombinant human TGF-β1 (R&D Systems) with medium changes every 2-3 days. For all assays except cell viability, hydrogels were cultured for 21 days.

Cell Viability

One day after encapsulation, cell-seeded-peptide hydrogels were stained with 350 ng/mL ethidium bromide (dead) and 12.5 μg/mL fluorescein diacetate (live) in PBS and imaged with a Nikon Eclipse fluorescent microscope.

DNA and ECM Biochemistry

On day 20 of culture, medium was additionally supplemented with 5 μCi/mL of ^{35}S-sulfate and 10 μCi/mL of ^{3}H-proline to measure cellular biosynthesis of proteoglycans and proteins, respectively. At day 21, hydrogels were rinsed 4x30-minutes in PBS with excess unlabeled sulfate and proline to remove excess free label. Hydrogels were weighed wet, lyophilized, weighed dry, and digested in 250 μg/mL proteinase-K (Roche) overnight at 60ºC. Digested samples were assayed for total DNA content by Hoechst dye binding[59], retained sulfated glycosaminoglycan (sGAG) content by DMMB dye binding assay[58], hydroxyproline (OH-Proline) content by chloramine T and p-dimethylaminobenzaldehyde reaction[58,88], and radiolabel incorporation with a liquid scintillation counter. Conditioned culture medium collected throughout the study was also analyzed for sGAG content by DMMB dye binding.

Mechanical Testing

After 21 days of culture, hydrogels were placed in PBS with protease inhibitors (Protease Complete, Roche) and a digital image was captured from which plug cross-sectional area was measured with the Matlab Image Processing Toolbox (The MathWorks, Natick, MA). For each cell type and medium condition, 6-9 hydrogel disks were tested (3 gels/animal x 2-3 animals). The dynamic stiffness of each plug was measured in unconfined uniaxial compression using a Dynastat mechanical spectrometer (IMASS, Hingham, MA) as described.[89] A 15% offset strain was applied via 3x5% ramp-and-hold steps (5% strain applied over 60 seconds, followed by 4-minute hold), followed by a frequency sweep of 0.5% amplitude sinusoidal strains at 0.05, 0.1, 0.3, 0.5, 1.0, and 5.0 Hz. The dynamic compressive stiffness was calculated as the ratio of the fundamental amplitudes of stress to strain.[89]

Proteoglycan Size-Exclusion Chromatography

For the final 24 hours, hydrogels were cultured in medium supplemented with 50 μCi/mL of ^{35}S-sulfate. Proteins were extracted from the minced sample with 4M guanidine HCl and 100mM sodium acetate with protease inhibitors (Protease Complete, Roche) for 48 hours at 4ºC with agitation.[82] Extract was desalted with a G-50 column (GE Healthcare Bio-Sciences, Piscataway, NJ), lyophilized and resuspended in 500mM ammonium acetate for separation on a Superose 6 column (GE Healthcare Bio-Sciences). ^{35}S-sulfate labeled proteoglycans were detected via an inline liquid scintillation counter. For native cartilage tissue extracts, 0.5mL fractions were collected and unlabeled proteoglycans were detected via DMMB dye binding.

Aggrecan Monomer Extraction and AFM Sample Preparation

Proteins were extracted from unlabeled, day 21 hydrogels with 4M guanidine as above. Extracts were adjusted to a density of 1.58 g/mL by the addition of CsCl and subjected to density gradient centrifugation at 470 000 g_{av} for 72 hours at 4ºC. The gradient was fractionated and fractions were assayed for density and sGAG content by DMMB dye binding. Fractions were combined according to density with fractions >1.54 g/mL (labeled D1)[82]. The D1 fraction was then desalted via dialysis and sGAG content was quantified by DMMB dye binding.

Aggrecan samples for AFM imaging were prepared as described previously[60]. Muscovite mica surfaces (SPI Supplies, West Chester, PA, #1804 V-5) were treated with 0.01% 3-amino-propyltriethoxysilane (APTES; Sigma Aldrich, St. Louis, MO) v/v in MilliQ water (18 MΩ · cm resistivity, Purelab Plus UV/UF, US Filter, Lowell, MA). Sixty microliters of APTES solution was deposited onto freshly cleaved mica, incubated for 20–30 min at room temperature in a humidity controlled environment, rinsed gently with MilliQ water, and air dried. The APTES-modified mica substrate was then incubated with 50 µL aliquots of 250 µg/ml GAG incubated for 20-30 min, gently rinsed with MilliQ water and air dried. Electrostatic interaction between the APTES-mica and the aggrecan GAG chains enabled retention of a population of aggrecan despite rinsing. Samples were imaged within a day of preparation.

AFM imaging

Imaging was performed as described previously[60]. The Nanoscope IIIa Multimode AFM (Digital Instruments (DI), Santa Barbara, CA) was used to image all samples via the EV or JV scanners. Tapping mode was employed in ambient temperature and humidity using Olympus AC240TS-2 rectangular Si cantilevers (k = 2 N/m). The cantilever was driven just below resonant frequency, ω_0, and a slow scan rate of 0.5-1 Hz was used to minimize sample disturbances giving a scan rate that was much slower (<25 000x) than the tap rate. The scans were tested for typical AFM imaging artifacts by varying scan direction, scan size, and rotating the sample.

The AFM height images were digitized into pixels and the aggrecan structure features were traced automatically with a custom Matlab program or manually with SigmaScan Pro image analysis software (SPSS Science, Chicago, IL). The core protein length and chondroitin sulfate GAG (CS-GAG) chain length were calculated according to the spatial coordinates of the traces.

Statistical Analysis

All data are presented as mean ± sem. Data were analyzed by a mixed model of variance with animal as a random factor. Residual plots were constructed for dependent variable data to test for normality and data were transformed if necessary to satisfy this assumption. *Post hoc* Tukey tests for significance of pairwise comparisons were performed with a threshold for significance of $p<0.05$.

3.3 Results

Cell Viability and DNA Content

Both BMSCs and chondrocytes from foal and adult donors survived seeding in peptide hydrogels and were >70% viable one day post-encapsulation in the presence of TGF-β1 (Fig. 3.1A). Similar viability was observed at day one in TGF-β1-free controls, however by day 21 decreased cell viability was apparent for both cell types and both donor ages in TGF-β1-free culture (not shown). No significant differences in DNA content were seen between days 0 and 21 for the TGF-β1-free controls suggesting minimal proliferation in these gels (Fig. 3.1B, note day 0 DNA content not available for adult BMSCs). In contrast, in the presence of TGF-β1, BMSC-seeded hydrogels from both foal and adult donors had approximately 2.5-fold higher DNA content than TGF-β1-free controls ($p<0.001$). In addition, chondrocytes from foal donors also proliferated in response to TGF-β1, but to a slightly lesser degree than BMSCs, with a 1.6-fold increase in DNA vs. TGF-β1-free controls ($p<0.001$). When chondrocytes were isolated from adult donors however, they no longer proliferated in response to TGF-β1, demonstrating a different phenotype than chondrocytes from young donors (Fig. 3.1B).

ECM Content and Biosynthesis

As expected, foal-chondrocyte-seeded peptide hydrogels accumulated significantly higher sGAG than adult chondrocytes both with and without TGF-β1[74]. In the absence of TGF-β1, accumulated sGAG was 7-fold higher for foal than for adult chondrocytes (Fig. 3.2A, $p<0.001$), and with TGF-β1 supplementation sGAG was more than 10-fold higher for the foal chondrocyte cultures ($p<0.001$). Minimal sGAG was

produced by BMSCs without TGF-β1 stimulation. However with TGF-β1 supplementation, foal and adult BMSCs accumulated 3-fold and 6-fold higher sGAG than adult chondrocytes, respectively ($p<0.001$). In addition, these day 21 sGAG contents for foal and adult BMSCs were a factor of 2-3 lower than foal chondrocyte sGAG accumulation.

Consistent with the sGAG content data, foal-chondrocyte-seeded peptide hydrogels had higher per cell proteoglycan biosynthesis rates (measured by ^{35}S-sulfate incorporation) than adult-chondrocyte hydrogels during the final day of culture (Fig. 3.2B), although there was only a 2-fold difference between foal and adult chondrocytes, both with and without TGF-β1 ($p<0.01$). Proteoglycan biosynthesis in BMSC-seeded peptide hydrogels was minimal without TGF-β1 stimulation, but was approaching the level of foal chondrocytes in the presence of TGF-β1 with foal BMSC cultures only a factor of 2 lower ($p<0.001$) and adult BMSC statistically equivalent to foal chondrocyte hydrogels.

The fraction of sGAG retained vs. the total amount produced (retained plus lost to the conditioned medium) was highest for foal chondrocytes at 76% (Fig. 3.2C), but both foal and adult BMSCs were only approximately 25% lower (56% and 66%, respectively, $p<0.001$). In contrast, adult chondrocytes retained only 20% of the sGAG produced in the presence of TGF-β1, nearly a factor of 4 less than the foal chondrocytes ($p<0.001$).

The hydroxyproline content of chondrocyte-seeded peptide hydrogels showed similar but less pronounced trends compared to sGAG content. Foal chondrocytes accumulated 10% and 50% higher hydroxyproline than adult chondrocytes, without and with TGF-β1, respectively (Fig. 3.2D, $p<0.001$). In contrast to sGAG, production of

hydroxyproline by adult chondrocytes did not increase with TGF-β1 stimulation. Also in contrast to sGAG, BMSC-seeded peptide hydrogels had higher hydroxyproline content than chondrocyte-seeded hydrogels. Without TGF-β1, both foal and adult BMSC cultures had 30-40% higher hydroxyproline content than either foal or adult chondrocytes ($p<0.001$). With TGF-β1 supplementation, hydroxyproline content of BMSC cultures was approximately a factor of 2 higher than foal and a factor of 3 higher than adult chondrocytes ($p<0.001$).

Protein synthesis rates during the final day of culture (measured by ^{3}H-proline incorporation) were largely consistent with total hydroxyproline content (Fig. 3.2E). In TGF-β1-free cultures the only significant difference was a lower rate for adult BMSC hydrogels by a factor of ~4 vs. the other cell types ($p<0.001$). TGF-β1 stimulation produced statistically comparable protein synthesis for adult and foal chondrocyte cultures with a 2- and 3-fold increase for foal- and adult-BMSC-seeded over chondrocyte-seeded peptide hydrogels, respectively ($p<0.01$).

The ratio of dry weight to wet weight, or the percentage solid, was higher for BMSC- than for chondrocyte-seeded peptide hydrogels, demonstrating greater total matrix density (Fig. 3.2F). In TGF-β1-free cultures, there was no significant difference between foal and adult chondrocytes (at approximately 1% solid), while foal and adult BMSCs were 20% and 80% higher, respectively (1.2% and 1.8%, $p<0.05$). Foal chondrocytes produced hydrogels that were nearly 2% solid with TGF-β1 stimulation, nearly 2-fold higher than adult chondrocytes ($p<0.001$). BMSCs were 2-3 fold higher still ($p<0.001$), at 4% and 6% solid for foal and adult BMSCs, respectively.

Mechanical Properties

Dynamic stiffness trended with both frequency and cell type (Fig. 3.3, $p<0.001$). Pairwise comparisons revealed four statistically significant groups. The group with the highest dynamic stiffness was group A, which contained TGF-β1-stimulated hydrogels seeded with BMSCs from both foal and adult donors. Group B contained foal chondrocytes cultured in TGF-β1 and was less stiff than group A ($p<0.05$). Foal BMSCs and chondrocytes cultured in TGF-β1-free control medium were in group C, which was lower than group B ($p<0.001$). Finally, group D had the lowest stiffness ($p<0.001$) and consisted of adult chondrocytes cultured either with or without TGF-β1, as well as cell-free controls.

Proteoglycan Size-Exclusion Superose 6 Chromatography

The majority of proteoglycans synthesized in all samples eluted as an aggrecan-like peak similar to proteoglycans extracted from young bovine cartilage tissue (Fig. 3.4). Both foal BMSCs and chondrocytes also produced a low, broad peak, to the right of the aggrecan peak, that returned to baseline levels by $K_{av}=0.3$, suggesting a population of smaller proteoglycans was present in these samples[84]. All proteoglycans produced by adult BMSCs and chondrocytes eluted with a K_{av} less than 0.2, showing that these samples contained fewer small proteoglycans than the foal cells and were more similar to the native cartilage tissue extract.

Aggrecan Monomer Morphology AFM Imaging

Purified proteoglycan extracts from BMSCs and chondrocytes of both animal ages contained molecules with a central backbone and numerous side chains, consistent with the known sGAG-functionalized core-protein structure of aggrecan (Fig. 3.5).[60] In all samples, full-length aggrecan was observed (for selected examples see green arrows in Figs. 3.5A, 3.5D, 3.5G, 3.5J) and in many cases globular domains were visible on both ends of the core protein, consistent with the presence of both G1- and G3-globular domains. Quantitative image analysis revealed that BMSCs from both foals and adults produced core protein with significantly longer average core-protein length than chondrocytes, 487-503 nm vs. 412-437 nm, respectively (Fig. 3.6A, $p<0.05$). Further analysis of the distribution of core-protein length for all cell types (Fig. 3.6B) reveals a main peak near 600 nm, likely representing full-length aggrecan, and a tail that extends below 200 nm, likely due to catabolic processing of the aggrecan core protein. Consistent with the trends in Fig. 3.6A, the full-length aggrecan peak in Fig. 3.6B is shifted larger for BMSC samples, where the peak is ≥600 nm, than for chondrocyte samples, where the peak is <600 nm. Furthermore, the frequency of aggrecan cleavage products <300 nm in length is higher for chondrocytes than for BMSCs of the corresponding age donors (i.e. foal chondrocytes produce more cleavage products than foal BMSCs and similarly for adult chondrocytes vs. BMSCs).

High magnification images of single aggrecan monomers have sufficient resolution to clearly distinguish and measure individual CS-GAG chains (example CS-GAGs highlighted in green on Figs 5C, 5F, 5I, and 5L). CS-GAG chains on BMSC produced aggrecan were longer than on chondrocyte produced aggrecan for both foal

cells (Figs. 3.5E-F vs. 3.5 B-C) and adult cells (Figs. 3.5K-L vs. 3.5H-I). Image quantification confirmed this trend with BMSCs from both foals and adults producing 63-73 nm CS-GAG chains while chondrocytes produced CS-GAG chains between 40-46 nm (Fig. 3.6A, $p<0.05$).

3.4 Discussion

The relative matrix forming capacity of BMSCs compared to that of primary chondrocytes was found to depend on the age of the tissue donor from which the cells are derived. For a skeletally-mature adult tissue source, BMSCs produced more sGAG and collagen and assembled a mechanically functional ECM with higher dynamic stiffness than primary chondrocytes. In addition, adult BMSCs proliferated during 3D peptide hydrogel culture in response to TGF-β1 stimulation, while adult primary chondrocytes did not. In contrast, BMSCs and chondrocytes from young tissue were both capable of proliferating and producing a mechanically functional tissue in 3D peptide hydrogel culture in the presence of TGF-β1. In the absence of TGF-β1, young primary chondrocytes demonstrated sGAG accumulation and proteoglycan synthesis that was greater than any other cell type in this study, but still not high enough to generate a tissue with more than an incremental increase in mechanical properties over cell-free controls.

The conclusion that young BMSCs produce a comparable cartilage-like ECM to young chondrocytes is in contrast to several recent reports, including studies by Mauck *et al.*[30], Erickson *et al.*[41], and Connelly *et al.*,[48] which showed inferior tissue forming capacity for BMSCs. However, these conclusions were all based on long-term, TGF-β1-stimulated culture in agarose hydrogels, whereas the present study focused on the initial

21 days of culture in a self-assembling peptide hydrogel, which is known to enhance chondrogenesis of BMSCs relative to agarose (Chapter 2). When peptide hydrogels were used by Erickson *et al*., close agreement with our results was observed early in culture for both neotissue ECM content and dynamic mechanical stiffness.

Young equine chondrocytes proliferated in response to TGF-β1, where adult equine chondrocytes did not, and had higher sGAG accumulation and proteoglycan synthesis than adult chondrocytes both with and without TGF-β1 stimulation. This is consistent with a recent report of decreased cellular proliferation and sGAG accumulation by human chondrocytes with age in pellet culture with TGF-β1 stimulation[71]. In addition, when Tran-Khanh *et al*. encapsulated bovine chondrocytes from fetal, young, and aged donors in agarose, a decrease in cell proliferation and sGAG per cell was observed with age[74]. However, Tran-Khanh *et al*. also saw a significant decrease in hydroxyproline content and protein synthesis per cell with age, which was not observed in the present study.

The dynamic stiffness of BMSC-seeded hydrogels from both young and adult sources was higher than for young chondrocytes, despite the higher sGAG content for young chondrocyte-seeded hydrogels, suggesting that a model where stiffness is linearly related to sGAG content is insufficient to describe these data. Given that dynamic stiffness was a function of frequency, a time-dependent model, such as poroelasticity, is required to describe the mechanical properties of the developing tissue constructs[89]. Poroelasticity predicts that mechanical properties will depend on both the equilibrium modulus and the hydraulic permeability of the solid matrix. While the equilibrium modulus and hydraulic permeability are both dependent on the sGAG content of the

neotissue, they also depend on the density of the solid matrix[90]. Since both young and adult BMSCs produced a denser solid matrix (with TGF-β1) than young chondrocytes, a lower hydraulic permeability may be expected than for BMSCs than for young chondrocytes. This higher solid matrix density and resulting lower hydraulic permeability for BMSC-seeded hydrogels corresponds to the higher dynamic stiffness measured for BMSC than for young chondrocyte samples, suggesting a poroelastic description for cell-seeded peptide hydrogel mechanical properties.

Size exclusion chromatography of the proteoglycans extracted from developing ECM of BMSC- and chondrocyte-seeded peptide hydrogels revealed that the predominant peak detected ran in the void volume of a Superose 6 column consistent with the size of aggrecan[84]. This aggrecan peak was observed from ECM extracts from both young and adult cells. However, for both young BMSCs and chondrocytes an additional minor population of proteoglycans was observed near $K_{av} = 0.2$ consistent with the size of decorin[84], whereas adult BMSCs and chondrocyte samples did not appear to contain a population of small proteoglycans. Due to the resolution limitations of the Superose 6 column in separating the various cleavage products of aggrecan monomers, more detailed analyses were performed via AFM imaging. In general, chromatography detected predominantly full-length aggrecan, which was generally consistent with the histograms of core-protein length observed by AFM imaging.

When purified aggrecan was imaged by tapping-mode AFM, predominantly full-length aggrecan monomers were observed for BMSCs and chondrocytes from both young and adult donors. This is in contrast to reports of significant variability in aggrecan size with age that were attributed to variation in core protein length[82,83,85]. These differences

are likely due to the use of primary tissue extracted aggrecan, which has a tissue half-life of 3.5 years[79], as compared to the newly synthesized aggrecan in the current study. Due to this long residence time, tissue-extracted aggrecan is susceptible to sustained catabolic activity[91] generating trends with age that were not seen in the present study. Nonetheless, aggrecan cleavage products were observed, although differences were mainly between chondrocytes and BMSCs and not related to age. One potential explanation for the difference in cleavage product formation is that TGF-β1 stimulation has been shown to increase catabolic processing of aggrecan in chondrocyte-seeded agarose[92]. In contrast, aggrecan catabolic activity by BMSCs in TGF-β1 stimulated peptide hydrogels is limited (Chapter 2). Thus, the observed catabolic processing of aggrecan may be a cell-type specific response to TGF-β1 stimulation.

In addition to differences in aggrecan cleavage product production, longer core-protein length for full-length aggrecan was observed for BMSCs than for chondrocytes. The trend for longer full-length aggrecan molecules produced in BMSC cultures may be related to the difference in CS-GAG chain length between the two cell types. BMSC samples had 40%-75% longer CS-GAG chains than chondrocyte samples. Given the high anionic charge density of these CS-GAGs and their close packing attachment on the core protein, an increase in their length would lead to a higher charge density and increased repulsive force, which would be expected to extend the core protein[60].

One potential mechanism by which longer CS-GAG chains may be synthesized is through altered core-protein post-translational processing kinetics[80,81,93]. These reports showed that slowing the rate of aggrecan core protein synthesis leads to a reduction in the rate of intracellular processing of core protein, which resulted in the synthesis of longer

CS-GAG chains. This effect was observed both for chemical inhibition of core protein synthesis by cycloheximide[80,81] and for mechanical inhibition of core protein synthesis by static compression[93]. To investigate whether a lower core protein synthesis rate in BMSC than in chondrocyte cultures would explain the longer CS-GAG chains observed for BMSCs, the rate of core protein synthesis was estimated by dividing the ^{35}S-sulfate incorporation rate (Fig. 3.2B) by the average CS-GAG chain length (Fig. 3.6A). The result is plotted in Fig. 3.7 along with rescaled CS-GAG data from Fig. 3.6A. Core protein synthesis for foal chondrocytes was 2-4-fold higher than for adult BMSCs, adult chondrocytes and foal BMSCs ($p<0.001$), while core protein synthesis rate differences between these three cell types were not significant (Fig. 3.7). These results showed an inverse relationship between core protein synthesis and CS-GAG chain length, with longer CS-GAG chains produced by BMSCs corresponding to lower core protein synthesis rates. Conversely, the higher core protein synthesis rate for foal chondrocytes corresponded with shorter CS-GAG chains. Adult chondrocytes were the exception to this trend, producing CS-GAG chains that were as short as foal chondrocytes, yet synthesizing core protein at a rate that was as low as BMSC samples. This suggests that a reduction in the post-translational processing capacity of adult chondrocytes compared to the other three cell types, and that this reduction is potentially responsible for the shorter CS-GAG chains produced.

3.5 Summary

BMSCs encapsulated in a self-assembling peptide hydrogel demonstrated robust cartilage ECM forming capacity that was sustained with aging, whereas similarly

cultured chondrocytes had reduced ECM forming capacity with age. The newly secreted ECM was mechanically functional and the matrix biochemical composition was consistent with a poroelastic model for the measured mechanical moduli. Detailed analysis of aggrecan monomers synthesized by BMSCs and chondrocytes, revealed longer core-protein length and CS-GAG chain length for BMSCs than for chondrocytes consistent with the synthesis of a younger tissue phenotype by BMSCs[72,82,83]. Taken together these differences suggest potential advantages for BMSCs over chondrocytes for use in cell-seeded cartilage repair strategies, especially when it is desirable to use autologous cells for treatment of adult patients. Future work on BMSC based therapies will need to develop techniques for maintaining the chondrogenic phenotype established during the early chondrogenesis described in this study, without inducing hypertrophy and terminal differentiation. These techniques could potentially involve modifying the cell-culture scaffold with bioactive motifs to control the BMSC differentiation state throughout the course of neotissue formation, integration with surrounding native tissue, and return to full mechanical and physiologic function.

3.6 Acknowledgements

Thank you to Hsu-Yi Lee for performing the AFM imaging and analysis. Thank you to Eric Vanderploeg and John Kisiday for helpful discussion on study design and hands on assistance with protocol development. Thank you to John Kisiday and Dave Frisbie for the generous supply of equine tissue. Thank you to Christine Ortiz and Alan Grodzinsky for scientific leadership and guidance.

This work was funded by the National Institutes of Health (NIH EB003805), the National Science Foundation (NSF-NIRT 0403903), and a National Institutes of Health Molecular, Cell, and Tissue Biomechanics Training Grant Fellowship (P.W.K.).

3.7 Figures

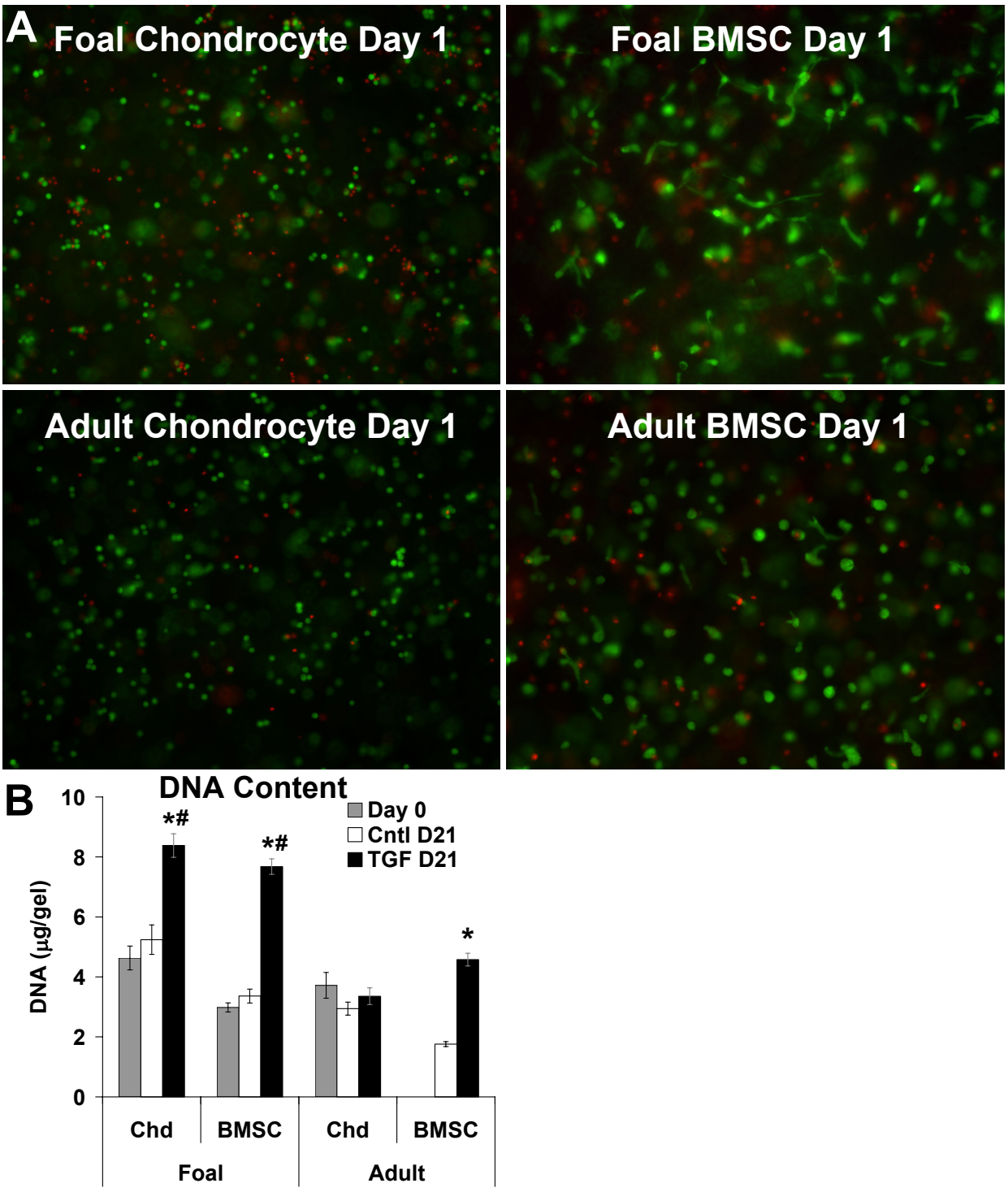

Figure 3.1 Cell Viability and Hydrogel DNA Content
(A) Live **(green)** and dead **(red)** staining of cell-seeded, self-assembling peptide hydrogels cultured with TGF-β1 at day 1. **(B)** DNA content for chondrocyte **(Chd)** and BMSC seeded hydrogels at day 0 **(Day 0)**, or after 21 days of culture in control **(Cntl D21)** or TGF-β1

supplemented **(TGF D21)** medium. **Stats:** mean ± sem, n=8 (4 gels x 2 foals), n=12 (4 gels x 3 adults); # vs. Day 0; * vs. Cntl D21; p<0.001.

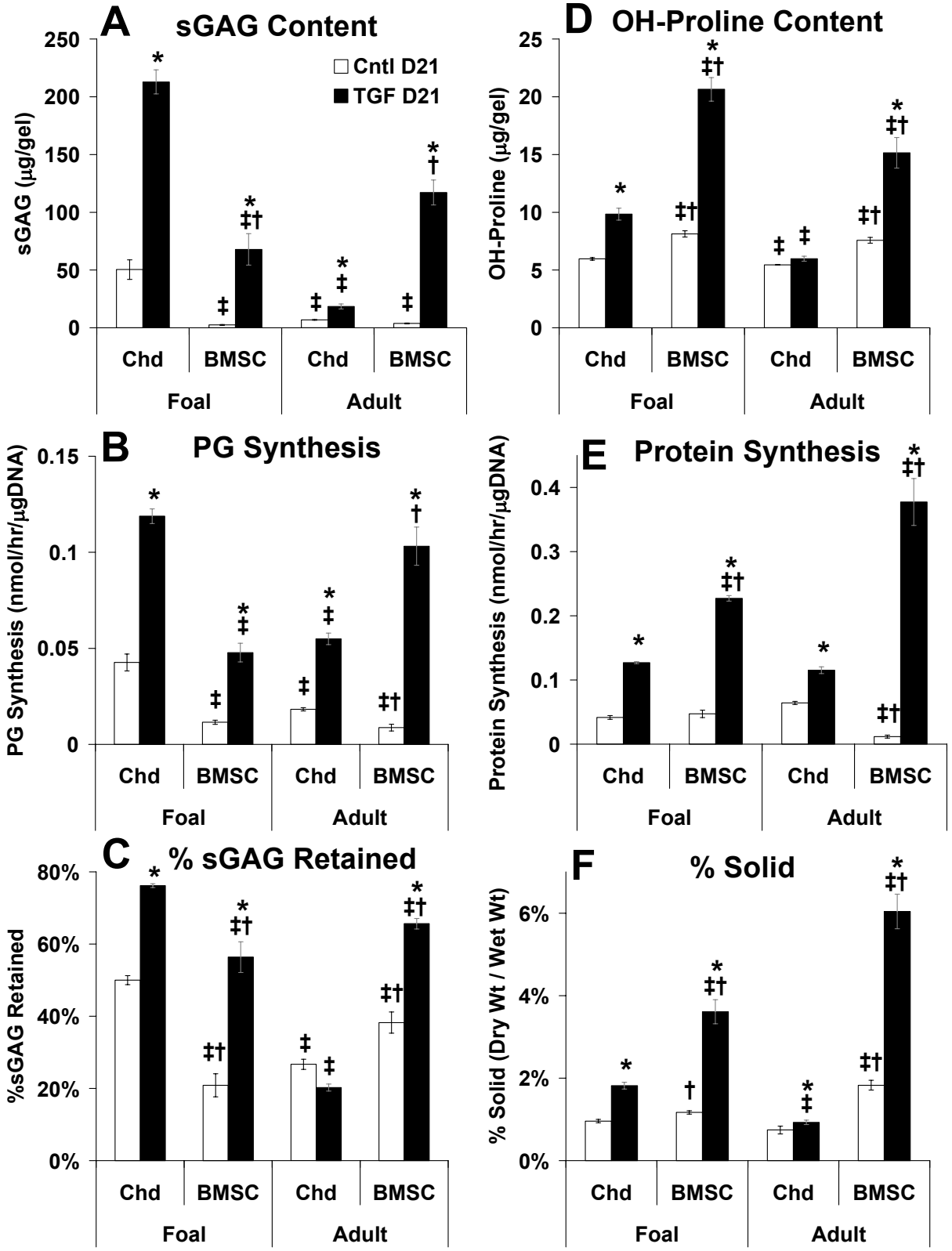

Figure 3.2 Hydrogel ECM Biosythesis Rates and Content
Chondrocyte **(Chd)** and BMSC seeded peptide hydrogels after 21 days of culture in control **(Cntl D21)** or TGF-β1 supplemented **(TGF D21)** medium. **(A)** sGAG content **(B)** Proteoglycan biosynthesis **(C)** Percent sGAG retention (hydrogel retained / total produced including lost to medium) **(D)** Hydroxyproline content **(E)** Protein biosynthesis **(F)** Percent solid matrix (dry weight / wet weight). **Stats:** mean ± sem, n=8 (4 gels x 2 foals) or n=12 (4 gels x 3 adults); ***** vs. Cntl D21; **‡** vs. foal chondrocyte; **†** vs. adult chondrocyte; $p<0.05$.

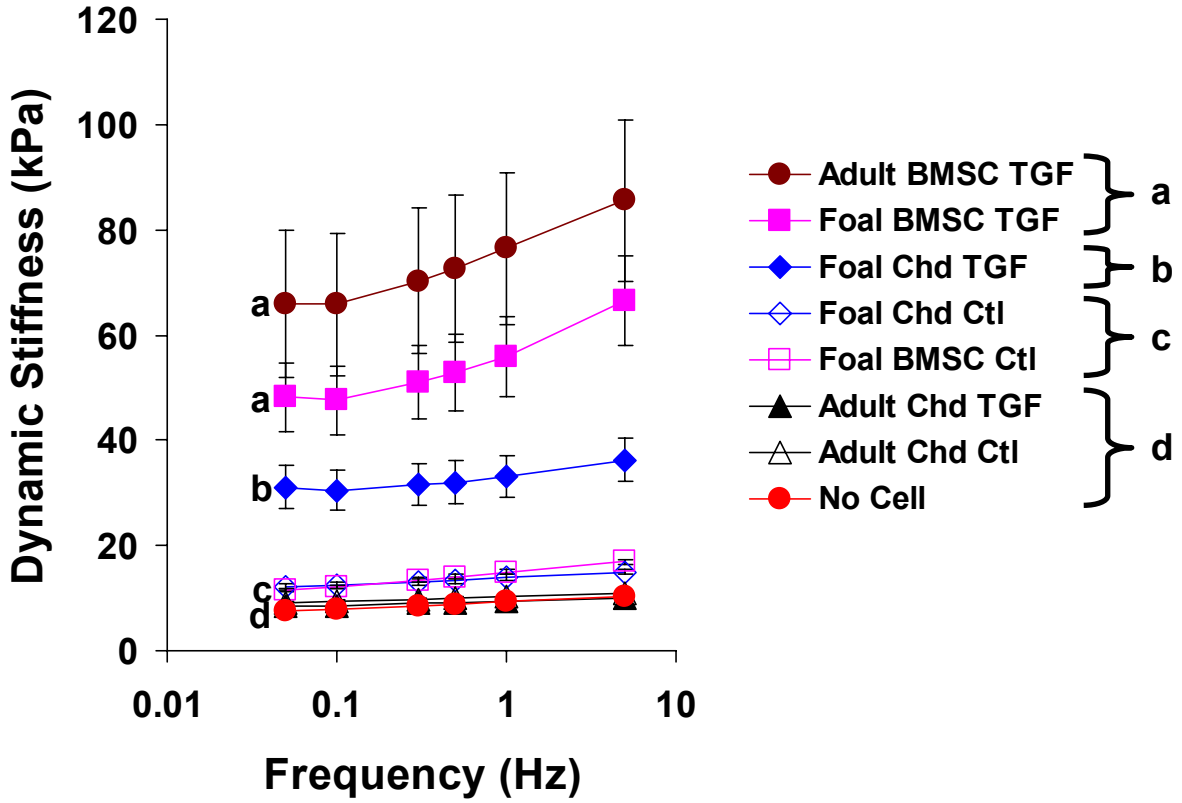

Figure 3.3 Hydrogel Dynamic Stiffness
Chondrocyte **(Chd)** and BMSC seeded peptide hydrogels after 21 days of culture in control **(Ctl)** or TGF-β1 supplemented **(TGF)** medium. **Stats:** mean ± sem, n=6 (3 gels x 2 foals) or n=9 (3 gels x 3 adults); **a, b, c, d** statistically unique groups; $p<0.05$.

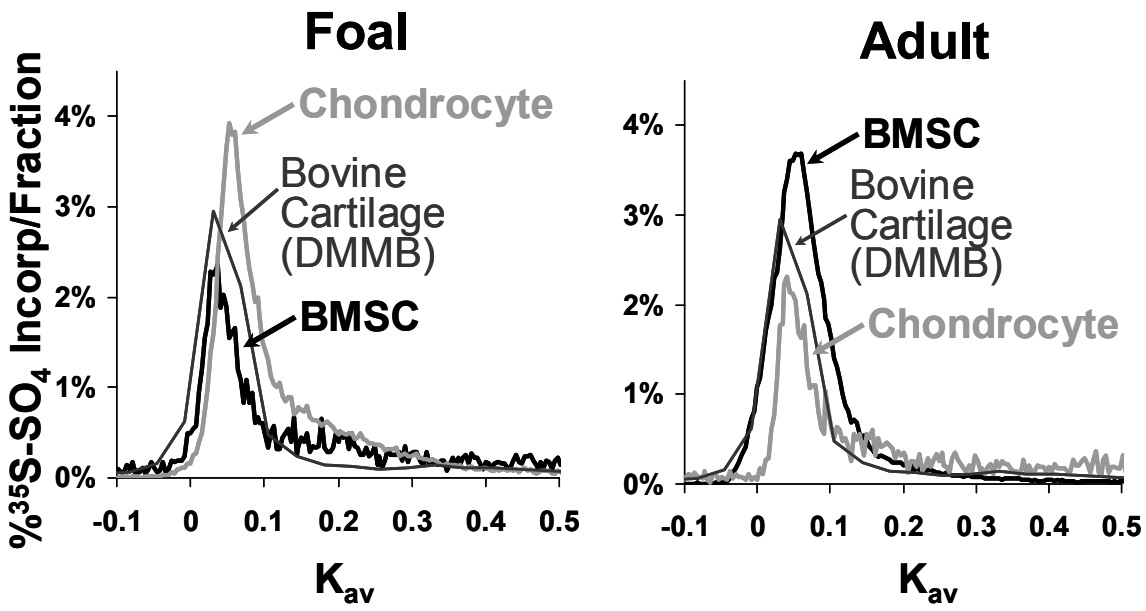

Figure 3.4 Superose 6, Size-Exclusion, Proteoglycan Chromatography
Proteoglycans extracted from either chondrocyte and BMSC seeded peptide hydrogels after 21 days of culture with TGF-β1 or from native cartilage tissue harvested from newborn bovine calves.

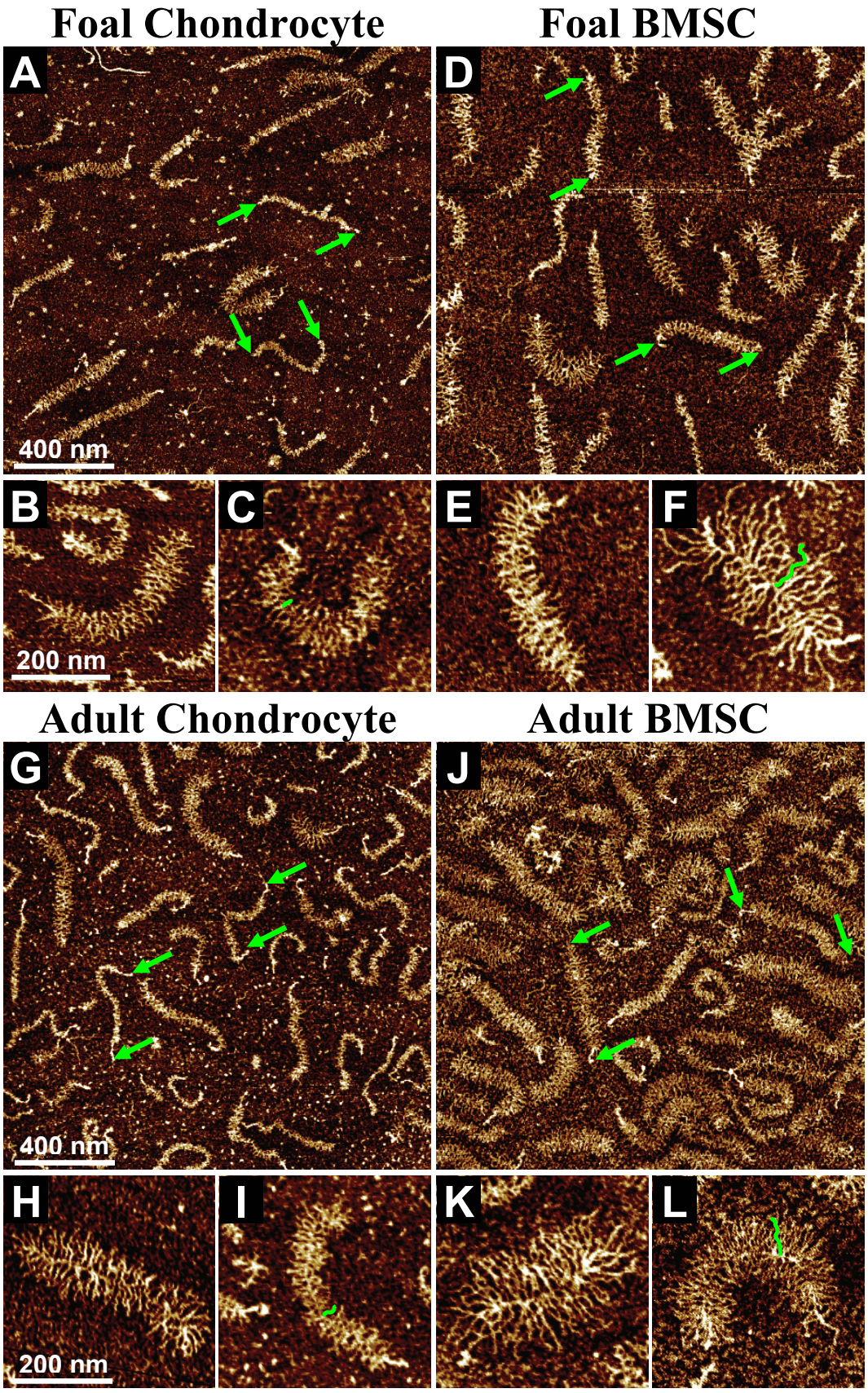
Foal Chondrocyte
Foal BMSC
A
D
400 nm
B
C
E
F
200 nm
Adult Chondrocyte
Adult BMSC
G
J
400 nm
H
I
K
L
200 nm

Figure 3.5 Tapping-mode AFM Imaging of Aggrecan Monomer Morphology
Proteoglycans extracted from cell-seeded peptide hydrogels after 21 days of culture with TGF-β1. **(A-C)** Foal chondrocytes, **(D-F)** Foal BMSCs, **(G-I)** Adult chondrocytes, **(J-L)** Adult BMSCs. Green arrows in A, D, G, and J denote ends of full-length aggrecan monomers. Example individual CS-GAG chains highlighted in green in C, F, I, and L.

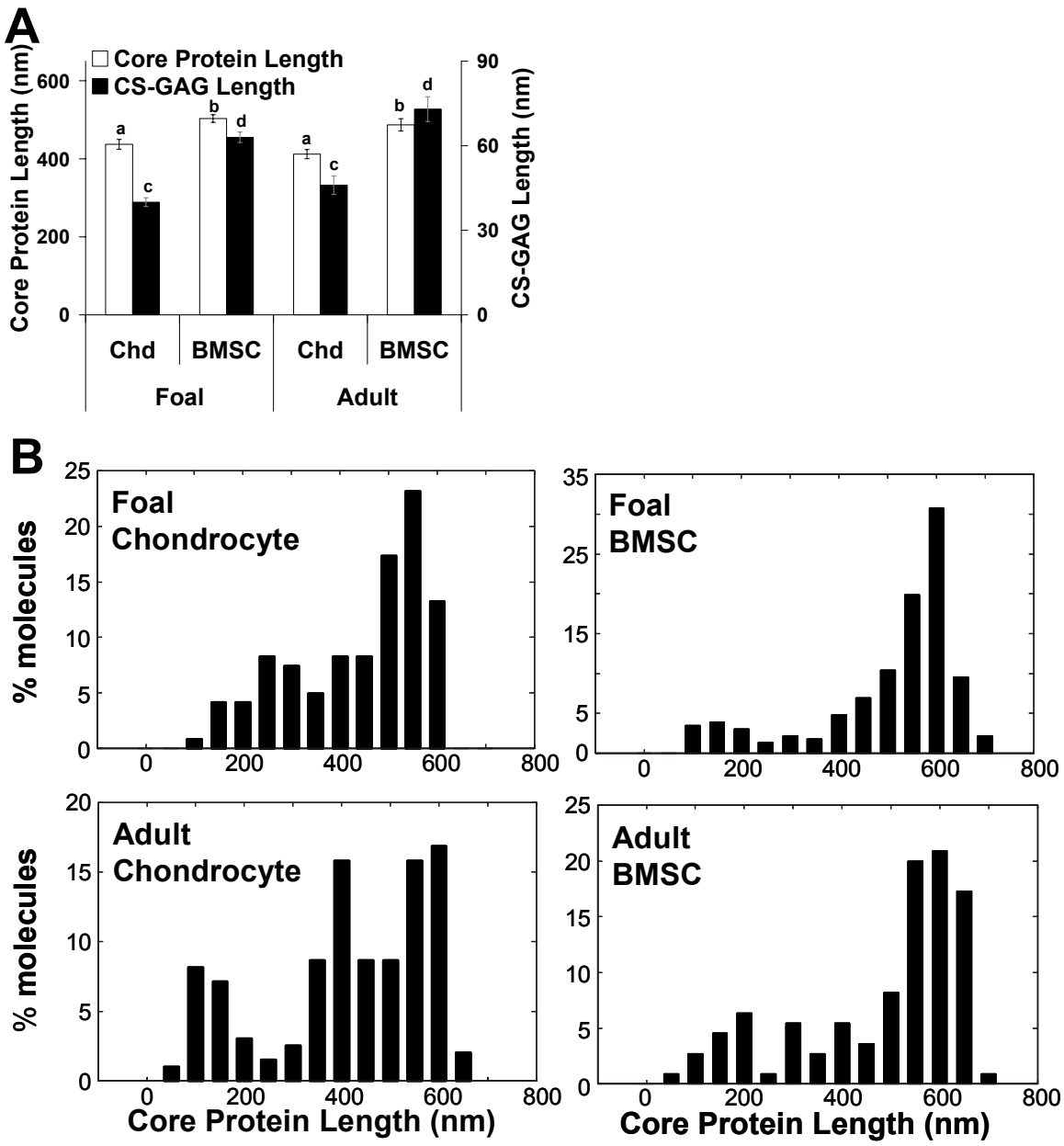

Figure 3.6 Aggrecan AFM Image Quantification
Aggrecan extracted from chondrocyte **(Chd)** and BMSC seeded peptide hydrogels after 21 days of culture with TGF-β1. **(A)** Core-protein length and CS-GAG chain length **(B)** Histogram of core-protein length. **Stats:** mean ± sem; core-protein length: **a, b** statistically unique groups, n=110-231; CS-GAG length: **c, d** statistically unique groups, n=28-35; $p<0.05$.

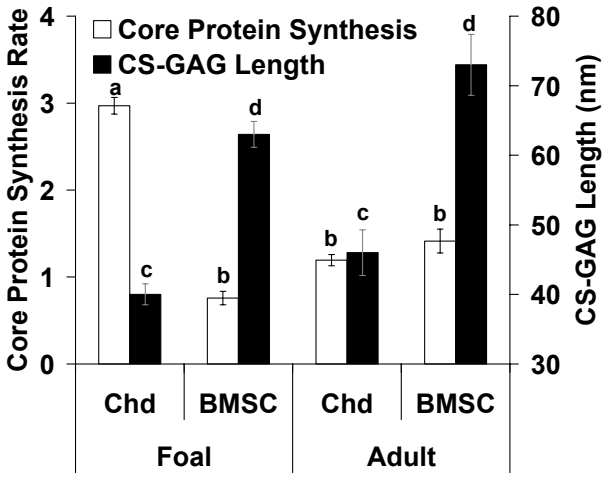

Figure 3.7 Core Protein Synthesis Rate and CS-GAG Chain Length
Chondrocyte **(Chd)** and BMSC seeded peptide hydrogels after 21 days of culture with TGF-β1. Core protein synthesis rate calculated by normalizing the ^{35}S-sulfate proteoglycan synthesis rate in Fig. 3.2B to the CS-GAG chain length in Fig. 3.6A (units=pmol/hr/µg DNA/nm). **Stats:** mean ± sem; core protein synthesis: **a, b** statistically unique groups, n=8-12; CS-GAG length: **c, d** statistically unique groups, n=28-35; $p<0.05$.

Chapter 4. Controlled delivery of TGF-β1 from self-assembling peptide hydrogels induces chondrogenesis in bone marrow stromal cells via Smad 2/3 signaling

Self-assembling peptide hydrogels were modified to deliver TGF-β1 to encapsulated bone-marrow derived stromal cells (BMSCs) via biotin-streptavidin tethering and growth factor adsorption. BMSCs encapsulated in peptide hydrogels with both tethered and adsorbed TGF-β1 were cultured in TGF-β1-free medium, and chondrogenesis was compared to that for BMSCs encapsulated in unmodified peptide hydrogels, with and without medium-delivered TGF-β1. Adsorbed TGF-β1 peptide hydrogels stimulated chondrogenesis of BMSCs as demonstrated by cell proliferation and cartilage-like ECM accumulation, while tethered TGF-β1 was not different from TGF-β1-free controls. Adsorbed TGF-β1 in both acellular peptide and agarose hydrogels was retained for 21 days with repeated bath changes, and peptide hydrogels retained 3-fold more TGF-β1 than agarose. Full-length aggrecan was produced by BMSCs in response to adsorbed TGF-β1 in both peptide and agarose hydrogels, while medium-delivered TGF-β1 stimulated elevated aggrecan cleavage product formation in agarose. Smad 2/3 was phosphorylated transiently in response to adsorbed TGF-β1, while medium-delivered TGF-β1 produced sustained signaling, suggesting dose and signal duration are potentially important for minimizing aggrecan cleavage product formation. TGF-β1 adsorbed to self-

assembling peptide hydrogels can stimulate BMSC chondrogenesis and neotissue production for cartilage tissue engineering applications.

4.1 Introduction

Due to the poor regenerative capacity of cartilage after injury or disease, cell-based, tissue-engineering strategies have been proposed to repair cartilage defects, resurface arthritic joints, and restore mechanical and physiologic tissue functions. To deliver a cell-based therapy, tissue engineering scaffolds seeded with bone-marrow-derived stromal cells (BMSCs) have been extensively studied with the goal of delivering and retaining cells in irregular defects, providing an appropriate environment for cell attachment, migration, proliferation, and differentiation, and stimulating production of cartilage neotissue that integrates with the surrounding native tissue[13,29,38]. To achieve all of these goals, a feature likely to be of critical importance will be to incorporate into scaffold design bioactive motifs which induce chondrogenesis and promote cartilage ECM synthesis[13].

Transforming growth factor β1 (TGF-β1) has been widely used to promote chondrogenesis of BMSCs in a variety of culture systems by supplying it in the medium for the duration of culture[16,31,32]. Due to the short *in vivo* half-life of TGF-β isoforms and their potent action on other cell types, various technologies have been engineered with the goal of local delivery and controlled release of these growth factors *in vivo*[94-99]. Given the wide range of functions controlled by TGF-β1[100-102], the goal of any such technology is to stimulate the appropriate intracellular signals to generate the desired effect on cell function. TGF-β1 signals through binding its type I and II receptor serine/threonine

kinases on the cell surface, forming an active complex that phosphorylates the Smad proteins, which in turn propagate the signal by ultimately translocating to the nucleus and promoting transcription[101,102]. The activated TGF-β1 receptor complex directly phosphorylates Smad2 and Smad3, two of the receptor-activated Smad proteins, to initiate this signal transduction pathway[100].

Self-assembling peptide hydrogels are a versatile new class of materials that have been developed for tissue engineering applications[22,103-106]. Benefits have been demonstrated for the use of these peptide hydrogels in cartilage[26,28], liver[42], and cardiovascular[20,86] tissue, and they have been shown to provide a microenvironment which enhances the chondrogenesis of BMSCs[28] (Chapter 2). These peptides can also control the delivery and release of functional proteins[104], therapeutic macromolecules[105], and bioactive motifs[103]. Taken together, these studies suggest the potential to simultaneously co-encapsulate growth factors and BMSCs in self-assembling peptide hydrogels and generate cartilage neotissue.

The goal of this study was to deliver TGF-β1 within a self-assembling peptide hydrogel to induce chondrogenesis of encapsulated BMSCs and the subsequent accumulation of a cartilage-like ECM. Two strategies for coupling TGF-β1 to the peptide scaffold were tested. The first employed biotin-conjugated TGF-β1 (bTGF-β1), biotin-conjugated peptide monomers, and multivalent streptavidin, which tethered TGF-β1 to the scaffold through a high-affinity "biotin sandwich" bond[20]. The second was to nonspecifically adsorb TGF-β1 to the unassembled-peptide hydrogel prior to encapsulating BMSCs. Functional assays for chondrogenesis of encapsulated BMSCs included cell content and biosynthesis of cartilage ECM components in cultured

hydrogels. TGF-β1 binding and release was characterized by release of radiolabeled growth factor from acellular peptide and agarose hydrogels. Finally, bioactivity of the peptide-delivered TGF-β1 was confirmed by Western blot analysis of phosphorylated Smad 2/3.

4.2 Materials and Methods

Materials

KLD peptide with the sequence AcN-$(KLDL)_3$-CNH_2 was synthesized by the MIT Biopolymers Laboratory (Cambridge, MA) using an ABI Model 433A peptide synthesizer with FMOC protection. All other materials were purchased from the suppliers noted below.

Tissue Harvest

Equine bone marrow was harvested from the sternum and iliac crest of immature (2-4-month-old foals) and skeletally-mature (2-5-year-old adults) mixed-breed horses as described previously.[28] Horses were euthanized at Colorado State for reasons unrelated to conditions that would affect bone marrow. Bovine bone marrow was harvested from newborn bovine calves (Research 87, Marlborough, MA).

Cell Isolation

BMSCs were isolated from equine (Chapter 3) and bovine (Chapter 2) marrow as described previously. Differential adhesion was used to separate BMSCs from the total nucleated cell population.[28] After reaching local confluence, BMSCs were cryopreserved

and stored for future use. Prior to peptide hydrogel encapsulation, BMSCs were expanded by plating at $6x10^3$ cells/cm^2 and culturing for three days in low glucose DMEM, 10% ES-FBS (Invitrogen, Carlsbad, CA), HEPES and PSA (100 U/mL penicillin, 100 μg/mL streptomycin, and 250 ng/mL amphotericin) plus 5 ng/mL bFGF (R&D Systems, Minneapolis, MN). After 3 days, cells were detached with 0.05% trypsin/1mM EDTA (Invitrogen) at ~$3x10^4$ cells/cm^2 (passage 1) and replated at $6x10^3$ cells/cm^2. Passage 2 cells were used for 3D peptide hydrogel culture.

Hydrogel Encapsulation and Culture

BMSCs were encapsulated in 0.35% (w/v) KLD or 2% low-melting-point Agarose (Invitrogen) using acellular agarose molds to initiate self-assembly (Chapter 2) and the resulting 50 μL initial volume, 6.35 mm diameter disks were cultured in high glucose DMEM (Invitrogen) supplemented with 1% ITS+1 (Sigma-Aldrich, St. Louis, MO), 0.1 μM dexamethasone (Sigma-Aldrich), 37.5 μg/mL ascorbate-2-phosphate (Wako Chemicals, Richmond, VA), PSA, HEPES, Proline, sodium pyruvate, and NEAA, with (TGF) or without (control) 10 ng/mL recombinant human TGF-β1 (R&D Systems). For TGF-β1 takeaway experiments, hydrogels were cultured in TGF-β1-supplemented medium for 4, 7, or 14 days followed by culture in control (TGF-β1-free) medium for the remainder of 21 days. BMSCs were alternatively encapsulated in either *TGF-β1 tethered KLD (Teth-KLD)*: 0.35% KLD with 35 μg/mL biotin-KLD [biotin-(aminocaproic acid)$_3$-(KLDL)$_3$], 2.1 μg/mL streptavidin (Pierce Biotechnology, Rockford, IL) and 100 ng/mL biotin-conjugated TGF-β1 (bTGF-β1, R&D Systems) or *TGF-β1 adsorbed KLD (Ads-KLD)*: 0.35% KLD with 100 ng/mL unlabeled TGF-β1 (R&D Systems). Both Teth-KLD

and Ads-KLD hydrogels were cultured in control (TGF-β1-free) medium. Hydrogels were cultured for up to 21 days.

DNA and ECM Biochemistry

During the last 24 hours of culture, medium was additionally supplemented with 5 μCi/mL of ^{35}S-sulfate and 10 μCi/mL of ^{3}H-proline to measure cellular biosynthesis of proteoglycans and proteins, respectively. Upon termination of culture, hydrogels were rinsed 4x30 minutes in excess unlabeled sulfate and proline, weighed wet, lyophilized, weighed dry, and digested in 250 μg/mL proteinase-K (Roche Applied Science, Indianapolis, IN) overnight at 60ºC. Digested samples were assayed for total DNA content by Hoechst dye binding[59], retained sulfated glycosaminoglycan (sGAG) content by DMMB dye binding assay[58], and radiolabel incorporation with a liquid scintillation counter. Conditioned culture medium collected throughout the study was also analyzed for sGAG content by DMMB dye binding.

TGF-β1 Controlled Delivery and Peptide Hydrogel Uptake

Immediately before use, ^{125}I-TGF-β1 (PerkinElmer, Waltham, MA) was purified by Sephadex G25 chromatography to remove small ^{125}I species that may result from time-dependent degradation of the label or incomplete purification as received from the supplier[107]. Sephadex G25 chromatography was performed with a 0.7 × 50 cm gravity fed column equilibrated in 1 M acetic acid supplemented with 0.1% BSA and 0.1% Triton X-100. Purified ^{125}I-TGF-β1 was collected in the void volume. Acellular 0.35% (w/v) KLD or 2% agarose solutions with and without ^{125}I-TGF-β1 (55pM, 1.4 ng/mL, 3500

Ci/mmol) or unlabeled TGF-β1 (10-100 ng/mL) were cast in acellular agarose molds as above. Hydrogels were incubated at 37ºC with agitation in a bath consisting of high glucose DMEM with 1% ITS+1 (Sigma-Aldrich), PSA, HEPES, Proline, sodium pyruvate, and NEAA. For TGF-β1 controlled delivery, the bath was changed every 2-3 days and saved for the duration of the experiment. At day 21, hydrogels were rinsed 3x to remove surface-bound TGF-β1 and mechanically disrupted (KLD) or melted (agarose) to measure retained TGF-β1. For peptide hydrogel TGF-β1 uptake, ^{125}I-TGF-β1 was added to the bath where indicated and the bath was not changed for 5 days. Bath and hydrogel samples were collected as before. The ^{125}I-radioactivity of all bath and hydrogel samples were quantified individually using a gamma counter. To account for the presence of small labeled species accumulated during the timecourse of experimentation, Sephadex G25 chromatography of the bath was performed weekly and at the end of all experiments and the fraction of free ^{125}I was determined[107]. The uptake ratio of free ^{125}I was also measured separately and included in the correction.

Aggrecan Extraction and Western Analysis

Aggrecan was extracted from hydrogel disks and analyzed as described previously[60]. Hydrogel disks were saturated with PBS and Complete Protease Inhibitors (Roche) and frozen at -20°C until extraction. Gels were extracted for 48 hours in 4M guanidinium hydrochloride, deglycosylated, and the resulting digest was lyophilized. Samples were reconstituted and 20 μg sGAG/lane was run on a 4-15% Tris-HCl gel at 100V for 1 hour. Proteins were transferred to a nitrocellulose membrane and probed with affinity-purified antibodies for aggrecan G1 domain (JSCATEG)[60].

Smad 2/3 and pSmad 2/3 Western Analysis

Hydrogels were mechanically disrupted via pipetting with extraction buffer consisting of Tris, NaCl, Triton X-100, and NP-40 with protease and phosphatase inhibitors. Extracts were sonicated, frozen, and stored in liquid nitrogen. For Western analysis, samples were thawed, vortexed, and analyzed for DNA content by Hoechst dye binding. Proteins were separated by 10% SDS-PAGE loaded with 0.1 μg DNA per lane. Proteins were transferred to a PVDF membrane and probed with Smad 2/3 or pSmad2 primary antibodies (Cell Signaling Technology, Danvers, MA) and HRP-conjugated, anti-rabbit secondary antibody. Membranes were stripped and reprobed with β-actin primary antibody (Cell Signaling Technology). For semi-quantification, band densitometry was performed using AlphaEaseFC (Alpha Innotech, Inc., San Leandro, CA) and Smad2/3 and pSmad2 were normalized both to β-actin as a loading control and to the day 4, medium-delivered TGF-β1 sample on each membrane.

Statistical analysis

All data are presented as mean ± sem. Data were analyzed with a mixed model of variance with animal as a random factor. Residual plots for dependent variable data were constructed to test for normal distribution. If this assumption was not met, data were transformed to ensure normality. Pairwise comparisons were made by *post hoc* Tukey tests with significance threshold set at $p<0.05$.

4.3 Results

bTGF-β1 Bioactivity and Peptide Hydrogel Tethering

The bioactivity of bTGF-β1 was verified by culturing bovine-BMSC-seeded peptide hydrogels in medium supplemented with both bTGF-β1 and TGF-β1 for 14 days. Peptide hydrogels cultured in bTGF-β1 and TGF-β1 accumulated 38 μg and 64 μg of sGAG, respectively, and both were significantly greater than 5 μg sGAG accumulated in TGF-β1-free controls ($p<0.001$). In addition, proteoglycan biosynthesis for bTGF-β1, TGF-β1, and TGF-β1-free controls were 109, 151, and 17 pmol/hr/μg DNA, respectively, with bTGF-β1 and TGF-β1 both significantly greater than TGF-β1-free ($p<0.001$). Thus, by both sGAG accumulation and proteoglycan biosynthesis bTGF-β1 stimulated chondrogenic differentiation of bovine BMSCs.

When combined with a molar excess of multivalent streptavidin, bTGF-β1 can be tethered to the biotinylated-KLD hydrogel via a high-affinity noncovalent bond (Teth-KLD). When bovine BMSCs were encapsulated in Teth-KLD and cultured for 14 days, no significant differences from TGF-β1-free controls were seen in either DNA or sGAG content (Fig. 4.1). However, with TGF-β1-supplemented medium non-tethered hydrogels had 4-fold higher DNA content than Teth-KLD by day 7 (Fig. 4.1A, $p<0.001$), which remained nearly 3-fold higher at day 14 ($p<0.001$). Similarly, sGAG content for untethered hydrogels with TGF-β1-supplemented medium was more than 6-fold higher than Teth-KLD at day 7 (Fig. 4.1B, $p<0.001$) and increased to nearly 18-fold higher by day 14 ($p<0.001$).

TGF-β1 Medium Takeaway

To investigate the duration of TGF-β1 medium supplementation required to stimulate chondrogenesis, TGF-β1 was removed from the culture medium at several timepoints during a 21-day culture experiment (Fig. 4.2). With only 4 days of culture in TGF-β1-supplemented medium, followed by 17 days of culture in TGF-β1-free medium, the DNA content of adult equine BMSC-seeded hydrogels was statistically equivalent to culture with 21 days of TGF-β1 stimulation (Fig. 4.2A) and more than 2-fold higher than TGF-β1-free controls ($p<0.001$). sGAG accumulation was more than 20-fold higher with 4 days of TGF-β1 stimulation than with TGF-β1-free culture (Fig. 4.2B, $p<0.001$). Furthermore sGAG accumulation with 4 days of TGF-β1 was only 30% lower than with 21 days of TGF-β1 supplementation ($p<0.01$).

Protein biosynthesis during day 20-21 of culture for hydrogels that were stimulated with TGF-β1 for the initial 4 days was more than 3-fold higher than TGF-β1-free controls (Fig. 4.2C, $p<0.001$) and was 10% of continuous TGF-β1 supplemented hydrogels ($p<0.001$). Proteoglycan biosynthesis for 4-day TGF-β1-stimulated hydrogels was nearly 5-fold higher than TGF-β1-free controls (Fig. 4.2D, $p<0.001$) and remarkably was over 30% of the continuous TGF-β1 stimulated hydrogels.

TGF-β1 Adsorbed Peptide Hydrogels Stimulate Chondrogenesis

Since 4 days of TGF-β1 supplementation stimulated BMSC chondrogenesis in peptide hydrogels, TGF-β1 was nonspecifically adsorbed onto KLD-peptide monomers (Ads-KLD) to determine if this method of delivery would provide sufficient pro-chondrogenic stimulus. When foal equine BMSCs were encapsulated in Ads-KLD and

cultured in TGF-β1-free medium, DNA content was 50% higher than TGF-β-free controls by day 7 (Fig. 4.3A, $p<0.001$) and was statistically equivalent to hydrogels with medium-delivered TGF-β1. No further increase in DNA content after day 7 was seen for Ads-KLD cultured BMSCs resulting in 60% lower DNA content for Ads-KLD than for medium-delivered TGF-β1 at day 21 ($p<0.001$). Ads-KLD cultured BMSCs accumulated equivalent sGAG to medium-delivered TGF-β1 throughout the entire 21 day culture period (Fig. 4.3B) with a final sGAG content that was 25-fold higher than TGF-β1-free controls ($p<0.001$). Consistent with sGAG content, proteoglycan biosynthesis in Ads-KLD was either higher or equivalent to hydrogels cultured with medium-delivered TGF-β1 through 21 days (Fig. 4.3C) and was 4-fold higher than the TGF-β1-free control at day 21 ($p<0.001$). In addition, the sGAG retained within the hydrogel as a percentage of the total produced (including sGAG lost to the conditioned medium) was 65% and 60% for BMSCs cultured in Ads-KLD and medium-delivered TGF-β1, respectively, at day 7 (difference was not significant), and remained constant over 21 days in culture (Fig. 4.3D).

The solid matrix as a percentage of the total wet mass for BMSCs in Ads-KLD was equivalent to hydrogels with medium-delivered TGF-β1 at days 7 and 14 (Fig. 4.3E), while by day 21 the Ads-KLD encapsulated BMSCs had produced 25% less solid matrix than hydrogels with medium-delivered TGF-β1 ($p<0.05$). However, Ads-KLD BMSCs still had more than 2-fold higher percentage solid than TGF-β1-free controls ($p<0.001$). Protein biosynthesis showed that Ads-KLD cultured BMSCs were equivalent to culture with medium-delivered TGF-β1 at day 7 (Fig. 4.3F), but dropped to 50% of medium-delivered TGF-β1 at days 14 and 21 ($p<0.001$). Ads-KLD encapsulated BMSCs still had

more than 2-fold higher protein biosynthesis than TGF-β1-free controls at day 21 ($p<0.01$).

Controlled Delivery of TGF-β1 with Peptide Hydrogels

^{125}I-labeled TGF-β1 was adsorbed onto KLD peptide monomers prior to self-assembly or adsorbed onto molten agarose prior to gelation (TGF-β1 loaded within the hydrogel) without cells. Independent experiments showed that the uptake ratio (ratio of TGF-β1 concentration in the gel to concentration in the bath) of TGF-β1 did not decrease after 2 days of diffusion out of the adsorbed hydrogels indicating that 2 days was sufficient for the system to reach equilibrium (data not shown). Bath changes were thus conducted every 2-3 days and TGF-β1-loaded hydrogels were incubated at 37°C in a TGF-β1-free bath for 21 days. Collected bath samples were analyzed for ^{125}I-TGF-β1 content (Fig. 4.4A). By day 3, 16% of the total ^{125}I-TGF-β1 loaded was washed out from KLD-peptide hydrogels, while nearly 40% was washed out from agarose hydrogels. By the end of 21 days, TGF-β1 washout had increased to 35% for KLD-peptide and nearly 60% for agarose (Figs. 4.4A, 4.4B, $p<0.001$). At day 21, hydrogels were melted at 70°C and mechanically disrupted to measure retained ^{125}I-TGF-β1. KLD peptide retained nearly 50% of the total ^{125}I-TGF-β1 loaded versus 14% for agarose hydrogels (Fig. 4.2B, $p<0.001$).

To determine the effect of TGF-β1 delivery method on hydrogel adsorption, ^{125}I-TGF-β1 was added to either the bath or the hydrogel itself (TGF-β1 loaded in bath and gel, respectively) and incubated with agitation at 37°C for 5 days without bath changes. The uptake ratio of ^{125}I-TGF-β1 (ratio of ^{125}I-TGF-β1 concentration in the gel to the bath)

was 5-fold higher for KLD-peptide than for agarose hydrogels (Fig. 4.4C, $p<0.001$). In addition, for both KLD peptide and agarose, the uptake ratio was more than 2-fold higher when ^{125}I-TGF-β1 was loaded in the gel rather than in the bath ($p<0.001$). Also, in both KLD peptide and agarose the uptake ratio of bath loaded ^{125}I-TGF-β1 was still greater than one (18.5 ± 1.3 and 2.9 ± 0.2, respectively, mean ± sem). When excess unlabeled TGF-β1 (100 ng/mL) was added to hydrogel-loaded ^{125}I-TGF-β1 KLD peptide and agarose, the uptake ratio decreased by 16% and 27%, respectively (Fig. 4.4D, $p<0.001$), and in both cases remained greater than one (72.2 ± 1.3 and 12.5 ± 0.2 for KLD and agarose, respectively).

TGF-β1-adsorbed Hydrogels Produce Full-Length Aggrecan

Bovine BMSCs encapsulated in both Ads-KLD and TGF-β1-adsorbed agarose (Ads-Agarose) produced equivalent sGAG to medium-delivered TGF-β1 by day 7 (Figs. 4.5A and 4.5B, respectively, $p<0.001$). By day 21, total sGAG produced in Ads-KLD and Ads-Agarose was 40% of medium-delivered TGF-β1 ($p<0.001$), but was 6-fold and 3-fold higher than TGF-β1-free controls, respectively ($p<0.001$). To further characterize the BMSC chondrogenic phenotype, proteoglycans were extracted from KLD-peptide and agarose samples and analyzed by Western blotting with an anti-G1 aggrecan antibody. With both adsorbed and medium-delivered TGF-β1, a large macromolecular species was identified running at the molecular weight of full-length aggrecan in KLD peptide and agarose (Fig. 4.5C). In KLD peptide, full-length aggrecan was the predominant species detected, consistent with the virtual absence of aggrecanase activity in peptide hydrogels (Chapter 2). In agarose with medium-delivered TGF-β1, a doublet band near 65 kDa was

the major immunoreactive band detected. However, in Ads-agarose the intensity of this doublet band was decreased and full-length aggrecan was the major product observed. This is consistent with a reduced level of aggrecanase activity when TGF-β1 was adsorbed to agarose hydrogels as compared to medium-delivered TGF-β1.

KLD Peptide Adsorbed TGF-β1 Signals via SMAD2/3

A 50-60 kDa species was detected via anti-Smad2/3 Western blotting in all samples after one day of culture (Fig. 4.6A). In samples encapsulated in Ads-KLD or treated with medium-delivered TGF-β1, pSmad2/3 was also detected at day 1. In addition, for a subset of animal donors (animal #2 in Fig. 4.4.6A) pSmad2/3 was detected in Teth-KLD hydrogels. pSmad2/3 was detected throughout 21 days of culture in peptide hydrogels cultured in TGF-β1 supplemented medium and through day 4 of culture in Ads-KLD samples (Fig. 4.6B). Total Smad2/3 was detected in all samples through day 21, however it was more abundant for Ads-KLD samples than any other condition from day 4-14 (Fig. 4.6B), making it a poor loading control. Semi-quantitative band densitometry showed statistically equivalent pSmad2/3 signaling for Ads-KLD and medium-delivered TGF-β1 samples at days 1 and 4, with Ads-KLD pSmad2/3 dropping to levels comparable to TGF-β1-free controls from day 14-21. For total Smad2/3, 2-factor ANOVA (for TGF condition and time) confirmed a significant trend with TGF condition ($p<0.05$), but not time, although no pairwise comparisons were significant.

4.4 Discussion

TGF-β1 adsorbed to KLD peptide hydrogels (Ads-KLD) stimulated chondrogenesis of encapsulated BMSCs, inducing cell proliferation and producing a cartilage-like ECM that was similar to hydrogels stimulated by medium-delivered TGF-β1. Delivery of an equivalent amount of TGF-β1 by an alternate method, tethering the growth factor to the KLD peptide via a biotin-streptavidin linkage (Teth-KLD), did not stimulate any marker for chondrogenesis above TGF-β1-free controls. Robust efficacy of Ads-KLD was demonstrated by the capacity to induce chondrogenesis of BMSCs isolated from two different species, equine and bovine, resulting in significant increases in hydrogel sGAG production over BMSCs cultured in TGF-β1-free conditions. In addition, equine BMSCs encapsulated in Ads-KLD produced neotissue with statistically equivalent cartilage ECM content and biosynthesis to KLD-encapsulated BMSCs stimulated by medium-delivered TGF-β1.

TGF-β1 encapsulation in both acellular KLD-peptide and agarose hydrogels resulted in TGF-β1 adsorption and retention in both hydrogels for 21 days. Uptake ratio experiments confirmed higher TGF-β1 affinity for KLD peptide than for agarose, and showed that TGF-β1 uptake was higher when it was mixed with peptide solutions prior to gel assembly than when diffusing into the assembled peptide hydrogel from the bath. These experiments demonstrate the capacity of TGF-β1 to adsorb to two very different biomaterials, and a specific interaction between TGF-β1 and KLD peptide that was not present with agarose. TGF-β1 has been adsorbed to a wide range of materials including titanium fiber[94], collagen-coated and uncoated titanium alloys[99], and acidic gelatin[108,109], which is consistent with our results showing TGF-β1 adsorption to both uncharged

agarose hydrogels and amphiphilic, zwitterionic KLD-peptide hydrogels. Given that the pore size of 2% low-melting-point (hydroxyethylated) agarose is approximately 35 nm[110] and the dimensions of TGF-β1 are less than 6 nm[111], while in KLD peptide individual node-to-node fiber lengths have been measured at 370nm[112], the higher TGF-β1 affinity for KLD peptide than agarose hydrogels is not likely to be due to restricted diffusion[113]. It may be related to the presence of negatively-charged aspartic acid residues in KLD peptide since basic TGF-β1 (pI=9.5)[108] has been shown to interact electrostatically with acidic gelatin[108,109]. In addition, electrostatic interactions determine the release of small dye molecules from self-assembling peptides[113,114], and these peptides have been shown to bind numerous growth factors including PDGF-BB, VEGF-A, bFGF, and angiopoietin-1 likely through non-covalent adsorption to the peptide nanofibers[86,113].

TGF-β1 uptake experiments also demonstrated that its affinity for KLD peptide depends on whether the peptide is in solution or assembled into an insoluble hydrogel (Fig. 4.4C). The dependence of the TGF-β1 interaction with KLD peptide on assembly may also involve electrostatic interactions. Since the assembled KLD peptide (pI=6.25, assuming pKa of each amino acid in the peptide is equal to the corresponding individual amino acid pKa as reported in Stryer Biochemistry[115]) has minimal net negative charge (-0.1) at neutral pH, most electrostatic charges are likely shielded by adjacent peptides in the assembled gel. Thus when TGF-β1 is added to KLD peptide solution prior to assembly, it may have an increased capacity to adsorb than when TGF-β1 is added to the physiologically buffered bath and diffuses into the assembled peptide hydrogel.

Chondrogenesis of BMSCs was shown to require TGF-β1 stimulation for just the initial 4 days of culture in peptide hydrogels. This may be due in part to the capacity of

KLD peptide to uptake TGF-β1 from the bath and thereby sustain TGF-β1 stimulation beyond the initial 4 days. Our results are consistent with a recent report where transient exposure to TGF-β1 for 2 weeks was shown to enhance the biomechanical and biochemical properties of chondrocyte-seeded agarose hydrogels[116] over medium-delivered TGF-β1 stimulation. Similarly, 3 weeks of transient TGF-β1 stimulation for BMSC-seeded agarose has been shown to produce equivalent cartilage-like biochemical properties to medium-delivered TGF-β1 stimulation[117].

Aggrecan Western analysis confirmed that full-length aggrecan was produced by Ads-KLD stimulated BMSCs, comparable to medium-delivered TGF-β1 stimulation of KLD encapsulated BMSCs and consistent with a recent report (Chapter 2). In agarose hydrogels stimulated by medium-delivered TGF-β1, the major immunoreactive product detected was a doublet band near 65 kDa consistent with the aggrecanase generated NITEGE neoepitope[61]. Consistent with these results, TGF-β1 has been shown to induce accumulation of aggrecan cleavage products in chondrocyte-seeded agarose[92] and in BMSC-seeded agarose hydrogels (Chapter 2). In contrast with medium-delivered TGF-β1, agarose hydrogels with adsorbed TGF-β1 stimulated the production of predominantly full-length aggrecan with reduced accumulation of aggrecan cleavage products (Fig. 4.5C). Clarke *et al*. has recently shown that cells sense TGF-β1 dose by depleting it through constitutive receptor trafficking processes[118]. In addition, tumor cells with impaired receptor trafficking led to TGF-β1 overproduction, which correlated with a poor disease prognosis. Thus, TGF-β1 dose and signaling duration can have a significant impact on cell decisions and function, suggesting that adsorbed TGF-β1, which would be expected to signal for an initial period and then deplete, may stimulate chondrogenesis. In

contrast, medium-delivered TGF-β1 may provide a sustained signal that potentially upregulates aggrecan catabolism in addition to chondrogenesis. Analysis of Smad 2/3 phosphorylation supported this idea of unique signaling paradigms for adsorbed and medium-delivered TGF-β1, with transient signaling for adsorbed TGF-β1, dissipating after one week, and sustained signaling for medium-delivered TGF-β1, with pSmad 2/3 levels steady for the first week and trending higher in weeks 2-3 (Fig. 4.6C).

Tethered TGF-β1 did not stimulate accumulation of a cartilage-like ECM or induce proliferation of BMSCs encapsulated in peptide hydrogels. This is in contrast to recent reports where covalently-tethered TGF-β1 stimulation induced myofibroblast differentiation[119], increased matrix production of vascular smooth muscle cells[120], and initiated cartilage-like ECM production in a magnetic-bead pellet culture system[96]. In addition, biotin-streptavidin sandwich tethered IGF-I in self-assembling peptide hydrogels improved cell survival and function after experimentally-induced myocardial infarction in a rat model[20]. It was thus surprising that tethered KLD in the current study was an ineffective chondrogenic stimulus. Potential explanations include improper presentation of the tethered TGF-β1 ligand to the cell surface preventing receptor binding, blocked ligand internalization by the high-affinity biotin-streptavidin linkage leading to altered intracellular signaling, and steric interference between the ligand and cell surface receptor generated by newly secreted matrix proteins shutting down signaling prematurely. Phosphorylation of Smad 2/3 by teth-KLD encapsulated BMSCs at day 1 for a subset of samples (Fig. 4.6A) suggests that tethered TGF-β1 can generate intracellular signal and that further optimization of the TGF-β tethering technology may enable effective chondrogenic stimulation, potentially through increasing TGF-β1 dose.

4.5 Summary

Adsorption of TGF-β1 to KLD peptide and agarose hydrogels stimulated chondrogenesis of BMSCs isolated from both bovine and equine sources. KLD peptide had significantly higher TGF-β1 uptake and retained significantly more TGF-β1 during wash out experiments than agarose hydrogels. Introducing unlabeled TGF-β1 at two orders of magnitude higher concentration than radiolabeled TGF-β1 had a minor impact on uptake. Adsorbed TGF-β1 stimulated the production of full length aggrecan by BMSCs in both KLD peptide and agarose hydrogels, while medium-delivered TGF-β1 stimulated aggrecan cleavage product formation in agarose hydrogels, potentially due to differences in Smad 2/3 phosphorylation. Given the wide diversity cell functions controlled by TGF-β1 signaling[101,102] and the importance of TGF-β1 signal duration and depletion kinetics in determining outcome[118], tuning the delivery duration and dose for pro-chondrogenic growth factors will likely be critical to the success of BMSC-based cartilage resurfacing technologies.

4.6 Acknowledgements

I would like to thank Dr. Richard T. Lee for numerous discussions and invaluable advice on strategies to tether and adsorb growth factors to self-assembling peptide hydrogels. Thank you to Sangwon Byun for generous assistance with uptake ratio and washout experiments. Thank you to Eric Vanderploeg and John Kisiday for helpful discussions on study design and hands on assistance with protocol development. Thank you to John Kisiday and Dave Frisbie for the supply of equine tissue. Thank you to John

Sandy for the donation of aggrecan antibodies. Finally, thank you to Alan Grodzinsky for scientific guidance and leadership.

This work was funded by the National Institutes of Health (NIH EB003805, NIH AR33236, and NIH AR45779) and a National Institutes of Health Molecular, Cell, and Tissue Biomechanics Training Grant Fellowship.

4.7 Tables

Table 4.1 Percent sGAG Retained

(† vs. TGF)

	KLD			Agarose		
	Day 7	**Day 14**	**Day 21**	**Day 7**	**Day 14**	**Day 21**
TGF	59±1	58±1	58±1	56±2	50±2	41±1
Ads-KLD	52±2	44±1†	30±1†	55±1	45±1	39±2

4.8 Figures

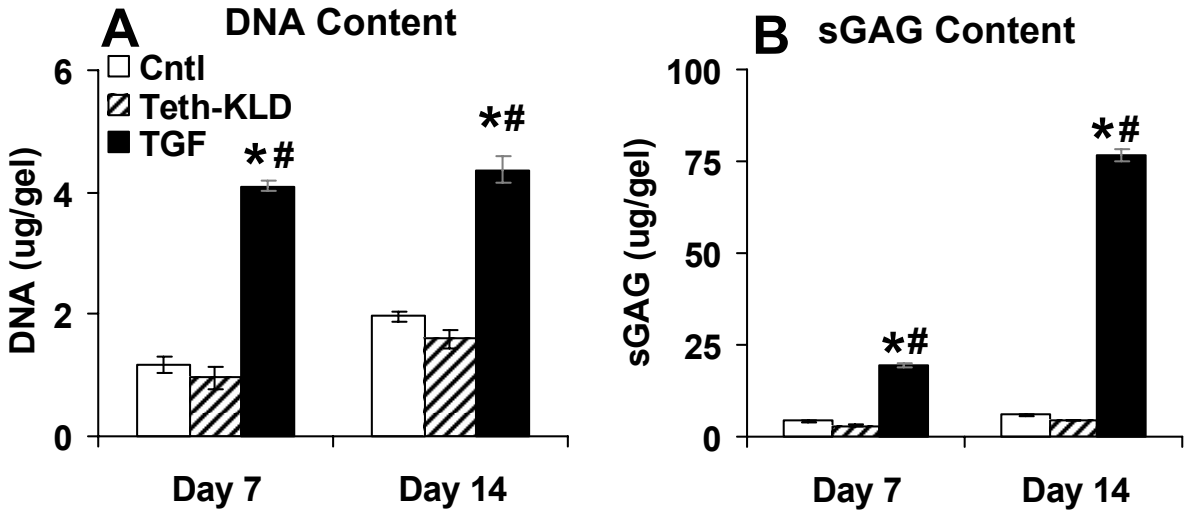

Figure 4.1 TGF-β1 tethered to KLD hydrogels (Teth-KLD); DNA and sGAG content Bovine BMSCs encapsulated in Teth-KLD or unmodified KLD peptide hydrogels and cultured in TGF-β1-free medium **(Cntl)**, or continuous TGF-β1 supplemented medium **(TGF)**. **(A)** DNA Content. **(B)** sGAG Content. **Stats:** mean ± sem, n=4; * vs. Cntl; # vs. Teth-KLD; $p<0.001$.

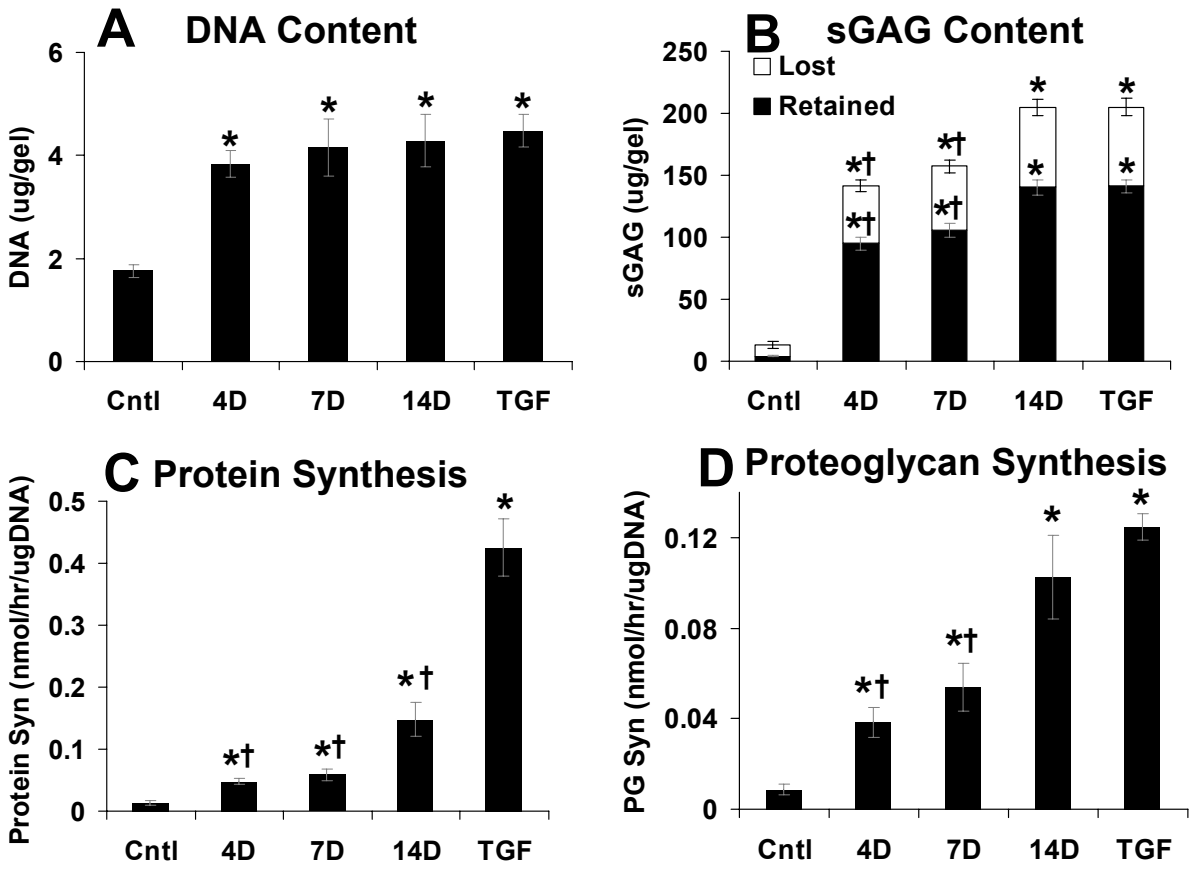

Figure 4.2 TGF-β1 takeaway DNA content, sGAG content, and ECM biosynthesis
Adult equine BMSCs encapsulated in KLD peptide hydrogel and cultured for 21 days in TGF-β1-free medium **(Cntl)**, 4, 7, or 14 days of TGF-β1 supplemented medium followed by TGF-β1-free medium (**4D**, **7D**, or **14D**, respectively), and continuous TGF-β1 supplemented medium **(TGF)**. **(A)** DNA Content. **(B)** sGAG Content. **(C)** Protein Biosynthesis. **(D)** Proteoglycan Biosynthesis. **Stats:** mean ± sem, n=8 (4 gels x 2 animals); * vs. Cntl; † vs. TGF; $p<0.01$.

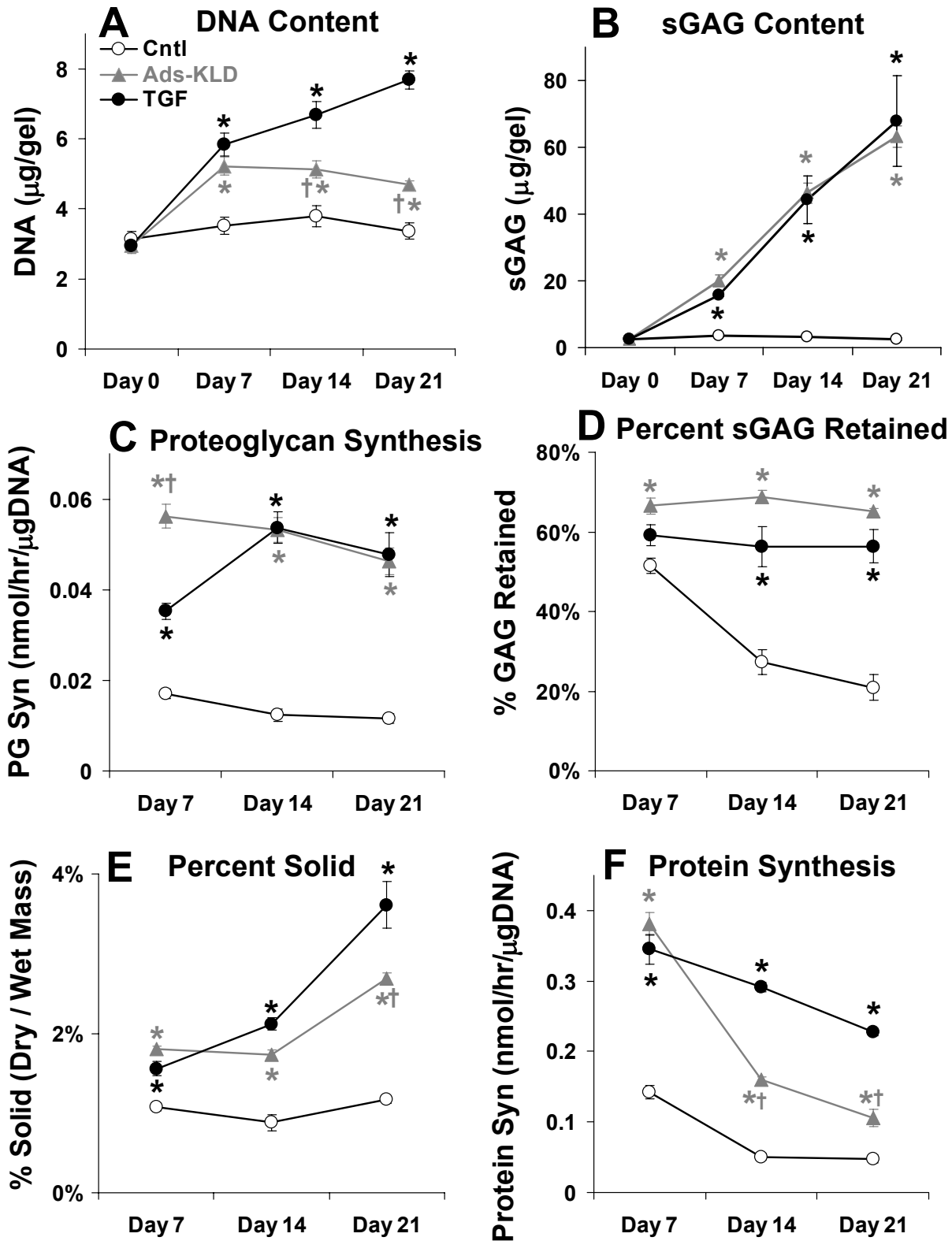

Figure 4.3 TGF-β1 adsorbed to KLD hydrogels (Ads-KLD); DNA content, sGAG content, and ECM biosynthesis

Young equine BMSCs encapsulated in Ads-KLD or unmodified KLD peptide hydrogels and

cultured in TGF-β1-free medium **(Cntl)**, or continuous TGF-β1 supplemented medium **(TGF)**. **(A)** DNA Content. **(B)** sGAG Content. **(C)** Proteoglycan Biosynthesis. **(D)** Percent sGAG retained in hydrogels vs. total produced (including sGAG lost to conditioned medium). **(E)** Percent solid matrix, dry weight vs. wet weight. **(F)** Protein Biosynthesis. **Stats:** mean ± sem, n=8 (4 gels x 2 animals); * vs. Cntl; † vs. TGF; $p<0.05$.

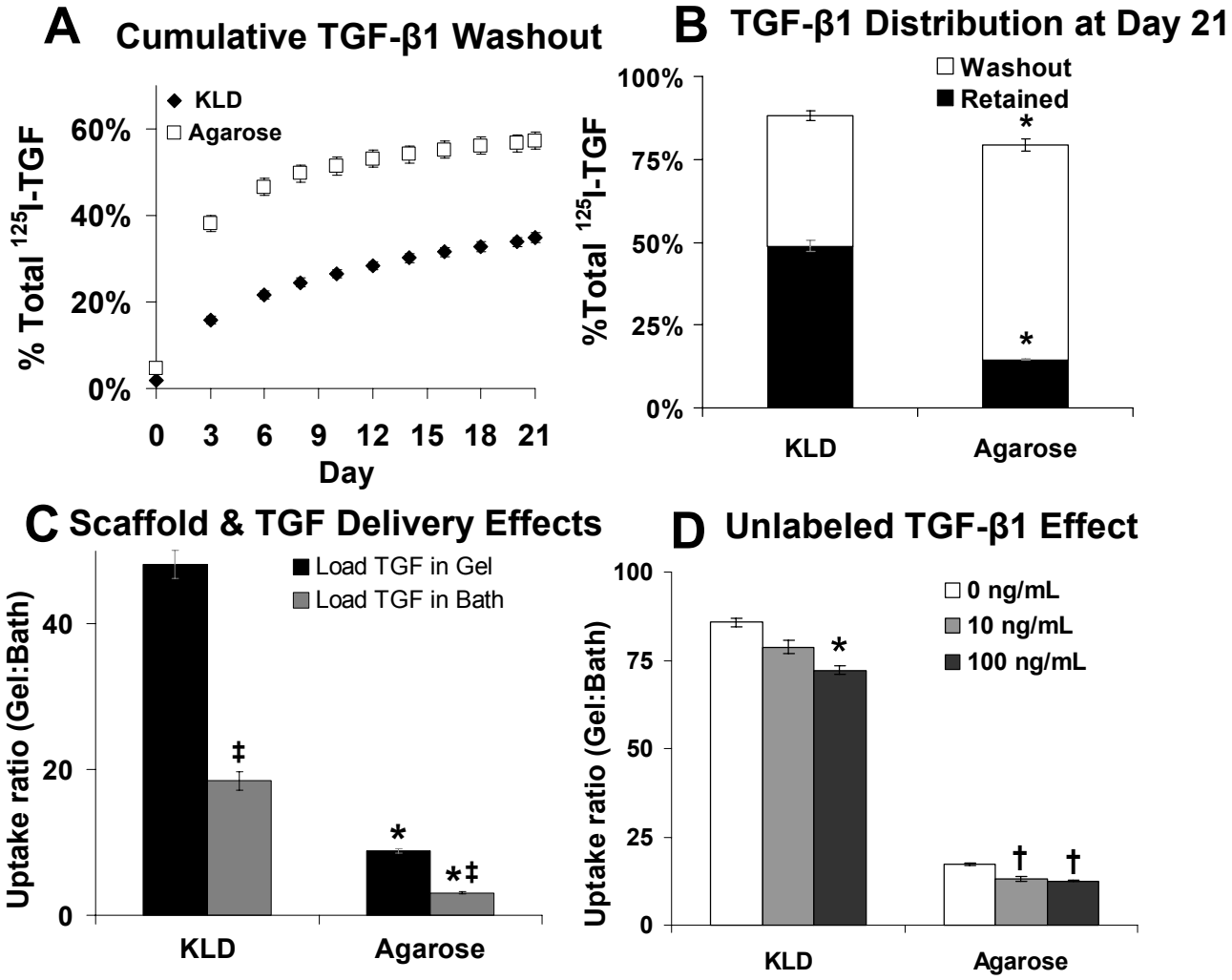

Figure 4.4 TGF-β1 adsorption to acellular KLD and agarose hydrogels
(A) Cumulative ^{125}I-TGF-β1 washout with bath changes after encapsulation in KLD or agarose hydrogels. Each datapoint corresponds to a complete bath change. **(B)** ^{125}I-TGF-β1 distribution in samples after 21-day washout shown in (A). **(C)** Uptake ratio of ^{125}I-TGF-β1 for KLD peptide and agarose hydrogels scaffolds when ^{125}I-TGF-β1 was encapsulated within the gel prior to gel casting **(Load TGF in Gel)** or when it diffused in from the bath after gel casting **(Load TGF in Bath)**. **(D)** Uptake ratio of ^{125}I-TGF-β1 when encapsulated with 0, 10, or 100 ng/mL of unlabeled TGF-β1 within KLD peptide or agarose hydrogels. **Stats:** mean ± sem, n=6 (A,B,C), n=4 (D); * vs. KLD without unlabeled-TGF-β1; † vs. agarose without unlabeled-TGF-β1; ‡ vs. Load TGF in Gel; $p<0.001$.

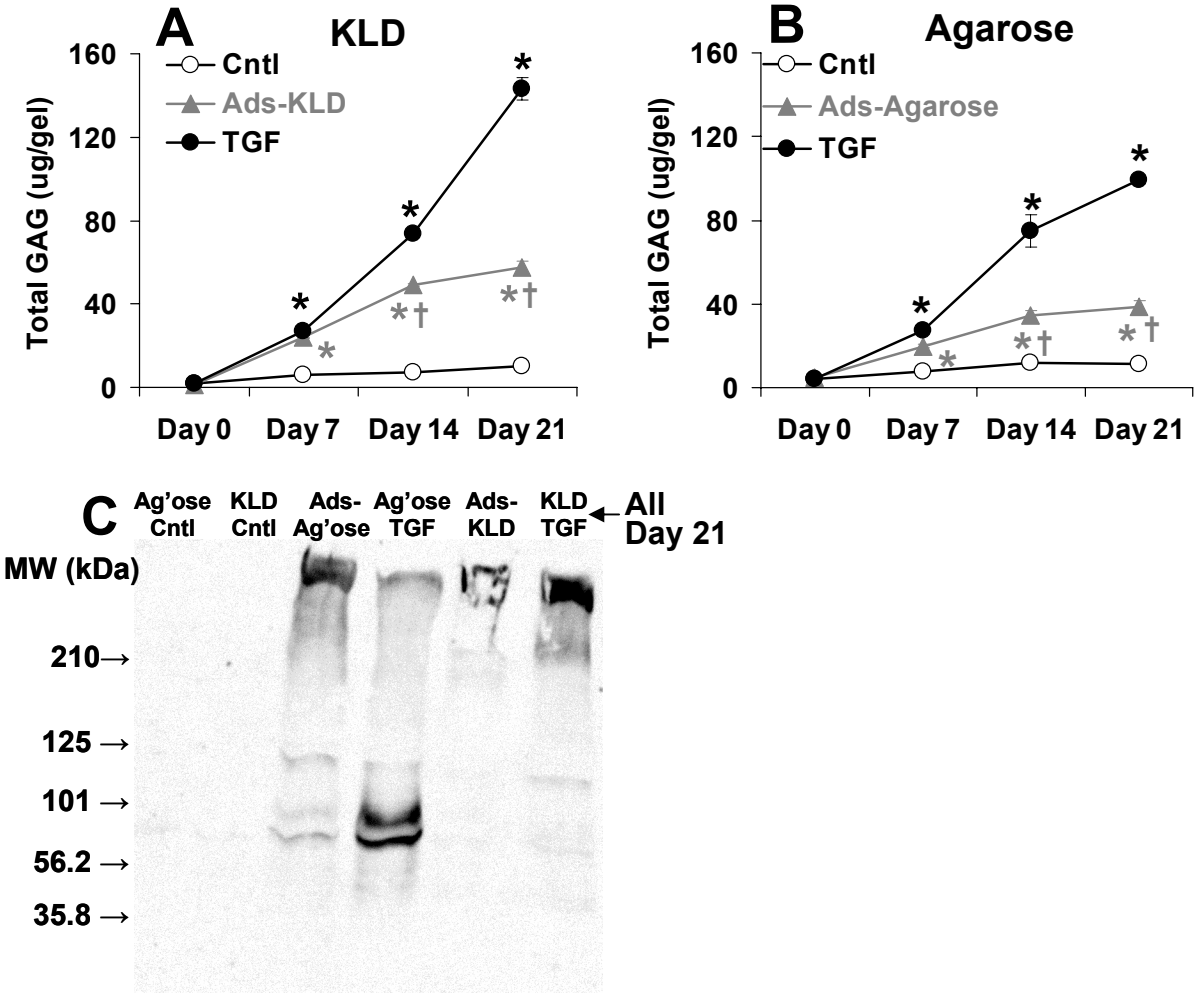

Figure 4.5 sGAG production in TGF-β1 adsorbed KLD peptide and agarose hydrogels
Total sGAG production by bovine BMSCs encapsulated in TGF-β1 adsorbed **(A)** KLD peptide **(Ads-KLD)** or **(B)** agarose **(Ads-Agarose)** or cultured in corresponding unmodified hydrogels with TGF-β1-free medium **(Cntl)** or continuous TGF-β1 supplemented medium **(TGF)**. **(C)** Anti-G1 domain aggrecan western blot of proteoglycans extracted from Ads-KLD, Ads-Agarose, and corresponding Cntl and TGF hydrogels. **Stats:** mean ± sem, n=4; * vs. Cntl; † vs. TGF; $p<0.001$.

A. Day 1

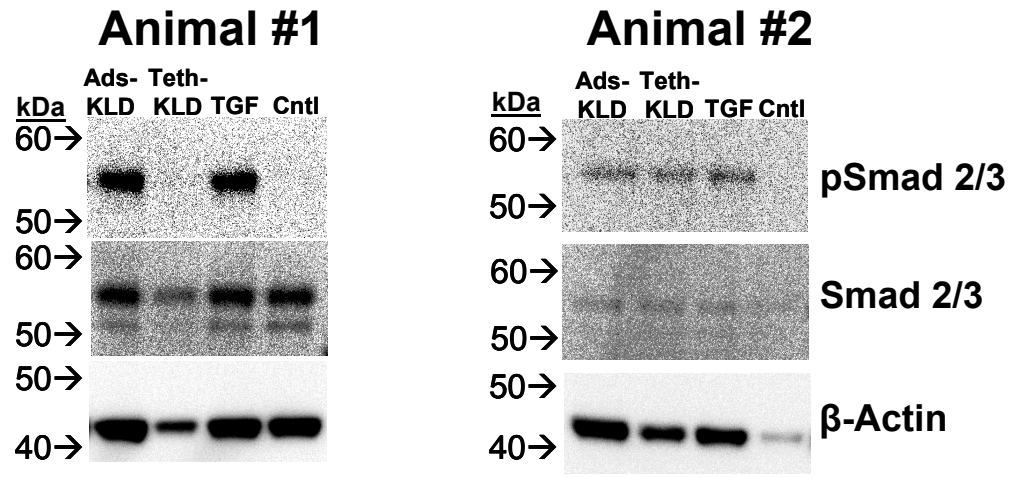

B. Day 4-21

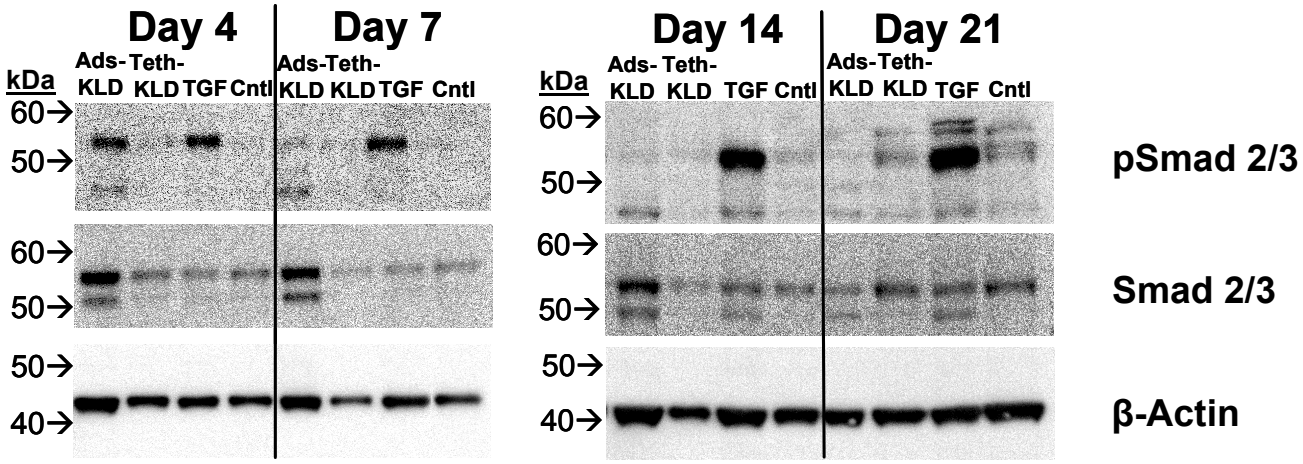

C. Semi-Quantification

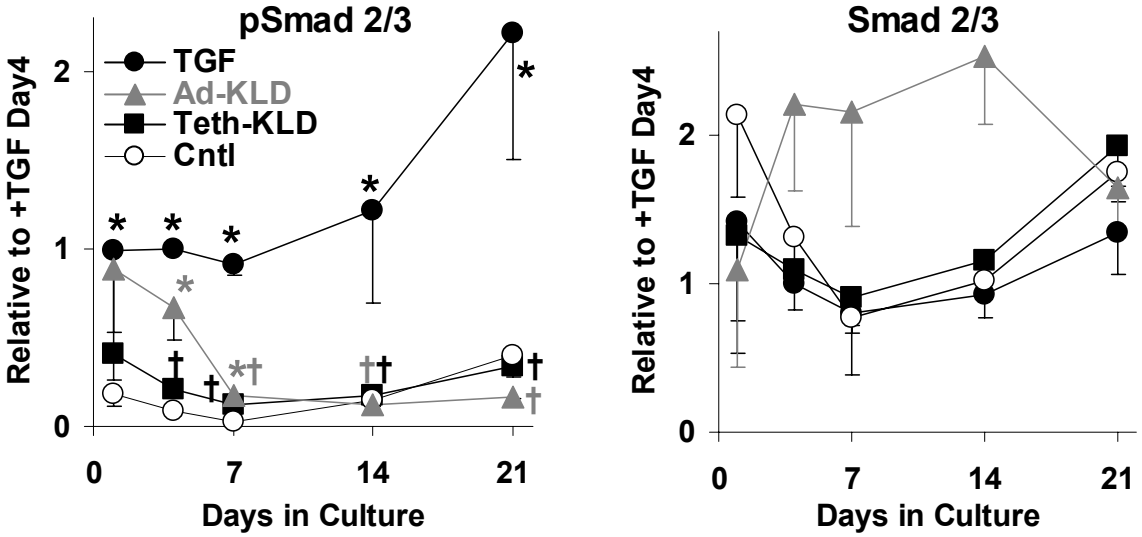

Figure 4.6 Smad 2/3 phosphorylation for bovine BMSCs encapsulated in KLD peptide hydrogels

BMSCs were stimulated by adsorbed, tethered, or medium-delivered TGF-β1 (**Ads-KLD, Teth-KLD, or TGF,** respectively) or cultured in TGF-β1-free medium **(Cntl)**. **(A)** Day 1 western blots for pSmad 2/3, Smad 2/3, and β1-actin from two different BMSC donors. **(B)** Day 4-21 western blots for animal #1. **(C)** Semi-quantification of Smad 2/3 phosphorylation by band densitometry. **Stats:** mean ± sem, n=3; ***** vs. Cntl; **†** vs. TGF; $p<0.05$.

Chapter 5. Summary and Conclusions

A technique for encapsulation of bone marrow stromal cells (BMSCs) within self-assembling peptide hydrogels and inducing chondrogenic differentiation has been developed (Chapter 2, Appendix C). Encapsulating BMSCs within peptide hydrogels enhanced ECM production, cell proliferation, and reduced aggrecan catabolism compared to BMSC chondrogenesis in agarose hydrogels. Given that chondrocyte-seeded tissue engineering strategies are established in clinical practice for cartilage repair (Chapter 1), neotissue forming capacity BMSC-seeded peptide hydrogels was compared to that for chondrocytes from both young and adult donors (Chapter 3). Young chondrocytes produced neotissue with the highest sGAG content, which is consistent with expectation for cells isolated from cartilage that is still developing and actively remodeling. However, young chondrocytes were not compatible with the goal of delivering an autologous-cell seeded therapy to adult patients in a single surgical procedure. Thus, it was a significant finding that ECM production of adult BMSCs was superior to adult chondrocytes and that the dynamic mechanical properties of adult BMSC-seeded neotissue exceeded those of even young chondrocytes.

Neotissue production by BMSCs is dependent upon chondrogenic differentiation, which must be induced by the addition of bioactive factors. For *in vitro* work, the culture medium has commonly been supplemented with transforming growth factor β1 (TGF-β1) and dexamethasone to stimulate chondrogenesis[16]. However, for *in vivo* applications cost of repeated dosing and undesirable systemic effects of potent prochondrogenic growth factors motivate the need for local, controlled release. A technology for adsorbing TGF-β1 to self-assembling peptide hydrogels was designed (Chapter 4), which retained TGF-

β1 within the peptide for up to 21 days and stimulated neotissue production comparable to medium-delivered TGF-β1.

One technical challenge of note is the sensitivity of BMSCs to soluble self-assembling peptide solutions. These solutions are inherently at low pH and BMSCs must be mixed with the viscous peptide solution and injected into the casting and assembly mold rapidly to maintain viability (60 seconds is a good maximum BMSC exposure to soluble peptide before assembly). Exceeding this time will likely cause cell death and inconsistent chondrogenesis for the surviving population. Two other factors that may be a source of variability in neotissue production are cell seeding density and peptide concentration. Both present technical challenges; cell seeding density because a miniscule fraction of the total cell population was counted by hand with a hemocytometry slide and peptide concentration because the mass of peptide was close to the lower sensitivity limit of the mass balance used. Given that cell-cell contact, cell-peptide adhesion, and hydrogel contraction were proposed to be central to enhanced chondrogenesis in peptide hydrogels (Chapter 2), variations in cell seeding density and peptide concentration may dramatically impact the nature of neotissue produced. Potentially related is the variation in uptake ratio at equilibrium for acellular peptide hydrogels (Figure 4.4). If peptide concentration is variable and responsible for the differences, it may suggest that different doses of TGF-β1 may have been administered in each experiment, contributing to variable ECM production.

The virtual absence of chondrogenesis in BMSCs seeded in TGF-β1 tethered peptide hydrogels was surprising and potentially should not be interpreted as a conclusive failure of this technology. Smad 2/3 analysis provided a glimmer of hope by showing

phosphorylation after one day in culture in a subset of samples (Figure 4.6). Looking at Smad 2/3 phosphorylation at multiple timepoints within the first 24 hours of culture may clarify the capacity for tethered TGF-β1 to signal. An additional potential complicating factor is the possibility that the high-affinity bond in the tether system changes the availability of TGF-β1 to signaling such that a higher dose may be needed than in the adsorbed case. For example, TGF-β1 trapped within peptide fibers during self-assembly may diffuse out when nonspecifically adsorbed but not when biotin-streptavidin tethered. Increasing the dose of tethered TGF-β1 may thus be necessary to generate sufficient bioavailability.

Another related question is whether TGF-β1 stimulates BMSC-mediated breakdown of the peptide scaffold. If so it may be that cells can access additional TGF-β1 stores as they degrade, remodel, and replace the peptide with newly secreted ECM. This is of particular interest in the adsorbed TGF-β1 system where 50% of the dose is retained in acellular peptide hydrogels after 21 days in washout experiments (Figure 4.4). A simple test of this hypothesis would be to culture BMSCs with ^{125}I-TGF-β1 adsorbed peptide hydrogels and measure radiolabel retention within the neotissue. BMSC-mediated remodeling would likely release any ^{125}I-TGF-β1 stores by day 21, in contrast to the acellular experiment.

The *in vitro* model system developed in this work is well suited to developing an understanding of neotissue formation sensitivity to all of the above mentioned parameters. However, successful cartilage repair in the clinic will require testing in animal models and human subjects with the goals of achieving durable cartilage repair, native physiological function, and stable integration with surrounding cartilage. The work in this

thesis provides a foundation for designing these *in vivo* studies. With the capacity to enhance chondrogenesis of BMSCs, reduce aggrecan catabolic activity, and deliver prochondrogenic factors, self-assembling peptide hydrogels are a promising candidate technology for cartilage repair and regeneration.

Appendix A. Chondrogenesis of BMSCs Genetically Modified to Express TGF-β1

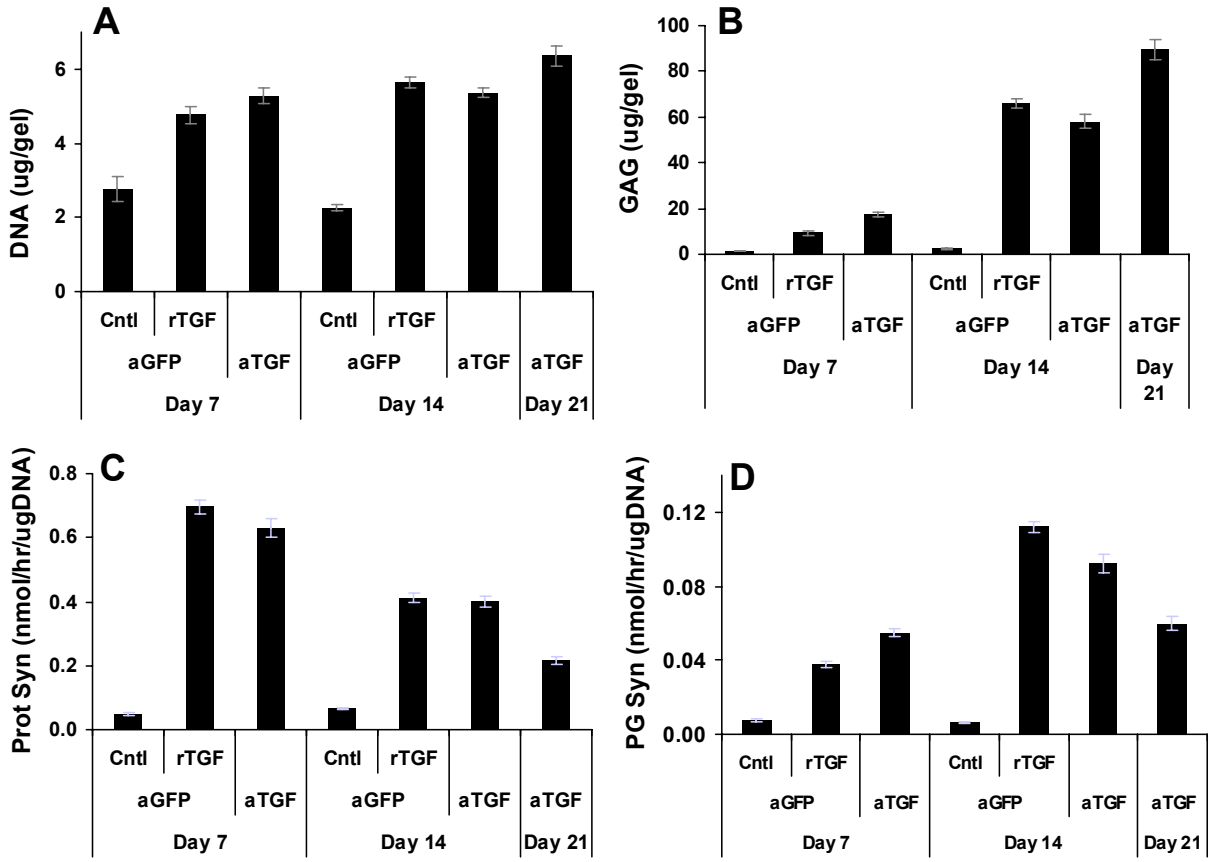

Figure A.1 Chondrogenesis of ads-TGF-β1 transfected bovine BMSCs encapsulated in peptide hydrogels

BMSCs transfected with 7000 adenoviral particles/cell of GFP or TGF-β1 vector (**aGFP** or **aTGF**, respectively). aGFP hydrogels were cultured with or without medium-delivered recombinant human TGF-β1 (**rTGF** or **Cntl**, respectively). **(A)** DNA Content, **(B)** sGAG Content, **(C)** Protein Biosynthesis, **(D)** Proteoglycan Biosynthesis.

Appendix B. BMSC Isolation from Bovine Tissue

Adapted from protocols developed by J Connelly, J Mouw, P Kopesky, and J Kisiday

Supplies
Bovine stifle joint (Research 87, Marlborough, MA)

Bone Marrow Harvest and Processing
1. Prepare 1x50mL conical with 25 mL PBS+PSA for each bone to be harvested
2. Remove all connective tissue and muscle around mid-diaphysus of each bone
3. Clean bone with 70% ethanol
4. Cut the bone with a sterilized hand-saw blade and transfer to the tissue culture hood
5. Carefully removed bone marrow with a forceps and small scoop and transfer to 50mL conical tubes with PBS. Avoid scraping the interior surface of the bone
6. Break up bone marrow by vigorous pipetting with a 25mL followed by 5mL pipette. May also need to use a syringe without a needle attached to apply enough pressure
7. Continue to homogenize bone marrow by passing the material through a 16 gauge needle
8. Centrifuge homogenized bone marrow 1000x g for 15 minutes
9. Carefully aspirate supernatant and the fatty layer
10. Resuspend in fresh PBS, pass material through an 18 gauge needle and then through a 70 μm cell strainer

Nucleated Cell Count and Cell Plating
1. Dilute cell suspension in Ammonium Chloride-Tris Base (7.6mg/mL AmCl, 2.4mg/mL Tris Base) (** JC suggested 1:1 dilution in 4% acetic acid); 1:20 dilution in AmCl/Tris for nucleated cell count via Trypan Blue (** Dilutions may need to be adjusted for each harvest.)
2. Obtain approximate nucleated cell count
3. Centrifuge cell suspension at 200 x g for 15 min
4. Aspirate supernatant and add low glucose DMEM + 10% ES-FBS, PSA, HEPES, & 1ng/mL b-FGF
5. Pre-plate approximately $75x10^6$ cells in 5mL on 100mm tissue culture treated petri dishes
6. Incubate for 30 min to allow rapidly adhering cells to attach
7. Transfer media and non-adherent cells to a T-flask and add another 10mL expansion medium (approximately $1x10^6$ cells/cm^2 in 15 mL media; ~$75x10^6$/T-75)
8. After 2 days in culture, remove expansion media and add fresh expansion medium
9. Continue to culture flasks until cells are nearly (75-80%) confluent [P0]
10. Remove cells with 0.05% trypsin-EDTA, centrifuge and resuspend in PBS, and count via Trypan Blue
11. Either freeze in 5 million cells/vial aliquots or re-plate at approximately 6,000/cm^2
12. Culture until 60%-70% confluent (2-3 days), passage [P1], and reseed again at 6,000/cm^2
13. Culture again until 60%-70% confluent (2-3 days), passage [P2], and seed into 3-D constructs for chondrogenesis

Appendix C. BMSC Encapsulation in Self-Assembling Peptide Hydrogels

Supplies
Custom 3-piece casting mold (Ring, Cap, Post)
2% LMP Agarose (Invitrogen)
1.25 mL sterile individually wrapped repeater pipette tips
24-well non-tissue culture treated plates
1X PBS without Ca^{2+} or Mg^{2+}, sterile, pH=7.2

Cast Acellular Agarose Rings (1-2 days prior to BMSC trypsinization)
1. Sterilize 2% agarose by autoclaving on the wet cycle for 20 min.
2. Place 2% agarose in 65°C water bath
3. Assemble 3-piece casting frames in each well of a 24-well plate in the following order: ring, cap, post. Make sure smooth side of ring and cap are touching. Use sterile forceps and spatula to position frames. See Figure 2.1
4. Assemble repeater pipette (old model) with 1.25 mL tip and set to 125 µL
5. Remove agarose from the water bath and place in the hood on styrofoam
6. Draw agarose into repeater pipette and inject into frames
7. Once all 24 wells are filled with agarose, cover plate and place at 4°C for 5 min. Be careful not to leave in hood too long or frame disassembly will be difficult
8. Return plate to hood and gently remove the frames in reverse order: post, cap, ring.
9. Add ~0.5mL 1X PBS to all wells
10. Store at 4°C for up to 4 days

Supplies
Casting medium: **25mM HEPES**, with hgDMEM, ITS+1, NEAA, Na Pyr, Proline, PSA
Culture medium: **10mM HEPES**, with hgDMEM, ITS+1, NEAA, Na Pyr, Proline, PSA
FBS medium: lgDMEM, 10% ES-FBS (Invitrogen), 10mM HEPES, PSA
1X PBS, sterile, pH=7.2
0.05% Trypsin/EDTA
10% Sucrose, Sterile
10% Sucrose, Sterile w/2.5mM HEPES
Peptide powder, sterile, (e.g. for 0.35% KLD12, 1.5mL x 3.5mg/mL x 1.2 = 6.3 mg/cast)
2mL screw top tubes, sterile
5mL polypropylene snap top tubes, sterile (BD Falcon)
1.0 or 1.25 mL sterile individually wrapped repeater pipette tips

Cast BMSC-seeded Self-Assembling Peptide Hydrogels (2 person procedure)
1. Aspirate PBS from each agarose ring and clean up loose agarose debris
2. Add ~0.5mL casting medium (above) to each well
3. Place plate(s) in 37°C incubator
4. Dissolve peptide at 4.375 mg/mL (for 3.5mg/mL final concentration) in sterile 10% sucrose by vortexing & sonicating. Leave peptide solution in sonicator.
5. Trypsinize cells and inactivate with FBS medium

6. Centrifuge cells and resuspend in FBS medium at >$10x10^6$ cells/mL (guess at count based on previous passage yield)
7. Count & aliquot $15x10^6$ cells into 2mL sterile screw top tubes. Store tubes at 4°C.
8. Prepare 5mL tubes with 1.2mL of 4.375 mg/mL peptide solution; return to sonicator
9. Spin 2mL tube with $15x10^6$ cells at 100 x g for 5 min
10. While spinning, aspirate 23 acellular agarose rings so that the center well is dry
11. Assemble repeater pipette with 1.0 mL or 1.25 mL tip and set to 50 µL
12. Person #1 aspirate medium from cells and resuspend in 300 µL of 10% sucrose + 2.5 mM HEPES
13. Person #2 hold 5mL tube with 1.2mL peptide solution
14. Person #1 inject cell suspension into 5mL tube
15. Starting from the time the cells are added to the peptide complete the following in 60 seconds: Gently vortex to ensure homogeneous cell distribution in peptide solution; gently draw cell-peptide suspension into repeater pipette, avoiding bubbles; rapidly but gently dispense 50 µL into the center well of up to 23 agarose rings
16. Wait at least 5 min and add 300 µL of casting medium to each plug to cover the top
17. Change medium replacing casting medium with culture medium
18. Place plate in incubator

Appendix D. Aggrecan Extraction and Purification

Adapted from protocols developed by J Sandy and Anna Plaas

Materials:
Guanidine HCl (4M)
Sodium Acetate (100mM)
Protease Complete Tablets (Roche, Cat #11 697 498 001)

1. Make desired volume of 4M Guanidine HCl in 100mM Sodium Acetate buffer and adjust pH to ~7.2. Rough guide: For tissue engineered plugs, make 1mL for every ~40mg of tissue wet weight with sGAG content of ~120ug (i.e. plug sGAG content is ~3ug/mg wet weight). I would double the amount of extraction solution if using native tissue instead of engineered samples.
2. Add appropriate fraction of protease complete tablet per manufacturer's instructions. (Inhibits a broad range of proteases).
3. Mechanically disrupt sample. May use a scalpel to dice (works for tissue engineered plugs). If using native cartilage tissue, may want to pulverize and homogenize.
4. Add appropriate volume of combined solution samples as per step #1 above.
5. Mix on shaker at 4C for 48hrs (probably excessive, but will maximize PG extraction)
6. Spin for 0.5-1hr at ~16,000 x g in microcentrifuge at 4C.
7. Transfer clarified supernatant to new tube and discard pellet.
8. Add CsCl powder until solution density is 1.58g/mL. Check density by weighing a known volume of solution.
9. Transfer sample to an appropriate tube for ultracentrifuge and balance ultracentrifuge rotor exactly!
10. Spin as long and as hard as you can. 72hrs at ~500,000 x g should produce a good density gradient.
11. Immediately at the end of the spin, carefully pipette fractions of the sample. Splitting 1mL into ~10 x 100uL fractions works well. Start by pipetting off the very top and working down the tube. Be aware that a hard pellet of CsCl may form at the bottom; the density gradient will likely still be sufficient for PG purification.
12. Measure the density of the fractions as in step #8.
13. Combine fractions based on density. D1>1.54g/mL; 1.46g/mL<D2<1.54g/mL[82]
14. Dialyze with 500 volumes of 1M NaCl for 12-24 hrs.
15. Dialyze with 500 volumes of MilliQ filtered, distilled H20.

Appendix E. Smad 2/3 Western Blot Analysis

Supplies:
NuPage 10% Bis-Tris Gel 1.5mm x 15 well; Invitrogen, Cat# NP0316BOX
Stds (Novex Sharp Pre-Stained, store -20C, Cat# LC5800)
Reducing Agent, NuPage, Invitrogen Cat# NP0004 (store 4C)
Sample Buffer, NuPage, Invitrogen Cat# NP0007 (store RT)
NuPage MOPS SDS Running Buffer, Invitrogen
Transfer Buffer (3.03g Tris, 14.4g Glysine, 800mL aqueous vol, pH=8.3; 200mL Methanol)
PVDF Membrane
P-SMAD2 antibody, Cell Signaling, Cat# 3101
Total SMAD2/3 antibody, Cell Signaling, Cat# 3102

Run Gel and Western Blot:
1. Max vol per lane = 25uL
2. Make sample buffer mix 2uL reducing agent+5uL sample buffer per lane (make up one lane, 7uL, extra)
3. Mix appropriate amount of protein from samples with 7uL of sample buffer
4. Boil 5min
5. Make 500 mL (800mL for 2 gels) MOPS running buffer by diluting 20X stock with DI H_2O
6. Assemble Gel apparatus, remove comb, fill inner chamber above white bar fill outer chamber with remaining buffer
7. Run 150V, ~90 min, @RT until stds reach bottom of gel (can increase to 200V)
8. While running, make transfer buffer (fresh each time)
9. Cut PVDF membrane to size
10. When gel is finished, activate PVDF membrane by wetting in 100% methanol (both sides) and rinsing in DI H_2O.
11. Place membrane in pan filled with transfer buffer. Also wet transfer apparatus in pan, black side down; stack sandwich in this order (item **a** on bottom, item **f** on top):
    a. sponge; **b.** blot paper; **c.** gel; **d.** membrane; **e.** blot paper; **f.** sponge
12. Disassemble gel, break cassette with putty knife, cut off comb and base of gel (the thick part)
13. Place gel in pan with transfer apparatus and allow to equilibrate for 10-15min
14. Complete assembly of sandwich and use test tube to roll out air bubbles
15. Insert sandwich into transfer chamber with ice block and stir bar.
16. Transfer in 4C room at 75V for 60 min.
17. Block 1 hr at RT in TBS + 0.1% Tween 20 + 5% BSA (SMAD2/3 antibody) (sonicate and filter this prior to use) or TBS-T + 5% milk (PSMAD2 antibody)
18. Incubate with primary antibody + TBS-T + 5% BSA/milk at 4C overnight
19. Wash 4x in TBS-T with 5 min between rinses (15 min total time)
20. Incubate with secondary antibody (1:2000)+TBS-T+5% BSA/milk for 1 hr at RT
21. Rinse 4x in TBS-T with 10 min between rinses (30 min total time)
22. 1:1 mix of imaging components, ~5mL per membrane, 1 min on shaker at RT

References

1. Felson DT, Lawrence RC, Dieppe PA, et al. Osteoarthritis: new insights. Part 1: the disease and its risk factors. Ann Intern Med. Oct 17 2000;133(8):635-646.

2. Wieland HA, Michaelis M, Kirschbaum BJ, Rudolphi KA. Osteoarthritis - an untreatable disease? Nat Rev Drug Discov. Apr 2005;4(4):331-344.

3. Gelber AC, Hochberg MC, Mead LA, Wang NY, Wigley FM, Klag MJ. Joint injury in young adults and risk for subsequent knee and hip osteoarthritis. Ann Intern Med. Sep 5 2000;133(5):321-328.

4. von Porat A, Roos EM, Roos H. High prevalence of osteoarthritis 14 years after an anterior cruciate ligament tear in male soccer players: a study of radiographic and patient relevant outcomes. Ann Rheum Dis. Mar 2004;63(3):269-273.

5. Brandt KD, Radin EL, Dieppe PA, van de Putte L. Yet more evidence that osteoarthritis is not a cartilage disease. Ann Rheum Dis. Oct 2006;65(10):1261-1264.

6. Willers C, Partsalis T, Zheng MH. Articular cartilage repair: procedures versus products. Expert Rev Med Devices. May 2007;4(3):373-392.

7. Kreuz PC, Steinwachs MR, Erggelet C, et al. Results after microfracture of full-thickness chondral defects in different compartments in the knee. Osteoarthritis Cartilage. Nov 2006;14(11):1119-1125.

8. Brittberg M, Lindahl A, Nilsson A, Ohlsson C, Isaksson O, Peterson L. Treatment of deep cartilage defects in the knee with autologous chondrocyte transplantation. N Engl J Med. Oct 6 1994;331(14):889-895.

9. Benya PD, Shaffer JD. Dedifferentiated chondrocytes reexpress the differentiated collagen phenotype when cultured in agarose gels. Cell. Aug 1982;30(1):215-224.

10. Knutsen G, Engebretsen L, Ludvigsen TC, et al. Autologous chondrocyte implantation compared with microfracture in the knee. A randomized trial. J Bone Joint Surg Am. Mar 2004;86-A(3):455-464.

11. Knutsen G, Drogset JO, Engebretsen L, et al. A randomized trial comparing autologous chondrocyte implantation with microfracture. Findings at five years. J Bone Joint Surg Am. Oct 2007;89(10):2105-2112.

12. Hettrich CM, Crawford D, Rodeo SA. Cartilage repair: third-generation cell-based technologies--basic science, surgical techniques, clinical outcomes. Sports Med Arthrosc. Dec 2008;16(4):230-235.

13. Steinert AF, Ghivizzani SC, Rethwilm A, Tuan RS, Evans CH, Noth U. Major biological obstacles for persistent cell-based regeneration of articular cartilage. Arthritis Res Ther. 2007;9(3):213.

14. Pittenger MF, Mackay AM, Beck SC, et al. Multilineage potential of adult human mesenchymal stem cells. Science. Apr 2 1999;284(5411):143-147.

15. Knippenberg M, Helder MN, Zandieh Doulabi B, Wuisman PI, Klein-Nulend J. Osteogenesis versus chondrogenesis by BMP-2 and BMP-7 in adipose stem cells. Biochem Biophys Res Commun. Apr 14 2006;342(3):902-908.

16. Johnstone B, Hering TM, Caplan AI, Goldberg VM, Yoo JU. In vitro chondrogenesis of bone marrow-derived mesenchymal progenitor cells. Exp Cell Res. Jan 10 1998;238(1):265-272.

17. Kisiday J, Frisbie DD, McIlwraith W, Grodzinsky A. Dynamic compression stimulates proteoglycan synthesis by mesenchymal stem cells in the absence of chondrogenic cytokines. Tissue Eng Part A. Feb 25 2009.
18. Bosnakovski D, Mizuno M, Kim G, Takagi S, Okumura M, Fujinaga T. Chondrogenic differentiation of bovine bone marrow mesenchymal stem cells (MSCs) in different hydrogels: Influence of collagen type II extracellular matrix on MSC chondrogenesis. Biotechnol Bioeng. Apr 20 2006;93(6):1152-1163.
19. Im GI, Jung NH, Tae SK. Chondrogenic Differentiation of Mesenchymal Stem Cells Isolated from Patients in Late Adulthood: The Optimal Conditions of Growth Factors. Tissue Eng. Mar 1 2006;12(3):527-537.
20. Davis ME, Hsieh PC, Takahashi T, et al. Local myocardial insulin-like growth factor 1 (IGF-1) delivery with biotinylated peptide nanofibers improves cell therapy for myocardial infarction. Proc Natl Acad Sci U S A. May 23 2006;103(21):8155-8160.
21. Zhang S, Marini DM, Hwang W, Santoso S. Design of nanostructured biological materials through self-assembly of peptides and proteins. Curr Opin Chem Biol. Dec 2002;6(6):865-871.
22. Zhang S, Holmes T, Lockshin C, Rich A. Spontaneous assembly of a self-complementary oligopeptide to form a stable macroscopic membrane. Proc Natl Acad Sci U S A. Apr 15 1993;90(8):3334-3338.
23. Zhang S, Gelain F, Zhao X. Designer self-assembling peptide nanofiber scaffolds for 3D tissue cell cultures. Semin Cancer Biol. Oct 2005;15(5):413-420.
24. Holmes TC. Novel peptide-based biomaterial scaffolds for tissue engineering. Trends Biotechnol. Jan 2002;20(1):16-21.
25. Davis ME, Motion JP, Narmoneva DA, et al. Injectable self-assembling peptide nanofibers create intramyocardial microenvironments for endothelial cells. Circulation. Feb 1 2005;111(4):442-450.
26. Kisiday J, Jin M, Kurz B, et al. Self-assembling peptide hydrogel fosters chondrocyte extracellular matrix production and cell division: implications for cartilage tissue repair. Proc Natl Acad Sci U S A. Jul 23 2002;99(15):9996-10001.
27. Mauck RL, Helm JM, Tuan RS. Chondrogenesis of human MSCs in a 3D self-assembling peptide hydrogel: Functional properties and divergent expression profiles compared to pellet cultures. Orthopedic Research Society, 52nd Annual Meeting. 2006:Abstract #775.
28. Kisiday JD, Kopesky PW, Evans CH, Grodzinsky AJ, McIlwraith CW, Frisbie DD. Evaluation of adult equine bone marrow- and adipose-derived progenitor cell chondrogenesis in hydrogel cultures. J Orthop Res. Mar 2008;26(3):322-331.
29. Noth U, Steinert AF, Tuan RS. Technology insight: adult mesenchymal stem cells for osteoarthritis therapy. Nat Clin Pract Rheumatol. Jul 2008;4(7):371-380.
30. Mauck RL, Yuan X, Tuan RS. Chondrogenic differentiation and functional maturation of bovine mesenchymal stem cells in long-term agarose culture. Osteoarthritis Cartilage. Feb 2006;14(2):179-189.
31. Mouw JK, Connelly JT, Wilson CG, Michael KE, Levenston ME. Dynamic compression regulates the expression and synthesis of chondrocyte-specific matrix molecules in bone marrow stromal cells. Stem Cells. Mar 2007;25(3):655-663.

32. Connelly JT, Garcia AJ, Levenston ME. Inhibition of in vitro chondrogenesis in RGD-modified three-dimensional alginate gels. Biomaterials. Feb 2007;28(6):1071-1083.
33. Hui TY, Cheung KM, Cheung WL, Chan D, Chan BP. In vitro chondrogenic differentiation of human mesenchymal stem cells in collagen microspheres: influence of cell seeding density and collagen concentration. Biomaterials. Aug 2008;29(22):3201-3212.
34. Schulz RM, Zscharnack M, Hanisch I, Geiling M, Hepp P, Bader A. Cartilage tissue engineering by collagen matrix associated bone marrow derived mesenchymal stem cells. Biomed Mater Eng. 2008;18(1 Suppl):S55-70.
35. Mohan N, Nair PD, Tabata Y. A 3D biodegradable protein based matrix for cartilage tissue engineering and stem cell differentiation to cartilage. J Mater Sci Mater Med. Jun 17 2008.
36. Haider M, Cappello J, Ghandehari H, Leong KW. In vitro chondrogenesis of mesenchymal stem cells in recombinant silk-elastinlike hydrogels. Pharm Res. Mar 2008;25(3):692-699.
37. Tuan RS. Stemming cartilage degeneration: adult mesenchymal stem cells as a cell source for articular cartilage tissue engineering. Arthritis Rheum. Oct 2006;54(10):3075-3078.
38. Raghunath J, Rollo J, Sales KM, Butler PE, Seifalian AM. Biomaterials and scaffold design: key to tissue-engineering cartilage. Biotechnol Appl Biochem. Feb 2007;46(Pt 2):73-84.
39. Rajangam K, Behanna HA, Hui MJ, et al. Heparin binding nanostructures to promote growth of blood vessels. Nano Lett. Sep 2006;6(9):2086-2090.
40. Haines-Butterick L, Rajagopal K, Branco M, et al. Controlling hydrogelation kinetics by peptide design for three-dimensional encapsulation and injectable delivery of cells. Proc Natl Acad Sci U S A. May 8 2007;104(19):7791-7796.
41. Erickson IE, Huang AH, Chung C, Li RT, Burdick JA, Mauck RL. Differential Maturation and Structure-Function Relationships in MSC- and Chondrocyte-Seeded Hydrogels. Tissue Eng Part A. Jan 2 2009.
42. Semino CE, Merok JR, Crane GG, Panagiotakos G, Zhang S. Functional differentiation of hepatocyte-like spheroid structures from putative liver progenitor cells in three-dimensional peptide scaffolds. Differentiation. Jun 2003;71(4-5):262-270.
43. Wang S, Nagrath D, Chen PC, Berthiaume F, Yarmush ML. Three-Dimensional Primary Hepatocyte Culture in Synthetic Self-Assembling Peptide Hydrogel. Tissue Eng. Jan 3 2008.
44. Knothe Tate ML, Falls TD, McBride SH, Atit R, Knothe UR. Mechanical modulation of osteochondroprogenitor cell fate. Int J Biochem Cell Biol. 2008;40(12):2720-2738.
45. Goldring MB, Tsuchimochi K, Ijiri K. The control of chondrogenesis. J Cell Biochem. Jan 1 2006;97(1):33-44.
46. Varghese S, Hwang NS, Canver AC, Theprungsirikul P, Lin DW, Elisseeff J. Chondroitin sulfate based niches for chondrogenic differentiation of mesenchymal stem cells. Matrix Biol. Jan 2008;27(1):12-21.

47. Kamiya N, Watanabe H, Habuchi H, et al. Versican/PG-M regulates chondrogenesis as an extracellular matrix molecule crucial for mesenchymal condensation. Journal of Biological Chemistry. Jan 27 2006;281(4):2390-2400.
48. Connelly JT, Wilson CG, Levenston ME. Characterization of proteoglycan production and processing by chondrocytes and BMSCs in tissue engineered constructs. Osteoarthritis Cartilage. Feb 20 2008.
49. Chung C, Burdick JA. Influence of three-dimensional hyaluronic Acid microenvironments on mesenchymal stem cell chondrogenesis. Tissue Eng Part A. Feb 2009;15(2):243-254.
50. Buschmann MD, Gluzband YA, Grodzinsky AJ, Kimura JH, Hunziker EB. Chondrocytes in agarose culture synthesize a mechanically functional extracellular matrix. J Orthop Res. Nov 1992;10(6):745-758.
51. Mauck RL, Soltz MA, Wang CC, et al. Functional tissue engineering of articular cartilage through dynamic loading of chondrocyte-seeded agarose gels. J Biomech Eng. Jun 2000;122(3):252-260.
52. Sieminski AL, Semino CE, Gong H, Kamm RD. Primary sequence of ionic self-assembling peptide gels affects endothelial cell adhesion and capillary morphogenesis. J Biomed Mater Res A. Jan 9 2008.
53. Sieminski AL, Was AS, Kim G, Gong H, Kamm RD. The stiffness of three-dimensional ionic self-assembling peptide gels affects the extent of capillary-like network formation. Cell Biochem Biophys. 2007;49(2):73-83.
54. Domm C, Schunke M, Christesen K, Kurz B. Redifferentiation of dedifferentiated bovine articular chondrocytes in alginate culture under low oxygen tension. Osteoarthritis Cartilage. Jan 2002;10(1):13-22.
55. Fitzgerald JB, Jin M, Dean D, Wood DJ, Zheng MH, Grodzinsky AJ. Mechanical compression of cartilage explants induces multiple time-dependent gene expression patterns and involves intracellular calcium and cyclic AMP. J Biol Chem. May 7 2004;279(19):19502-19511.
56. Bosnakovski D, Mizuno M, Kim G, Takagi S, Okumura M, Fujinaga T. Isolation and multilineage differentiation of bovine bone marrow mesenchymal stem cells. Cell Tissue Res. Feb 2005;319(2):243-253.
57. Pfaffl MW. A new mathematical model for relative quantification in real-time RT-PCR. Nucleic Acids Res. May 1 2001;29(9):e45.
58. Farndale RW, Sayers CA, Barrett AJ. A direct spectrophotometric microassay for sulfated glycosaminoglycans in cartilage cultures. Connect Tissue Res. 1982;9(4):247-248.
59. Kim YJ, Sah RL, Doong JY, Grodzinsky AJ. Fluorometric assay of DNA in cartilage explants using Hoechst 33258. Anal Biochem. Oct 1988;174(1):168-176.
60. Ng L, Grodzinsky AJ, Patwari P, Sandy J, Plaas A, Ortiz C. Individual cartilage aggrecan macromolecules and their constituent glycosaminoglycans visualized via atomic force microscopy. J Struct Biol. Sep 2003;143(3):242-257.
61. Patwari P, Kurz B, Sandy JD, Grodzinsky AJ. Mannosamine inhibits aggrecanase-mediated changes in the physical properties and biochemical composition of articular cartilage. Arch Biochem Biophys. Feb 1 2000;374(1):79-85.

62. Hall BK, Miyake T. Divide, accumulate, differentiate: cell condensation in skeletal development revisited. Int J Dev Biol. Dec 1995;39(6):881-893.
63. Hall BK, Miyake T. All for one and one for all: condensations and the initiation of skeletal development. Bioessays. Feb 2000;22(2):138-147.
64. Lee CR, Grodzinsky AJ, Spector M. Modulation of the contractile and biosynthetic activity of chondrocytes seeded in collagen-glycosaminoglycan matrices. Tissue Eng. Feb 2003;9(1):27-36.
65. Lee CR, Grodzinsky AJ, Spector M. The effects of cross-linking of collagen-glycosaminoglycan scaffolds on compressive stiffness, chondrocyte-mediated contraction, proliferation and biosynthesis. Biomaterials. Dec 2001;22(23):3145-3154.
66. Barry F, Boynton RE, Liu B, Murphy JM. Chondrogenic differentiation of mesenchymal stem cells from bone marrow: differentiation-dependent gene expression of matrix components. Exp Cell Res. Aug 15 2001;268(2):189-200.
67. Bosnakovski D, Mizuno M, Kim G, Takagi S, Okumur M, Fujinag T. Gene expression profile of bovine bone marrow mesenchymal stem cell during spontaneous chondrogenic differentiation in pellet culture system. Jpn J Vet Res. Feb 2006;53(3-4):127-139.
68. Huang CY, Hagar KL, Frost LE, Sun Y, Cheung HS. Effects of cyclic compressive loading on chondrogenesis of rabbit bone-marrow derived mesenchymal stem cells. Stem Cells. 2004;22(3):313-323.
69. Jiang Y, Mishima H, Sakai S, Liu YK, Ohyabu Y, Uemura T. Gene expression analysis of major lineage-defining factors in human bone marrow cells: effect of aging, gender, and age-related disorders. J Orthop Res. Jul 2008;26(7):910-917.
70. Scharstuhl A, Schewe B, Benz K, Gaissmaier C, Buhring HJ, Stoop R. Chondrogenic potential of human adult mesenchymal stem cells is independent of age or osteoarthritis etiology. Stem Cells. Dec 2007;25(12):3244-3251.
71. Barbero A, Grogan S, Schafer D, Heberer M, Mainil-Varlet P, Martin I. Age related changes in human articular chondrocyte yield, proliferation and post-expansion chondrogenic capacity. Osteoarthritis and Cartilage. Jun 2004;12(6):476-484.
72. Bolton MC, Dudhia J, Bayliss MT. Age-related changes in the synthesis of link protein and aggrecan in human articular cartilage: implications for aggregate stability. Biochem J. Jan 1 1999;337 (Pt 1):77-82.
73. Plaas AH, Sandy JD. Age-related decrease in the link-stability of proteoglycan aggregates formed by articular chondrocytes. Biochem J. May 15 1984;220(1):337-340.
74. Tran-Khanh N, Hoemann CD, McKee MD, Henderson JE, Buschmann MD. Aged bovine chondrocytes display a diminished capacity to produce a collagen-rich, mechanically functional cartilage extracellular matrix. J Orthop Res. Nov 2005;23(6):1354-1362.
75. Martin JA, Ellerbroek SM, Buckwalter JA. Age-related decline in chondrocyte response to insulin-like growth factor-I: the role of growth factor binding proteins. J Orthop Res. Jul 1997;15(4):491-498.
76. Hickery MS, Bayliss MT, Dudhia J, Lewthwaite JC, Edwards JC, Pitsillides AA. Age-related changes in the response of human articular cartilage to IL-1alpha and

transforming growth factor-beta (TGF-beta): chondrocytes exhibit a diminished sensitivity to TGF-beta. J Biol Chem. Dec 26 2003;278(52):53063-53071.
77. Blaney Davidson EN, Scharstuhl A, Vitters EL, van der Kraan PM, van den Berg WB. Reduced transforming growth factor-beta signaling in cartilage of old mice: role in impaired repair capacity. Arthritis Res Ther. 2005;7(6):R1338-1347.
78. Chen FH, Tuan, R.S. Mesenchymal stem cells in arthritic diseases. Arthritis Research & Therapy. 2008;10(223).
79. Dudhia J. Aggrecan, aging and assembly in articular cartilage. Cell Mol Life Sci. Oct 2005;62(19-20):2241-2256.
80. Kimura JH, Caputo CB, Hascall VC. The effect of cycloheximide on synthesis of proteoglycans by cultured chondrocytes from the Swarm rat chondrosarcoma. J Biol Chem. May 10 1981;256(9):4368-4376.
81. Mitchell D, Hardingham T. The control of chondroitin sulphate biosynthesis and its influence on the structure of cartilage proteoglycans. Biochem J. Feb 15 1982;202(2):387-395.
82. Roughley PJ, White RJ. Age-related changes in the structure of the proteoglycan subunits from human articular cartilage. J Biol Chem. Jan 10 1980;255(1):217-224.
83. Buckwalter JA, Roughley PJ, Rosenberg LC. Age-related changes in cartilage proteoglycans: quantitative electron microscopic studies. Microsc Res Tech. Aug 1 1994;28(5):398-408.
84. Hascall VC, Calabro A, Midura RJ, Yanagishita M. Isolation and characterization of proteoglycans. Methods Enzymol. 1994;230:390-417.
85. Buckwalter JA, Rosenberg LC. Electron microscopic studies of cartilage proteoglycans. Direct evidence for the variable length of the chondroitin sulfate-rich region of proteoglycan subunit core protein. J Biol Chem. Aug 25 1982;257(16):9830-9839.
86. Hsieh PC, Davis ME, Gannon J, MacGillivray C, Lee RT. Controlled delivery of PDGF-BB for myocardial protection using injectable self-assembling peptide nanofibers. J Clin Invest. Jan 2006;116(1):237-248.
87. Ragan PM, Chin VI, Hung HH, et al. Chondrocyte extracellular matrix synthesis and turnover are influenced by static compression in a new alginate disk culture system. Arch Biochem Biophys. Nov 15 2000;383(2):256-264.
88. Woessner JF, Jr. The determination of hydroxyproline in tissue and protein samples containing small proportions of this imino acid. Arch Biochem Biophys. May 1961;93:440-447.
89. Frank EH, Grodzinsky AJ. Cartilage electromechanics--I. Electrokinetic transduction and the effects of electrolyte pH and ionic strength. J Biomech. 1987;20(6):615-627.
90. Williamson AK, Chen AC, Sah RL. Compressive properties and function-composition relationships of developing bovine articular cartilage. J Orthop Res. Nov 2001;19(6):1113-1121.
91. Patwari P, Gao G, Lee JH, Grodzinsky AJ, Sandy JD. Analysis of ADAMTS4 and MT4-MMP indicates that both are involved in aggrecanolysis in interleukin-1-treated bovine cartilage. Osteoarthritis Cartilage. Apr 2005;13(4):269-277.

92. Wilson CG, Nishimuta JF, Levenston ME. Chondrocytes and Meniscal Fibrochondrocytes Differentially Process Aggrecan During De Novo Extracellular Matrix Assembly. Tissue Eng Part A. Mar 2 2009.
93. Kim YJ, Grodzinsky AJ, Plaas AH. Compression of cartilage results in differential effects on biosynthetic pathways for aggrecan, link protein, and hyaluronan. Arch Biochem Biophys. Apr 15 1996;328(2):331-340.
94. Vehof JW, Haus MT, de Ruijter AE, Spauwen PH, Jansen JA. Bone formation in transforming growth factor beta-I-loaded titanium fiber mesh implants. Clin Oral Implants Res. Feb 2002;13(1):94-102.
95. Holland TA, Tessmar JK, Tabata Y, Mikos AG. Transforming growth factor-beta 1 release from oligo(poly(ethylene glycol) fumarate) hydrogels in conditions that model the cartilage wound healing environment. J Control Release. Jan 8 2004;94(1):101-114.
96. Motoyama M, Deie M, Kanaya A, et al. In vitro cartilage formation using TGF-beta-immobilized magnetic beads and mesenchymal stem cell-magnetic bead complexes under magnetic field conditions. J Biomed Mater Res A. Jan 26 2009.
97. Park JS, Yang HJ, Woo DG, Yang HN, Na K, Park KH. Chondrogenic differentiation of mesenchymal stem cells embedded in a scaffold by long-term release of TGF-beta3 complexed with chondroitin sulfate. J Biomed Mater Res A. Mar 11 2009.
98. Park H, Temenoff JS, Tabata Y, et al. Effect of dual growth factor delivery on chondrogenic differentiation of rabbit marrow mesenchymal stem cells encapsulated in injectable hydrogel composites. J Biomed Mater Res A. Mar 15 2009;88(4):889-897.
99. Fischer U, Hempel U, Becker D, et al. Transforming growth factor beta1 immobilized adsorptively on Ti6Al4V and collagen type I coated Ti6Al4V maintains its biological activity. Biomaterials. Jul 2003;24(15):2631-2641.
100. Heldin CH, Miyazono K, ten Dijke P. TGF-beta signalling from cell membrane to nucleus through SMAD proteins. Nature. Dec 4 1997;390(6659):465-471.
101. Moustakas A, Souchelnytskyi S, Heldin CH. Smad regulation in TGF-beta signal transduction. J Cell Sci. Dec 2001;114(Pt 24):4359-4369.
102. Shi Y, Massague J. Mechanisms of TGF-beta signaling from cell membrane to the nucleus. Cell. Jun 13 2003;113(6):685-700.
103. Rajangam K, Arnold MS, Rocco MA, Stupp SI. Peptide amphiphile nanostructure-heparin interactions and their relationship to bioactivity. Biomaterials. Aug 2008;29(23):3298-3305.
104. Koutsopoulos S, Unsworth LD, Nagai Y, Zhang S. Controlled release of functional proteins through designer self-assembling peptide nanofiber hydrogel scaffold. Proc Natl Acad Sci U S A. Mar 24 2009;106(12):4623-4628.
105. Branco MC, Pochan DJ, Wagner NJ, Schneider JP. Macromolecular diffusion and release from self-assembled beta-hairpin peptide hydrogels. Biomaterials. Mar 2009;30(7):1339-1347.
106. Branco MC, Schneider JP. Self-assembling materials for therapeutic delivery. Acta Biomater. Mar 2009;5(3):817-831.

107. Garcia AM, Szasz N, Trippel SB, Morales TI, Grodzinsky AJ, Frank EH. Transport and binding of insulin-like growth factor I through articular cartilage. Arch Biochem Biophys. Jul 1 2003;415(1):69-79.
108. Yamamoto M, Ikada Y, Tabata Y. Controlled release of growth factors based on biodegradation of gelatin hydrogel. J Biomater Sci Polym Ed. 2001;12(1):77-88.
109. Holland TA, Tabata Y, Mikos AG. In vitro release of transforming growth factor-beta 1 from gelatin microparticles encapsulated in biodegradable, injectable oligo(poly(ethylene glycol) fumarate) hydrogels. J Control Release. Sep 4 2003;91(3):299-313.
110. Serwer P. Agarose gels: Properties and use for electrophoresis. Electrophoresis. 1983;4(6):375-382.
111. Schlunegger MP, Grutter MG. An unusual feature revealed by the crystal structure at 2.2 A resolution of human transforming growth factor-beta 2. Nature. Jul 30 1992;358(6385):430-434.
112. Sieminski AL, Semino CE, Gong H, Kamm RD. Primary sequence of ionic self-assembling peptide gels affects endothelial cell adhesion and capillary morphogenesis. J Biomed Mater Res A. Nov 2008;87(2):494-504.
113. Segers VF, Lee RT. Local delivery of proteins and the use of self-assembling peptides. Drug Discov Today. Jul 2007;12(13-14):561-568.
114. Nagai Y, Unsworth LD, Koutsopoulos S, Zhang S. Slow release of molecules in self-assembling peptide nanofiber scaffold. J Control Release. Sep 28 2006;115(1):18-25.
115. Stryer L. Biochemistry. Third ed: W.H. Freeman; 1988.
116. Byers BA, Mauck RL, Chiang IE, Tuan RS. Transient exposure to transforming growth factor beta 3 under serum-free conditions enhances the biomechanical and biochemical maturation of tissue-engineered cartilage. Tissue Eng Part A. Nov 2008;14(11):1821-1834.
117. Mauck RL, Byers BA, Yuan X, Rackwitz L, Tuan RS. Cartilage tissue engineering with MSC-laden hydrogels: Effect of seeding density, exposure to chondrogenic medium, and dynamic loading. Trans 52nd Mtg ORS, Chicago, IL. 2006.
118. Clarke DC, Brown ML, Erickson RA, Shi Y, Liu X. Transforming growth factor beta depletion is the primary determinant of Smad signaling kinetics. Mol Cell Biol. May 2009;29(9):2443-2455.
119. Metzger W, Grenner N, Motsch SE, Strehlow R, Pohlemann T, Oberringer M. Induction of myofibroblastic differentiation in vitro by covalently immobilized transforming growth factor-beta(1). Tissue Eng. Nov 2007;13(11):2751-2760.
120. Mann BK, Schmedlen RH, West JL. Tethered-TGF-beta increases extracellular matrix production of vascular smooth muscle cells. Biomaterials. Mar 2001;22(5):439-444.